MCDONNELL DOUGLAS CORPORATION

BERTHING MECHANISM FINAL TEST REPORT AND PROGRAM ASSESSMENT (CDRL 13 & 14)

OCTOBER 1988

MDAC H3913

PREPARED BY: Control Dynamics Company
Huntsville, Alabama
&
McDonnell Douglas
Astronautics Company
Huntington Beach, California

APPROVED BY:

G. C. BURNS
Program Manager
Berthing Mechanisms

Prepared for George C. Marshall Space Flight Center
Under Contract NAS8-36417

MCDONNELL DOUGLAS ASTRONAUTICS COMPANY-HUNTINGTON BEACH
5301 Bolsa Avenue Huntington Beach, California 92647 (714) 896-3311

Final Test Report

1. Introduction

The purpose of this report is to document the testing performed on both hardware and software developed under the Space Station Berthing Mechanisms Program. The mechanism testing was accomplished under Phase 7 of the NASA/MSFC Advanced Development Contract NAS8-36417.

The docking and berthing mechanism, henceforth to be called simply the docking mechanism, was designed by McDonnell Douglas Astronautics Company (MDAC) located in Huntington Beach, California. Assembly of the mechanism was performed by the Space Flight Systems (SFS) division of United Technologies Corporation. Testing of the mechanism has occurred at three locations. Several system components, e.g. actuators and computer system, were functionally tested at MDAC-HB before assembly. A series of post assembly tests were performed at the United Technologies facilities in Huntsville and the dynamic testing was undertaken at the MSFC 6-DOF simulation facility. The post assembly tests, as well as the dynamic testing of the mechanism, are the subject of the remainder of this report.

2. Post Assembly Tests

The post assembly tests, as specified in the "Berthing Mechanism Program Full Scale Test Plan" (Ref. 1), began immediately after the final assembly of the docking mechanism was complete. The tests were of three basic types - the pressure tests, the latch actuation tests, and the bellows spring rate test. This report will document the results of each of these tests.

2.1 Pressure Tests

Before the seal leak tests were performed, a proof pressure test was conducted at 15 psig to ensure integrity of the mechanism. This pressure was maintained for 10 minutes without evidence of a leak through the seal port. No bubbles were released into the flask (see Figures 2.1a and b), nor was there any visible drop of indicated pressure on the gage.

A number of thermocouples were attached to the outer surface of the mechanism. Unfortunately the thermocouples tended to track the room temperature, not the gas temperature inside the mechanism. There was no apparent way to put a temperature sensor inside the mechanism without compromising the seal integrity. The temperature measurements were recorded on a strip-chart recorder at UTC.

2.1.1 Seal Leak Test # 1

This test was used to verify the capability of the permanent seals to maintain pressure in the mechanism. The test basically consisted of pressurizing the mechanism to 10 psig without the o-ring seal (1D58545) in place. The seal leak port is located between the two permanent seals, thus any leakage past the inner seal would be sensed as a series of bubbles in the outer water filled flask. The test was conducted in all four clocking positions to insure that the seals perform satisfactorily in any of the possible clocking orientations.

Figures 2.2 - 2.5 are the pressure vs. time plots for each of the four clocking positions. It can be seen in the plots, the pressure drops by approximately 2% over the course of an hour. The fact that no bubbles were released into the flask indicates that there was no gas escaping past the inner permanent seal. There are several possible explanations of the pressure loss. Temperature accommodation of the pressure change is quite possible. However, since the gas temperature is not available this cannot be verified. It is also possible that a small gas leak existed where the cover plate (1D58772) seats into the flex half. The cover plate did have its own seal, and it is installed in such a way that the pressure tends to force the plate into the seal, thus minimizing any gap that may have been present. Finally, there might have been a very small leak in the bellows or at some interior weld point, but this cannot be determined from the data. It should be kept in mind

PRESSURE TEST SET-UP

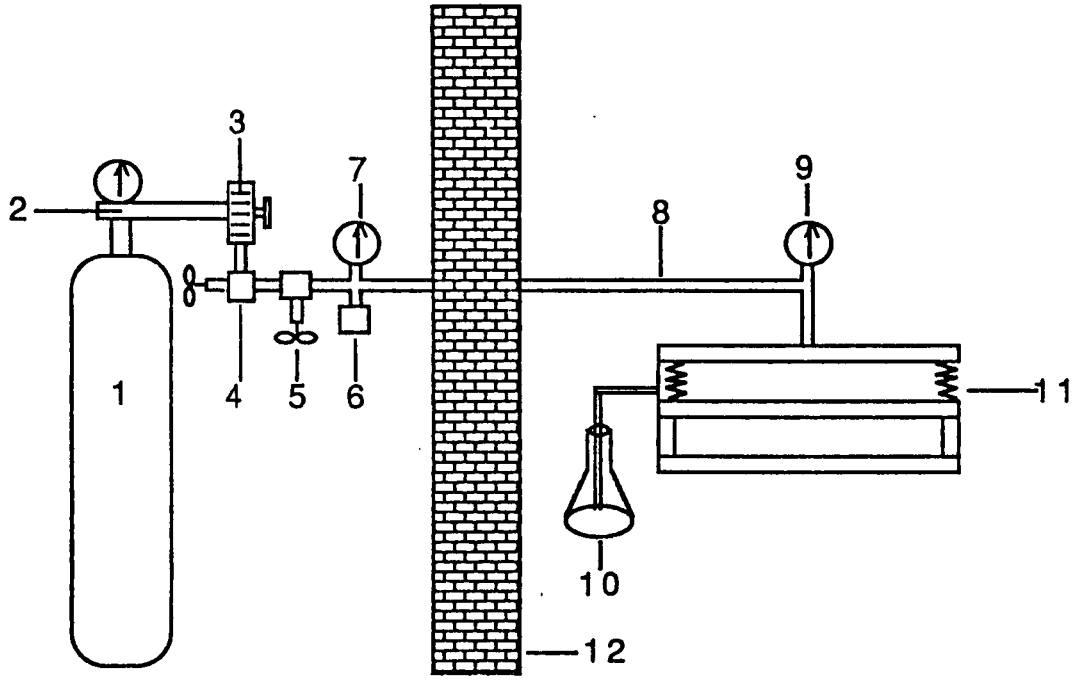

1. N2 BOTTLE
2. REGULATOR (50 PSIG)
3. FLOW METER (0-1000 FT/HR)
4. REGULATOR (0-50 PSIG)
5. SHUT OFF VALVE
6. POP-OFF VALVE (18 PSIG)
7. PRESSURE GUAGE (0-15 PSI)
8. PRESSURE LINE
9. GAUGE (0-30 PSIG)
10. LEAK DETECTOR (BETWEEN SEALS)
11. TEST ARTICLE
12. SAFETY WALL

FIGURE 2.1a

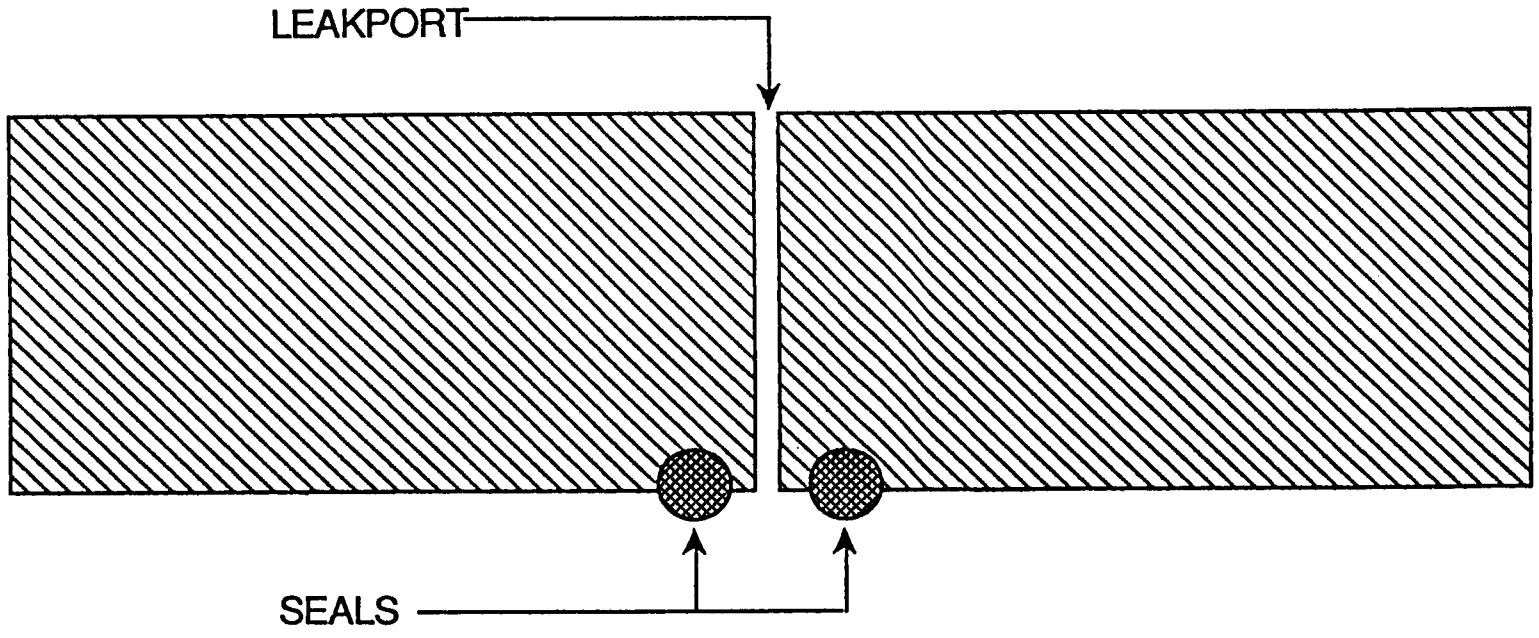

FIGURE 2.1b

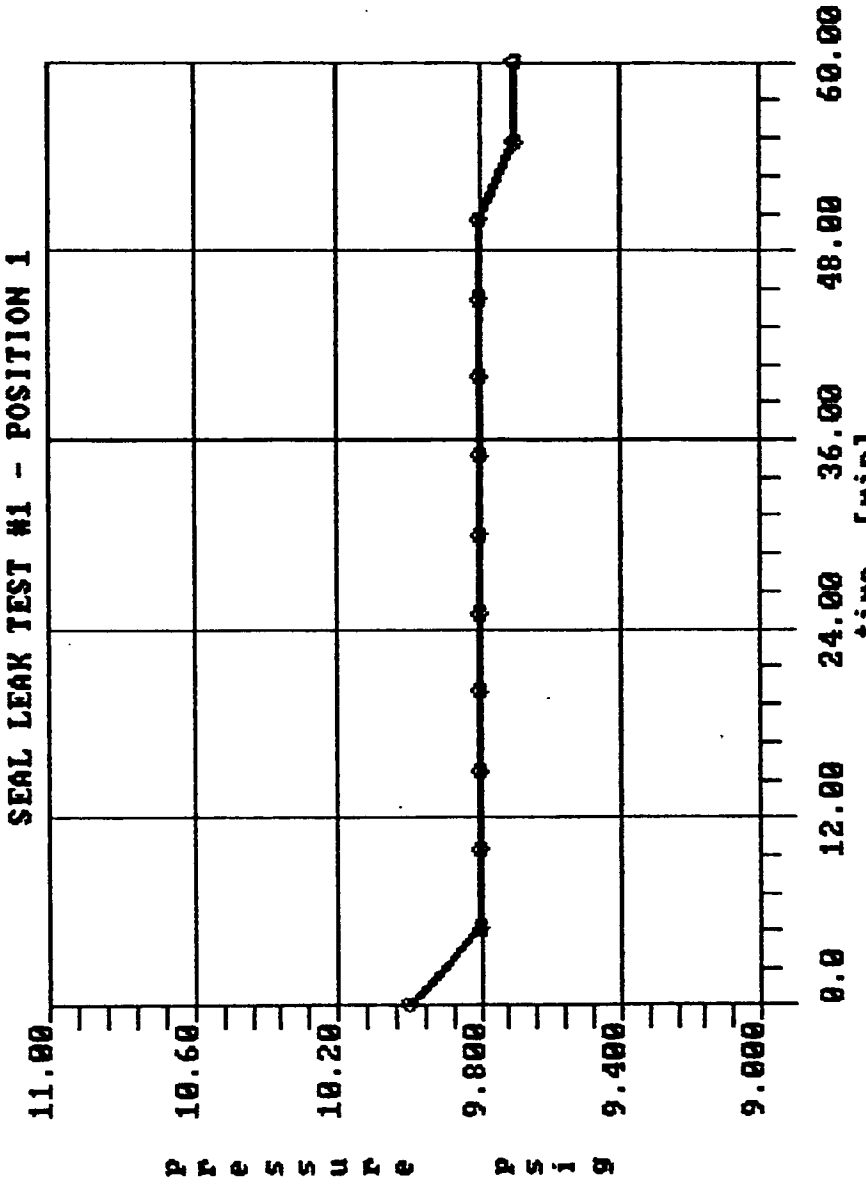
SEAL LEAK TEST #1 - POSITION 1
11.00
10.60
10.20
9.800
9.400
9.000
pressure psig
0.0
12.00
24.00
36.00
48.00
60.00
time [min]

FIGURE 2.2

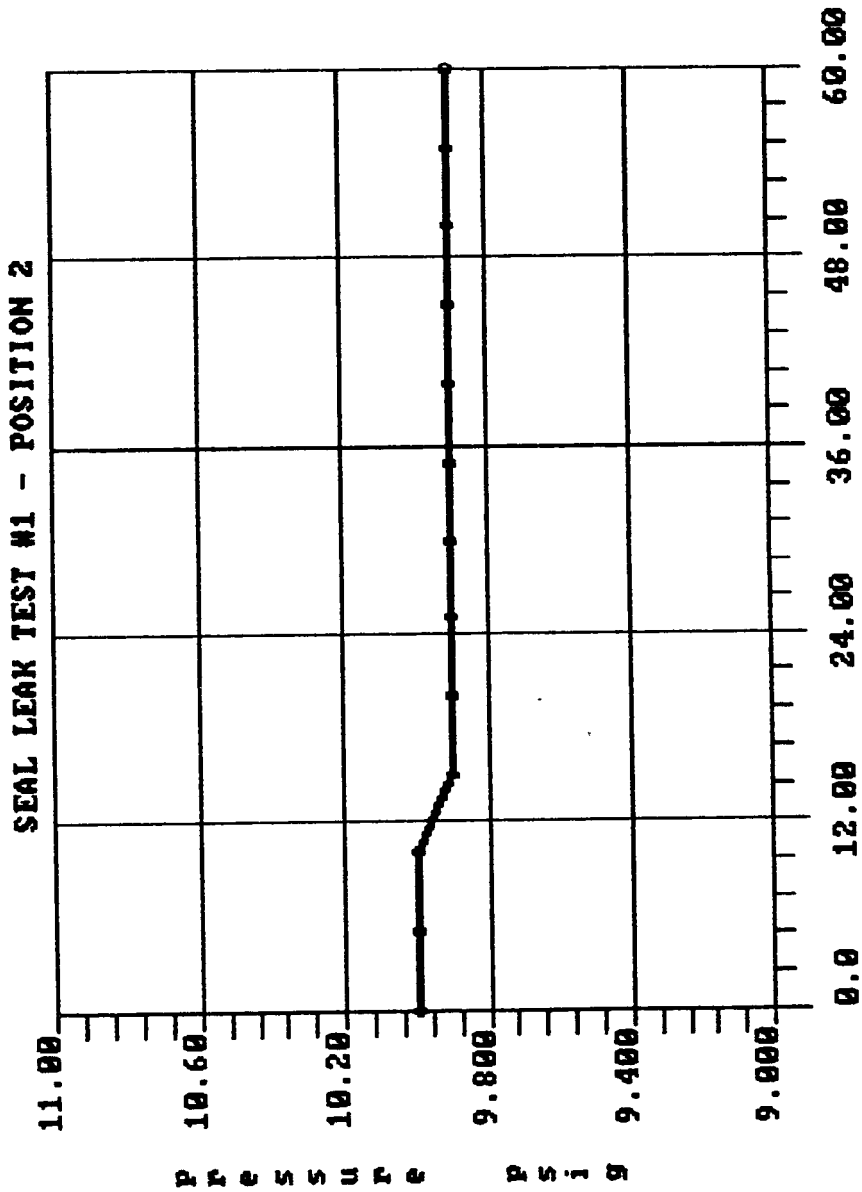
SEAL LEAK TEST #1 - POSITION 2
pressure psig
11.00
10.60
10.20
9.800
9.400
9.000
0.0
12.00
24.00
36.00
48.00
60.00
time [min]

FIGURE 2.3

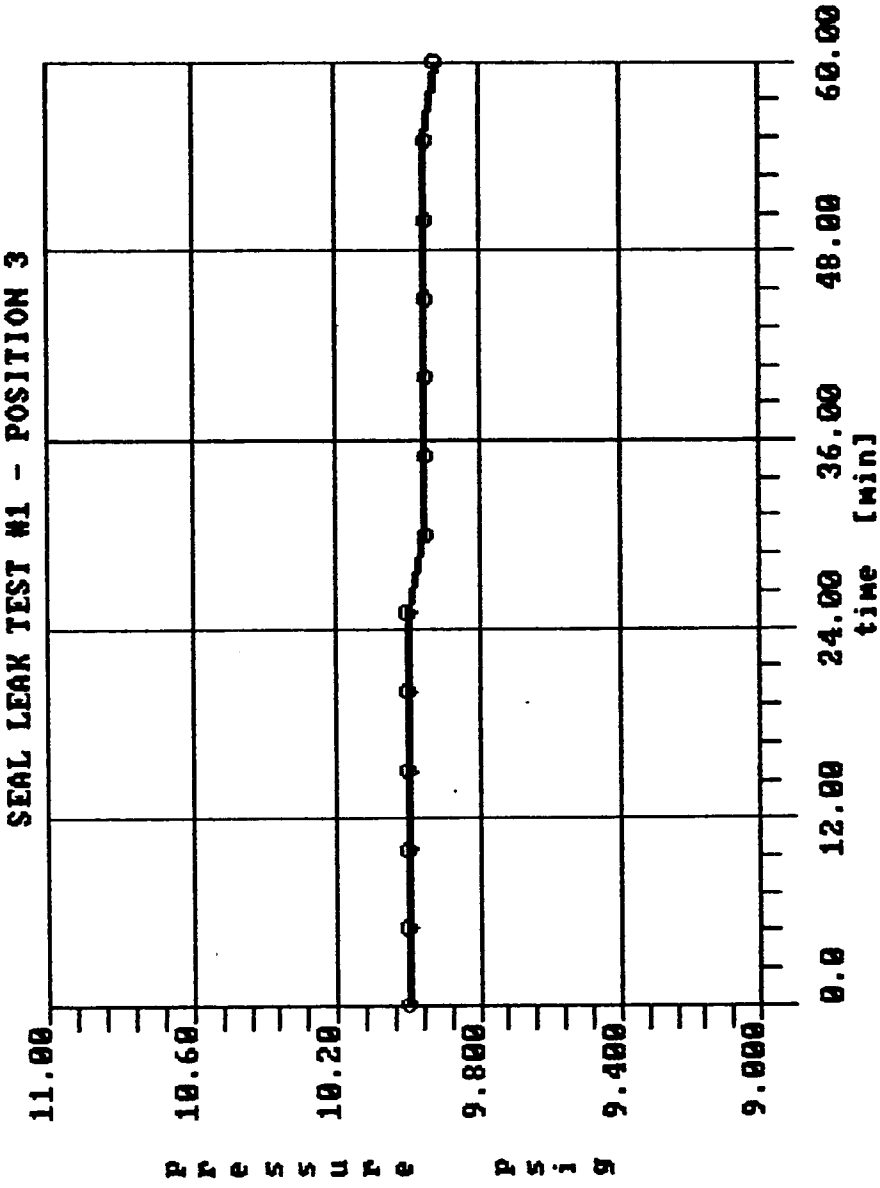
SEAL LEAK TEST #1 - POSITION 3
pressure psig
11.00
10.60
10.20
9.800
9.400
9.000
0.0
12.00
24.00
36.00
48.00
60.00
time [min]

FIGURE 2.4

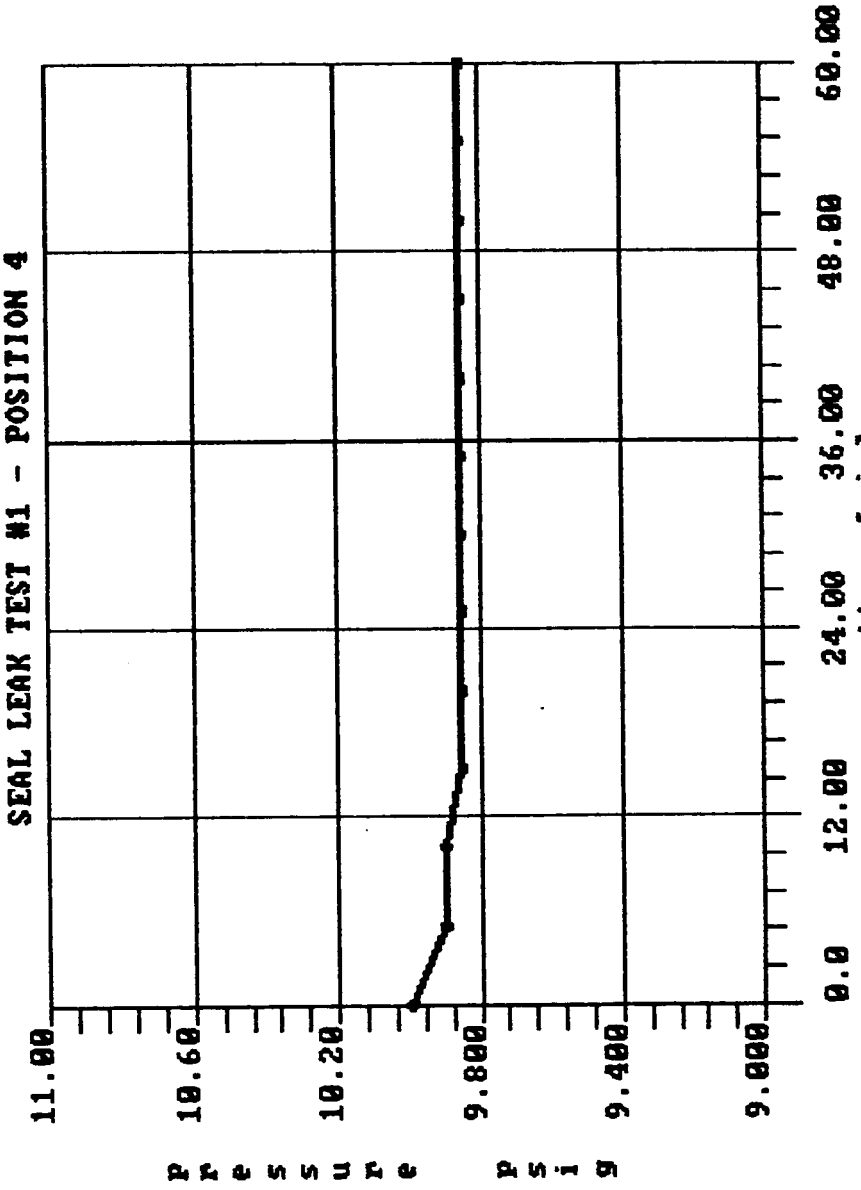
SEAL LEAK TEST #1 - POSITION 4
pressure psig
11.000
10.600
10.200
9.800
9.400
9.000
0.0
12.00
24.00
36.00
48.00
60.00
time [min]

FIGURE 2.5

that the purpose of Seal Leak Test # 1 was to verify the permanent seals, which had no detectable leak.

2.1.2 Seal Leak Test # 2

The second pressure test was used to verify the capability of the manually installed o-ring seal (1D58545) to maintain pressure in the mechanism. For this test the inner permanent seal was removed before mating the two mechanism halves. After the mechanism is mated, but before the structural latches are engaged and torqued to 500 in-lbs, the o-ring is installed from inside the mechanism. If any gas should escape past the o-ring it will have a direct path to the leakport since the inner permanent seal has been removed.

The mechanism was pressurized to 15 psig and held there for 10 minutes as a safety precaution. No bubbles were seen to enter the flask from the leakport. At the end of the 10 minute proof test the pressure was reduced to approximately 10 psig and monitored for 1 hour. Figure 2.6 is the pressure vs. time plot for the 1 hour test. It is seen that the pressure actually increases by about 2% during the course of the hour. This is almost certainly caused by an increase of the interior gas temperature. There were no nitrogen bubbles released into the flask, thus indicating that the manually installed o-ring does in fact seal the interface between the two mechanism halves as designed.

2.2 Bellows Flex Test

The purpose of the Bellows Flex Test was to measure the bellows angular spring rate. Figure 2.7 shows the test setup. The top sketch in this figure shows the upper plate of the flexible (bellows) half of the docking mechanism, the attached beam fixture, and weight cage. Omitted from the sketch is the actual bellows, the lower (active) half of the docking mechanism, and an overhead crane assembly which was attached to the end of the beam through a load cell. The overhead crane was used to lift up on the beam, while putting weights in the cage was used to pull down on the beam.

The bellows spring rate was measured about two perpendicular axes. These axes are identified in Figure 2.8. The numbers 1-16 on the figure are the numbers associated with the structural latches. These identifying numbers are located on the base plate of the bellows half of the mechanism. The data used to form the load vs. deflection curves is contained in TABLE 2.1. The angle and moment convention used is such that a positive angle and moment result when a downward load is applied to the end of the beam fixture.

Figures 2.9a and 2.9b are the load-deflection curves for Tests 1 and 2 respectively. The linear region (close to zero load) slope from Test 1 yields an approximate spring stiffness of 31,000 in-

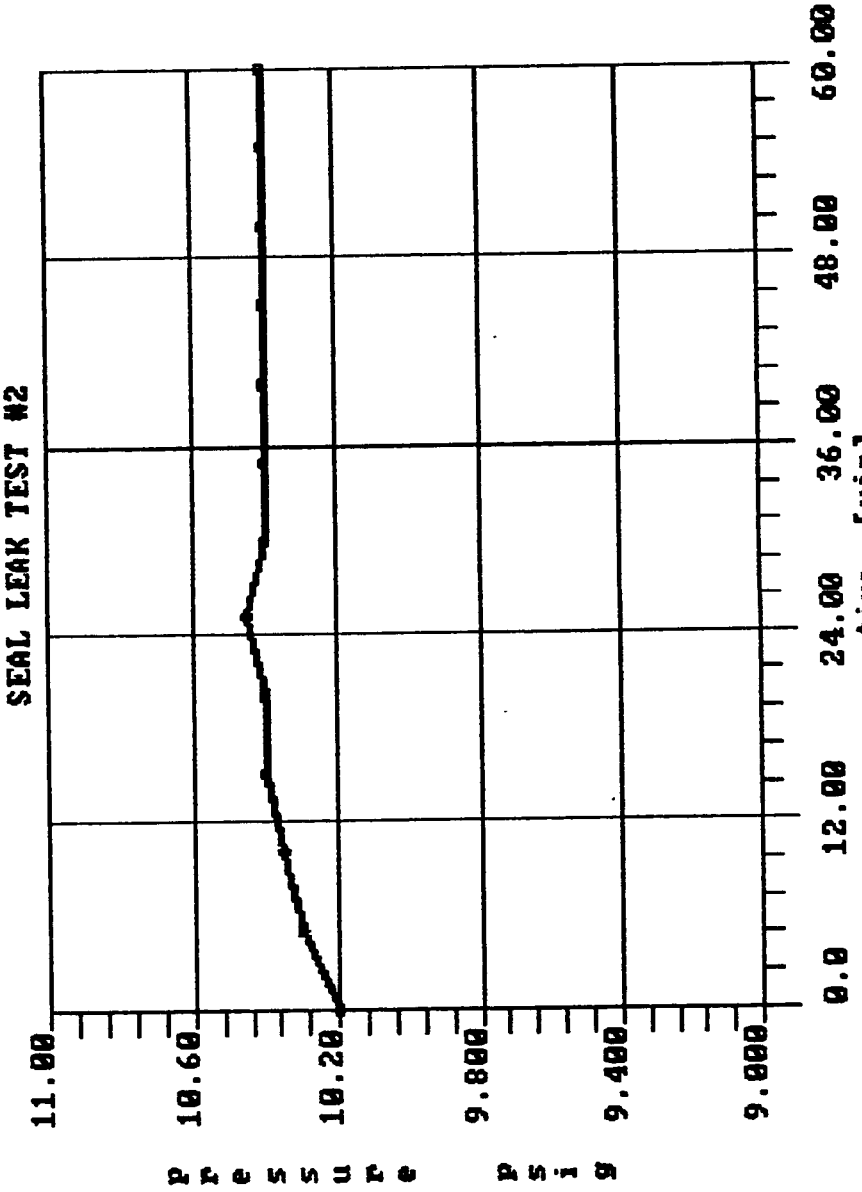
SEAL LEAK TEST #2
11.00
10.60
10.20
9.800
9.400
9.000
pressure psig
0.0
12.00
24.00
36.00
48.00
60.00
time [min]

FIGURE 2.6

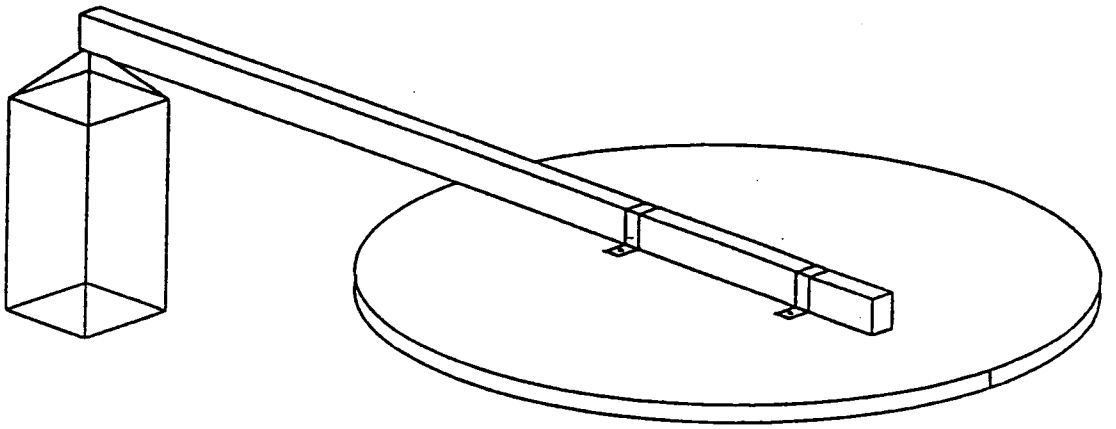

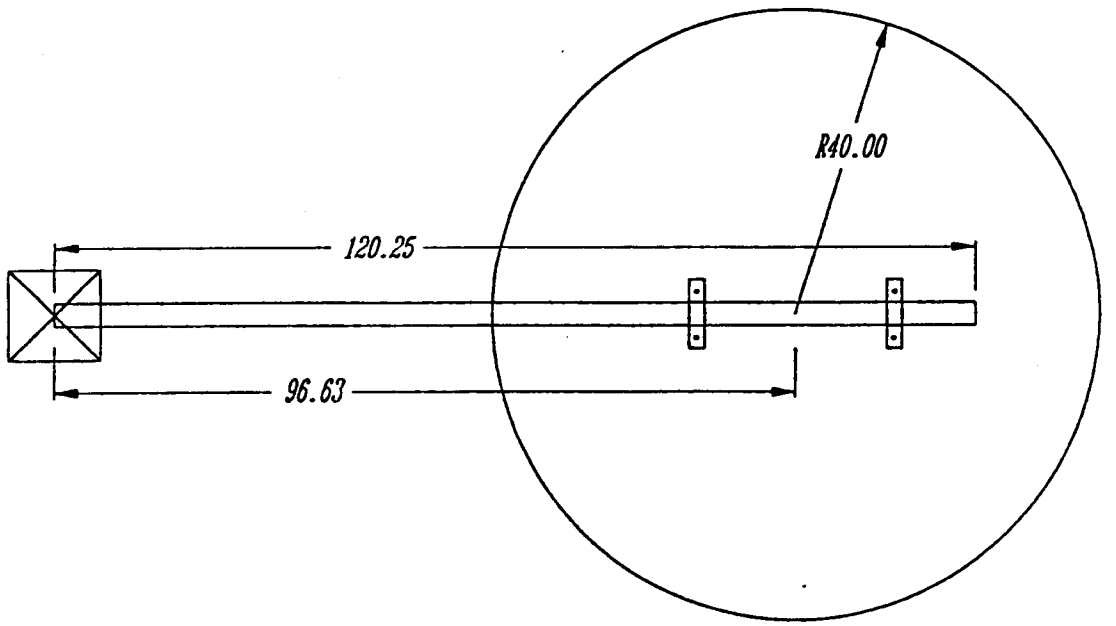

NOTE: THE 40.00 INCH RING RADIUS IS APPROXIMATE

FIGURE 2.7

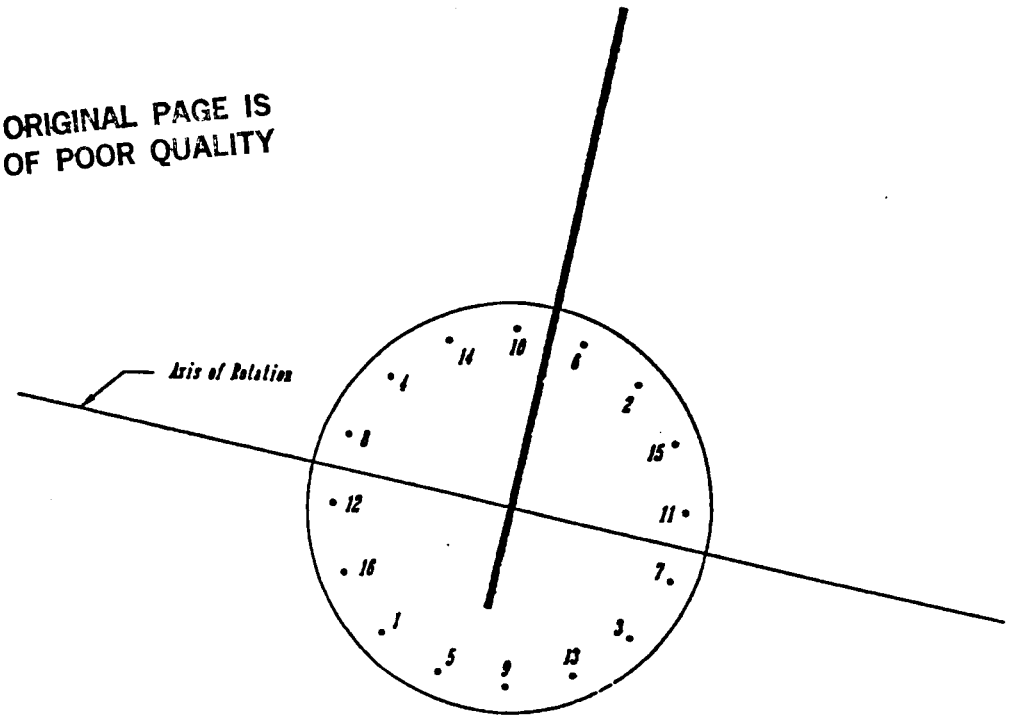

TEST 2 POSITION

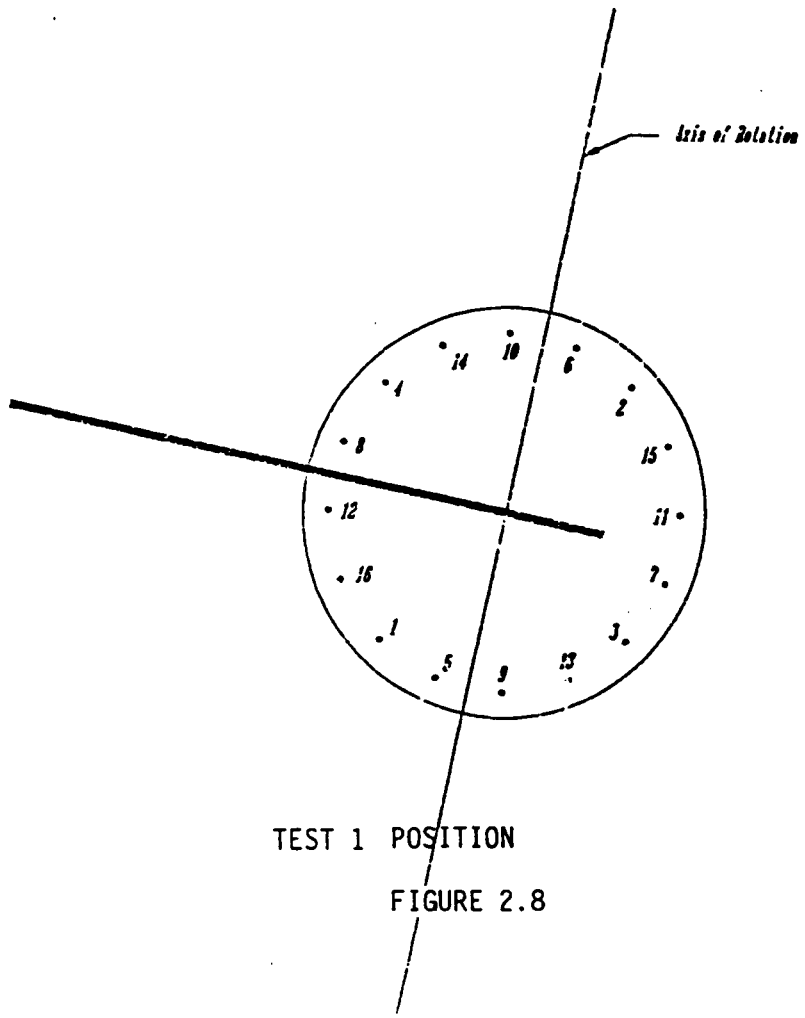

TEST 1 POSITION

FIGURE 2.8

TEST 1

	M (in-lb)	θ (deg)
1	3944	0.39
2	6529	0.48
3	10877	0.63
4	14162	0.71
5	17737	0.82
6	20732	0.91
7	23631	0.96
8	25757	1
9	28269	1.03
10	30685	1.07
11	27303	1.07
12	25854	1.07
13	23921	1.06
14	21022	1.03
15	18607	1
16	16191	0.94
17	13776	0.87
18	11360	0.77
19	8944	0.66
20	6529	0.58
21	4113	0.5
22	1697	0.42
23	-718	0.34
24	-3134	0.27
25	-5549	0.18
26	-7965	0.12
27	-10381	0.08
28	-12796	0.03
29	-15212	-0.01
30	-17628	-0.08
31	-20043	-0.12
32	-22459	-0.17
33	-19560	-0.18
34	-17628	-0.17
35	-15212	-0.15
36	-12796	-0.12
37	-10381	-0.08
38	-7965	0
39	-5549	0.06
40	-3134	0.15
41	-718	0.25
42	1697	0.32
43	4113	0.39
44	6529	0.48

TEST 2

	M (in-lb)	θ (deg)
1	3944	0.38
2	6529	0.39
3	10877	0.46
4	14452	0.53
5	17447	0.58
6	20732	0.65
7	23631	0.69
8	26047	0.75
9	28173	0.79
10	30685	0.84
11	27786	0.84
12	25854	0.84
13	23438	0.82
14	21022	0.79
15	18607	0.78
16	16191	0.75
17	13776	0.72
18	11360	0.7
19	8944	0.66
20	6529	0.62
21	4113	0.58
22	1697	0.47
23	-718	0.35
24	-3134	0.27
25	-5549	0.22
26	-7965	0.16
27	-10381	0.09
28	-12796	0.03
29	-15212	0
30	-17628	-0.06
31	-20043	-0.14
32	-22459	-0.21
33	-19560	-0.19
34	-17628	-0.17
35	-15212	-0.11
36	-12796	-0.06
37	-10381	0
38	-7965	0.05
39	-5549	0.1
40	-3617	0.16
41	-718	0.22
42	1697	0.28
43	4596	0.34
44	6529	0.38
45	8944	0.43
46	11360	0.47

TABLE 2.1

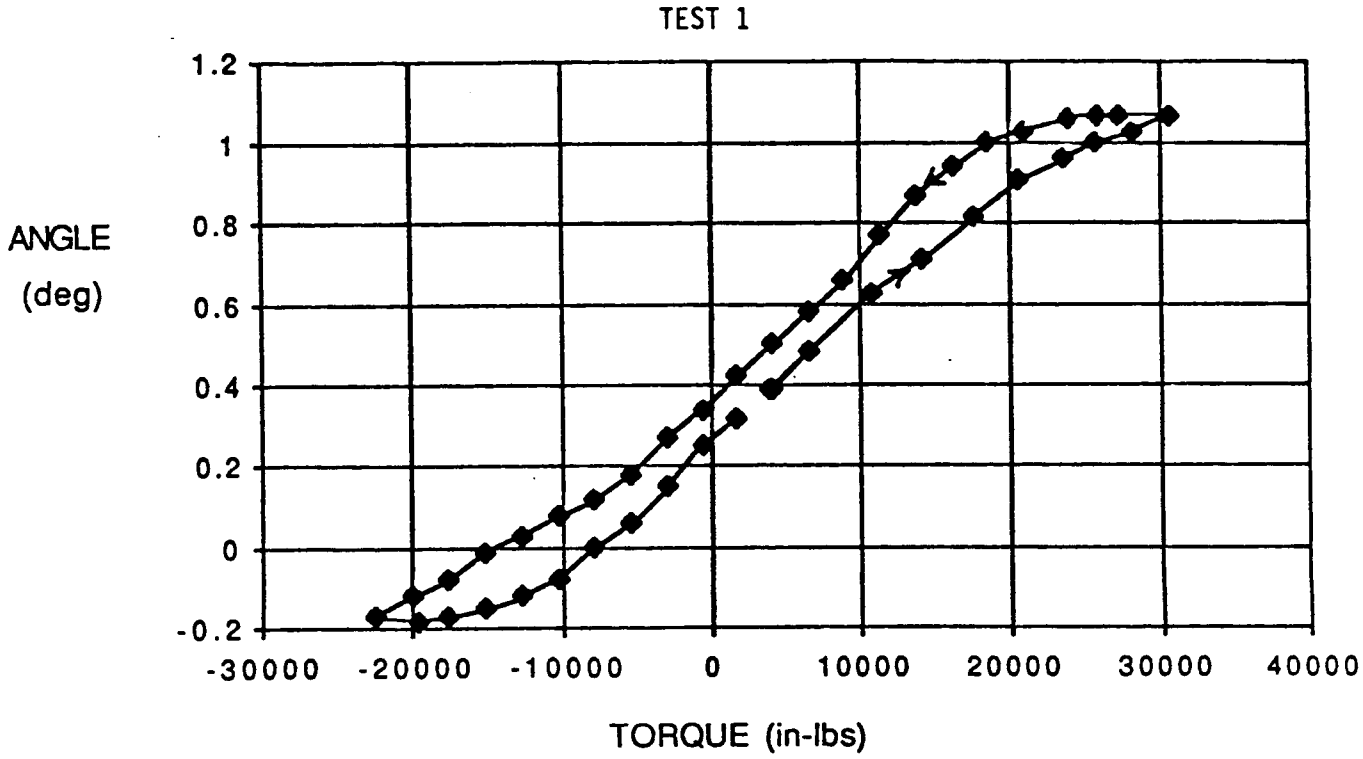

FIGURE 2.9a

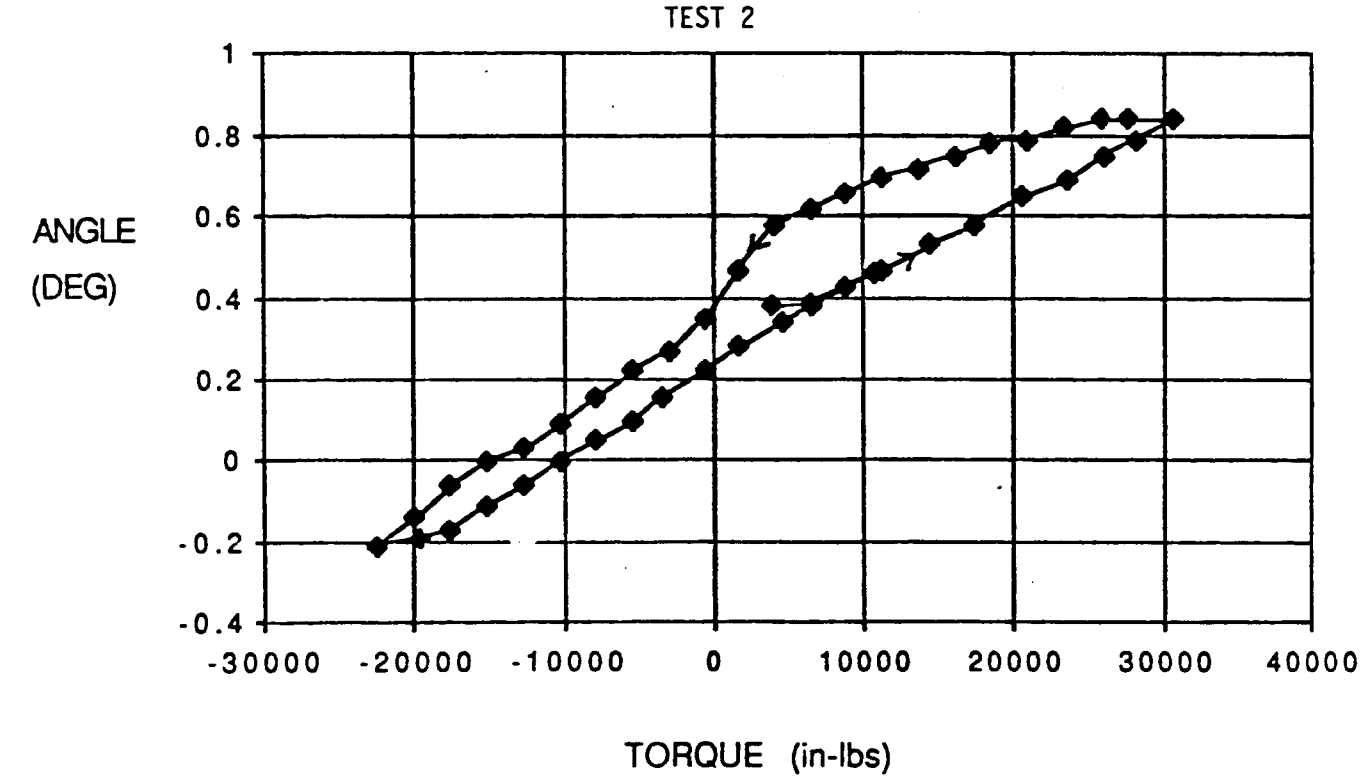

FIGURE 2.9b

lb/deg about the axis of rotation indicated in Figure 2.8. The spring rate measured in Test 2 is approximately 40,000 in-lb/deg about the appropriate axis of rotation. The differences in these two spring rate values may have been caused by several sources. Among these sources are:

1. Non-uniform cable pulley friction

2. Non-uniform bellows fold spacing

3. Non-uniform bellows ply thickness and separation

4. Inaccurate load cell measurements

The fact that load-deflection curves shown in Figure 2.9 are not centered about zero torque and zero angle is partially because of the initial torque and deflection imparted to the mechanism by the beam fixture and weight cage. It is also known that the base plate, which is attached to the bellows, does not sit perfectly level on top of the bellows. The reason that the bellows deflection test was not carried out to 2°, as stipulated in the procedure, was because the spacing between the bellows folds was reduced to zero before the 2° angular deflection was achieved. This is due in part to the fact that the moment applied to the base plate was generated by applying a compressive load through a 96 inch moment arm. The compressive load on the bellows clearly reduces the amount of "stroke" that the bellows can absorb from any other loading - namely the applied moment.

2.3 Mechanical Validation/Exercise

The mechanical validation tests performed at USBI basically consisted of exercising both the quick-acting capture latches and the long-reach capture latches. The major mechanical elements of the docking mechanism are the electromechanical actuators. These actuators were individually tested by MDAC at their Huntington Beach facility.

It was found during the initial operation of the long-reach capture latches that the latches could not open all the way because of contact with the center flange. A portion of the center flange material was removed from each latch, thus correcting the problem.

The quick-acting capture latches were found to be rather sensitive to the position of the adjustable cams which actuate the travel limit switches. When the cams are not positioned correctly, the latch tends to go into a limit cycle oscillation instead of closing down and securing the mechanism halves together. After the cams were adjusted, the quick-acting latches performed correctly through repeated cycles. Upon completing the test it was found that a bearing had failed on latch #4. As a result of this failure, a slight design modification was implemented in the latch.

3. Docking/Berthing Mechanism System Tests

The docking mechanism systems tests were performed at the NASA/MSFC 6-DOF Motion Simulation Facility. The system tests can be basically classified as preliminary functionality/troubleshooting tests and actual dynamic simulation tests. A basic layout of the test setup is shown in Figure 3.1.

The MSFC 6-DOF Motion Simulation Facility, hereafter to be termed simply the "6-DOF," is a relative motion simulation capable of handling test articles up to 20,000 lbs. Certainly the 1600 lb active docking mechanism presented no excess weight problem to the 6-DOF. Figure 3.2 shows the basic operating concepts of the 6-DOF. The data output from the 6-DOF for this test is in two forms. A strip-chart recorder located in the 6-DOF control room records the force and moment data coming from force/torque sensor mounted between the ceiling support structure and the bellows-half mechanism. Additionally, the relative kinematic variables as well as contact forces and torques are available as a time history for each dynamic run of the 6-DOF. An example of these plots can be found in Figures 3.8 through 3.25. Figure 3.3 defines the output variables with respect to the mechanism.

The "docking mechanism" is actually a system composed of the actual mechanical mechanism (rings, actuators, latches, etc.), the electronic equipment rack, and control computer. The system is schematically shown in Figure 3.4, while the equipment rack, control computer, and berthing mechanisms are seen in Figure 3.5. Data output from the docking mechanism was recorded on a strip chart recorder. The data recorded for each actuator includes the load cell value, motor torque, position, current, and commanded force. An example of this data is contained in Figure 3.32.

3.1 System Functionality Tests

After installation of the mechanism in the MSFC 6-DOF, a series of functionality tests were conducted. These tests included a check-out of the quick-acting capture latches and operation of the mechanism in the pre-capture, capture, and alignment modes.

3.1.1 Latch Test

A test of the quick-acting capture latches was performed to ensure that the entire latch system was functioning properly. The latch system is composed of the contact switches, the relays and associated electronics, and the latches themselves. The system was exercised at UTC during the post assembly tests. It was found that if the cam which engages the latch limit switches (see Figures 3.6 and 3.7) is not adjusted properly, the capture latch can get into a limit cycle type oscillation. Since the mechanism had been moved from UTC to MSFC, it was considered prudent to recheck the system.

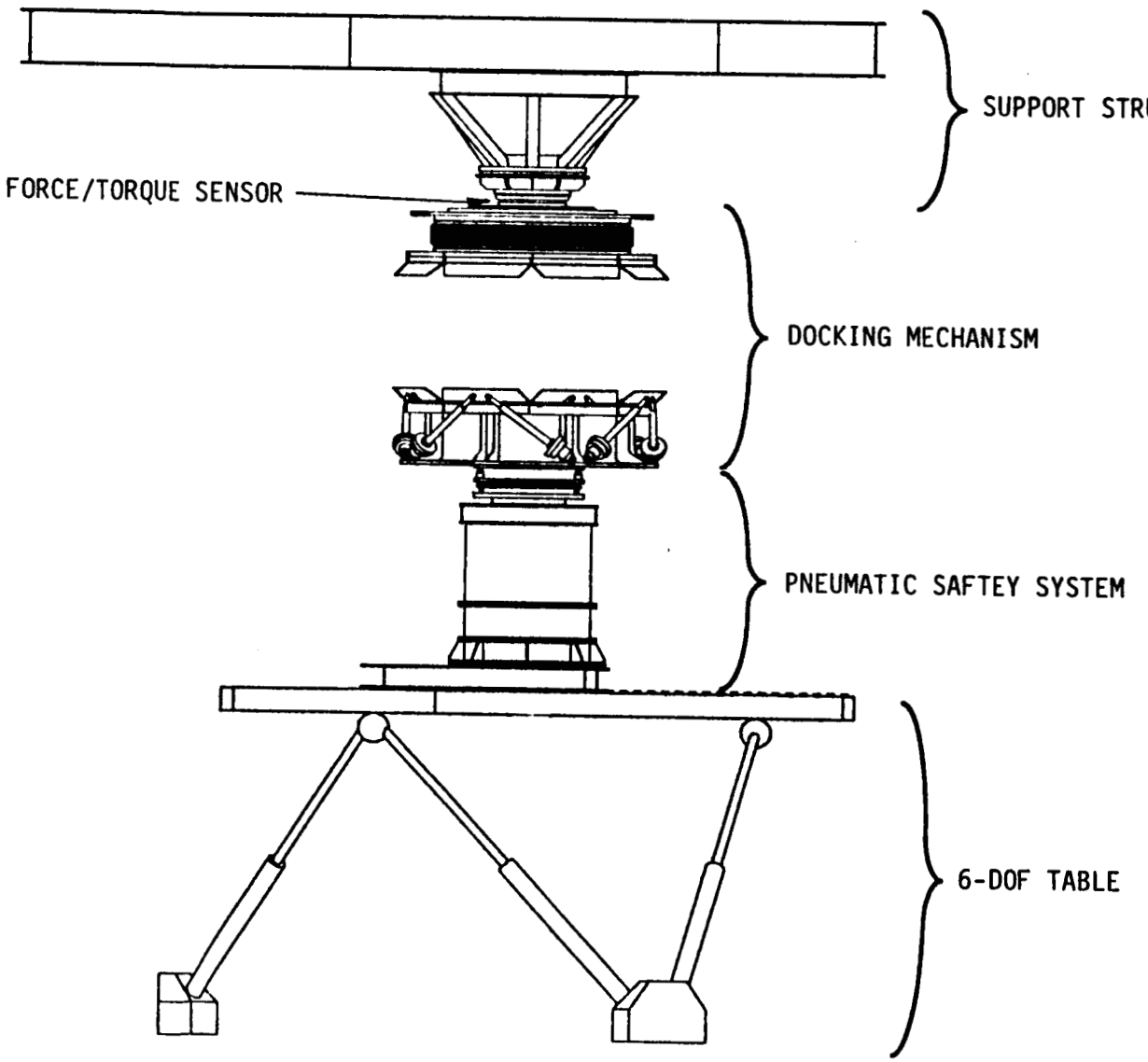

FIGURE 3.1

COURTESY MSFC/B. MITCHELL EP-65

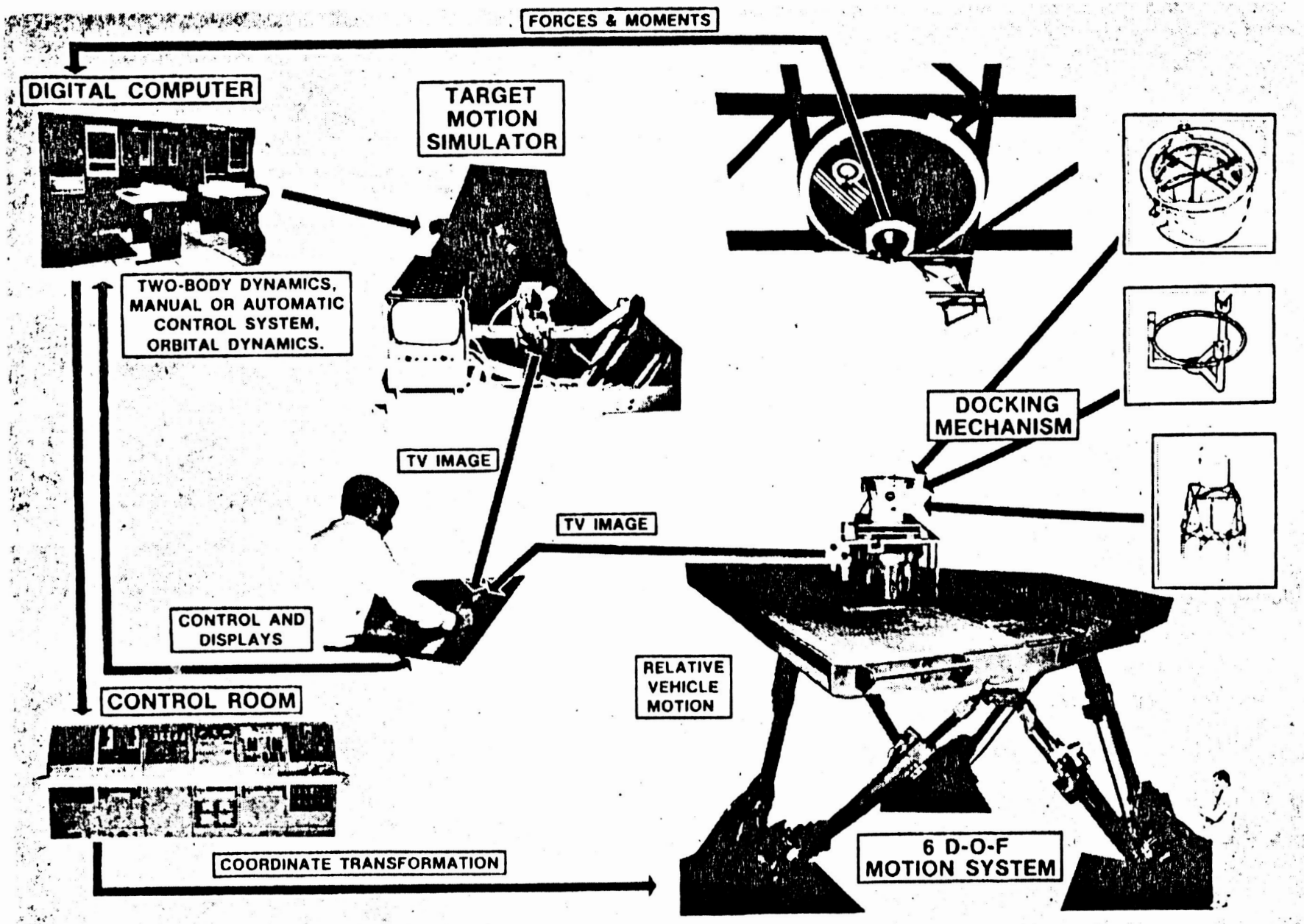

DOCKING MECHANISM DEVELOPMENT

FIGURE 3.2

(Courtesy MSFC/EB-44)

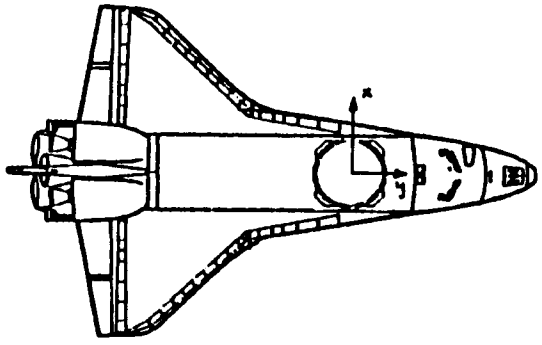

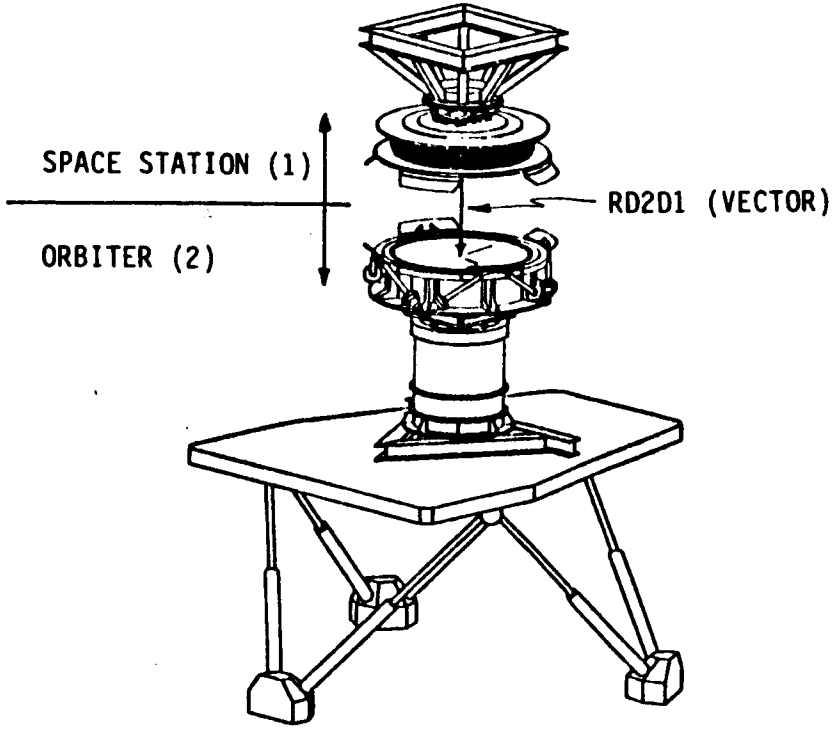

D1 FRAME ATTACHED TO UPPER MECHANISM HALF, ORIGIN COINCIDENT WITH RING CENTER

D2 FRAME ATTACHED TO LOWER MECHANISM HALF, ORIGIN COINCIDENT WITH RING CENTER WHEN FULLY RETRACTED

6-DOF OUTPUT VARIABLES

RD2D1D1(X,Y,Z)	-	VECTOR COMPONENTS (X,Y,Z) OF THE VECTOR FROM D1 TO D2, EXPRESSED IN THE D1 FRAME
RD2D1D1(X,Y,Z)	-	TIME DERIVATIVE OF ABOVE VECTOR
OMV2V1D1(X,Y,Z)	-	RELATIVE ANGULAR RATE OF V2 (ORBITER) W.R.T. V1 (STATION), EXPRESSED IN D1 FRAME
F1CD1(X,Y,Z)	-	FORCE MEASURED BY SENSOR, EXPRESSED IN D1 FRAME
T1CD1(X,Y,Z)	-	TORQUE MEASURED BY SENSOR, EXPRESSED IN D1 FRAME
THETA(X,Y,Z)	-	1-2-3 EULER ANGLES, D2 WRT TO D1

FIGURE 3.3

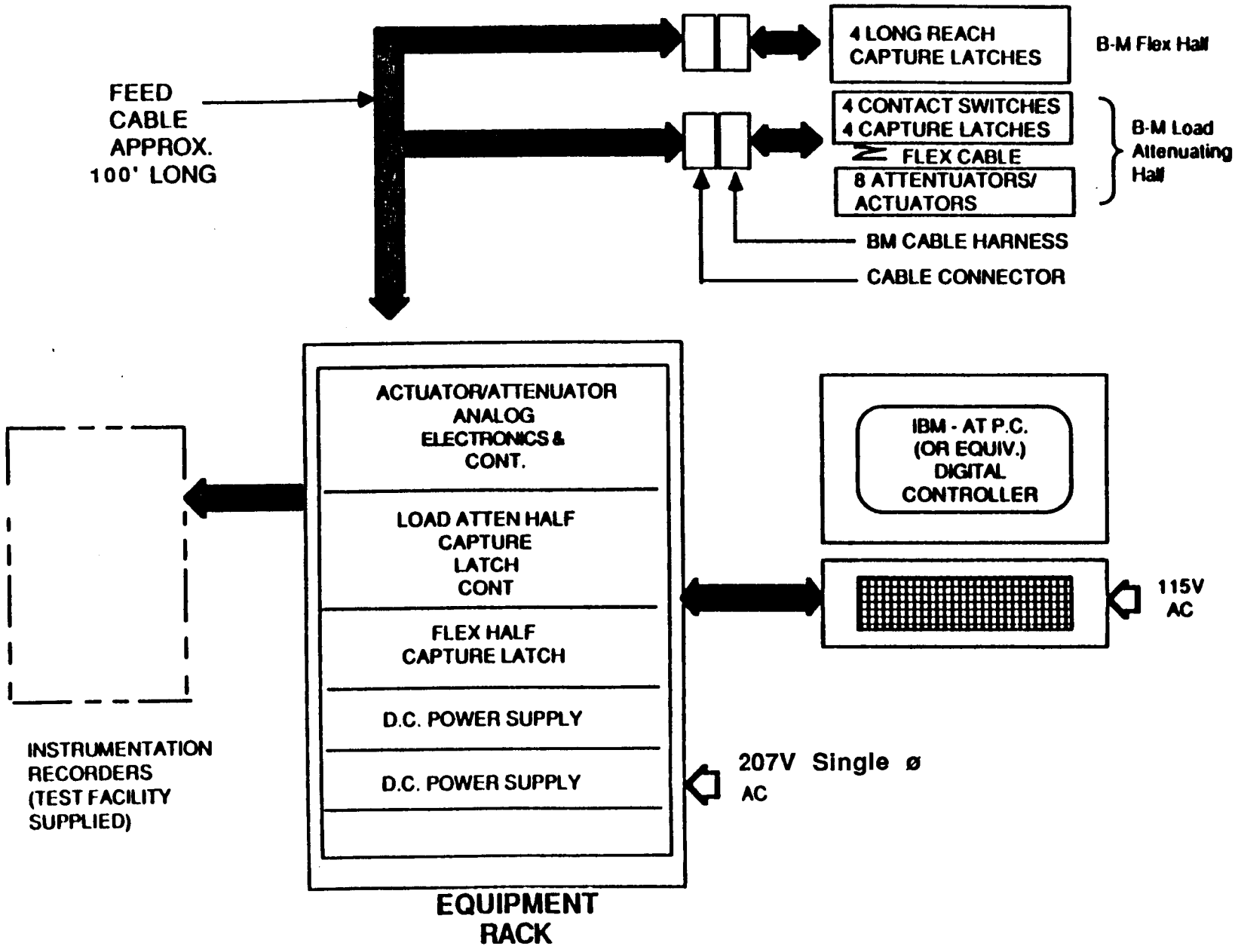
FEED CABLE APPROX. 100' LONG
4 LONG REACH CAPTURE LATCHES
B-M Flex Half
4 CONTACT SWITCHES
4 CAPTURE LATCHES
FLEX CABLE
8 ATTENTUATORS/ ACTUATORS
B-M Load Attenuating Half
BM CABLE HARNESS
CABLE CONNECTOR
ACTUATOR/ATTENUATOR ANALOG ELECTRONICS & CONT.
LOAD ATTEN HALF CAPTURE LATCH CONT
FLEX HALF CAPTURE LATCH
D.C. POWER SUPPLY
D.C. POWER SUPPLY
IBM - AT P.C. (OR EQUIV.) DIGITAL CONTROLLER
115V AC
207V Single ø AC
INSTRUMENTATION RECORDERS (TEST FACILITY SUPPLIED)
EQUIPMENT RACK

FIGURE 3.4

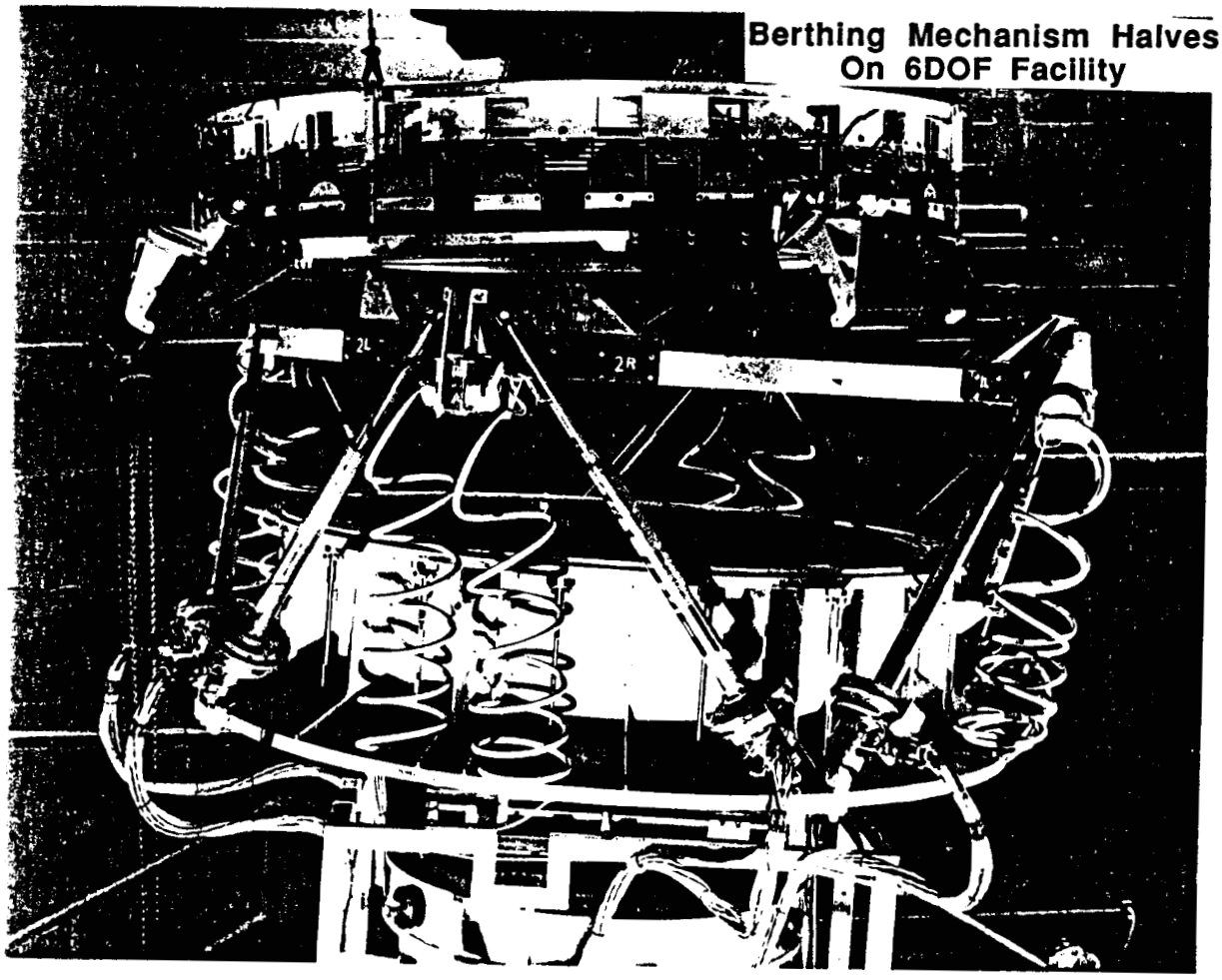

Berthing Mechanism Halves
On 6DOF Facility

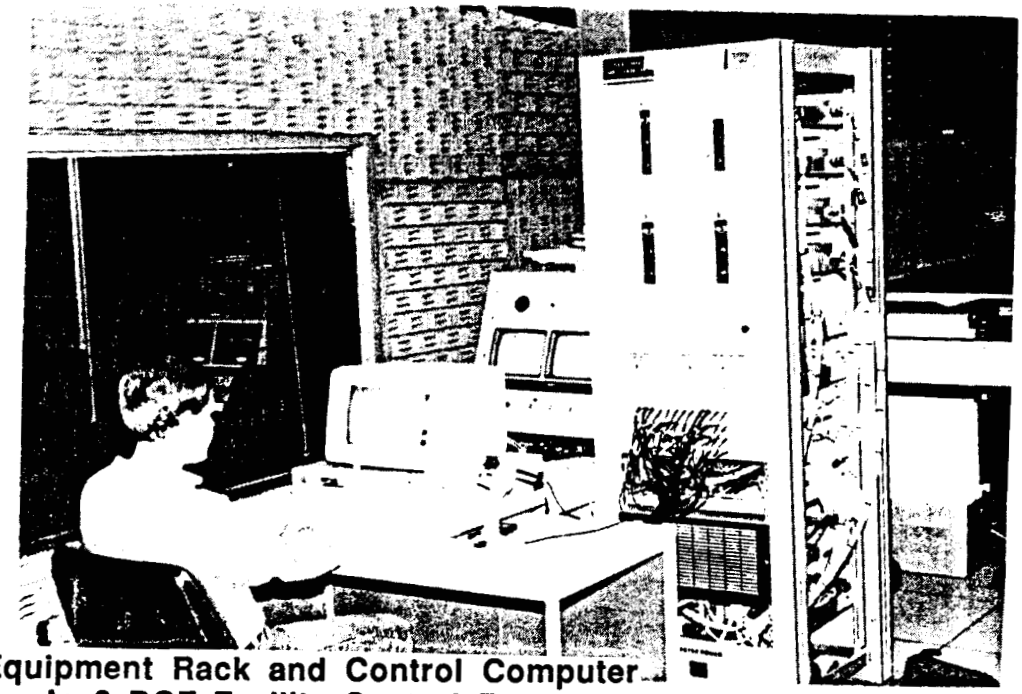

Equipment Rack and Control Computer
In 6 DOF Facility Control Room

Figure 3.5

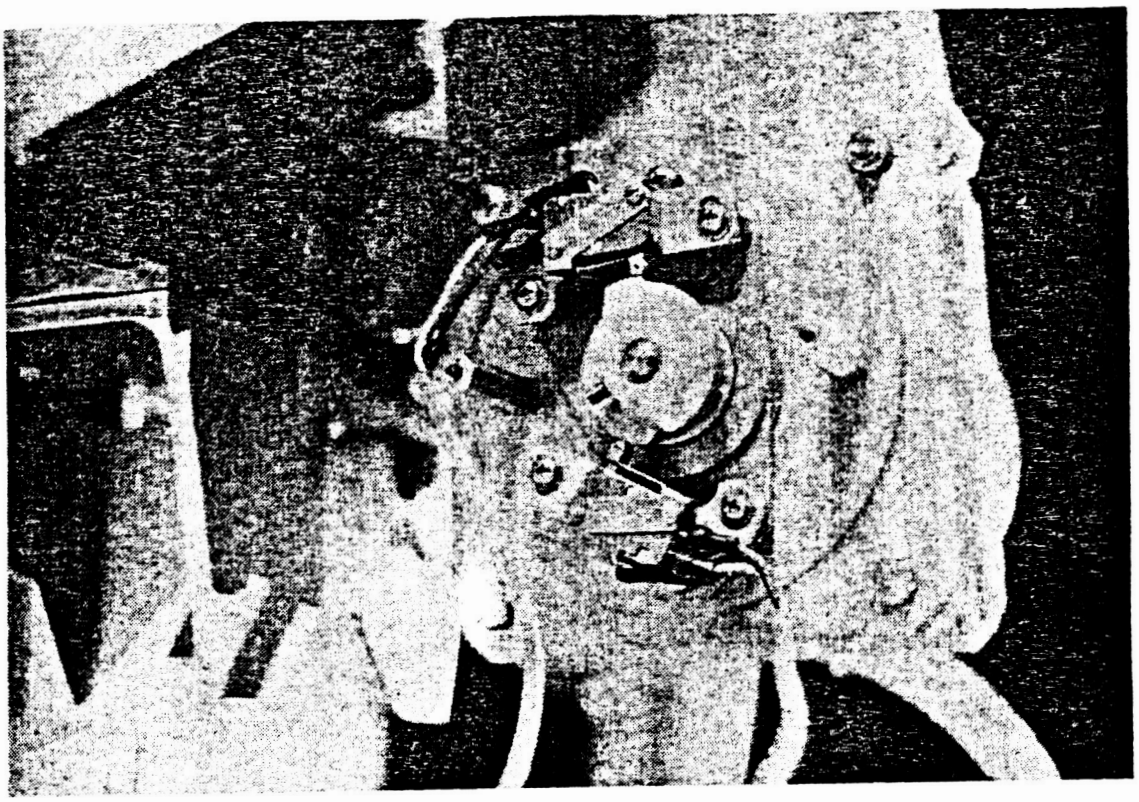

FIGURE 3.6 LATCH IN CLOSED POSITION

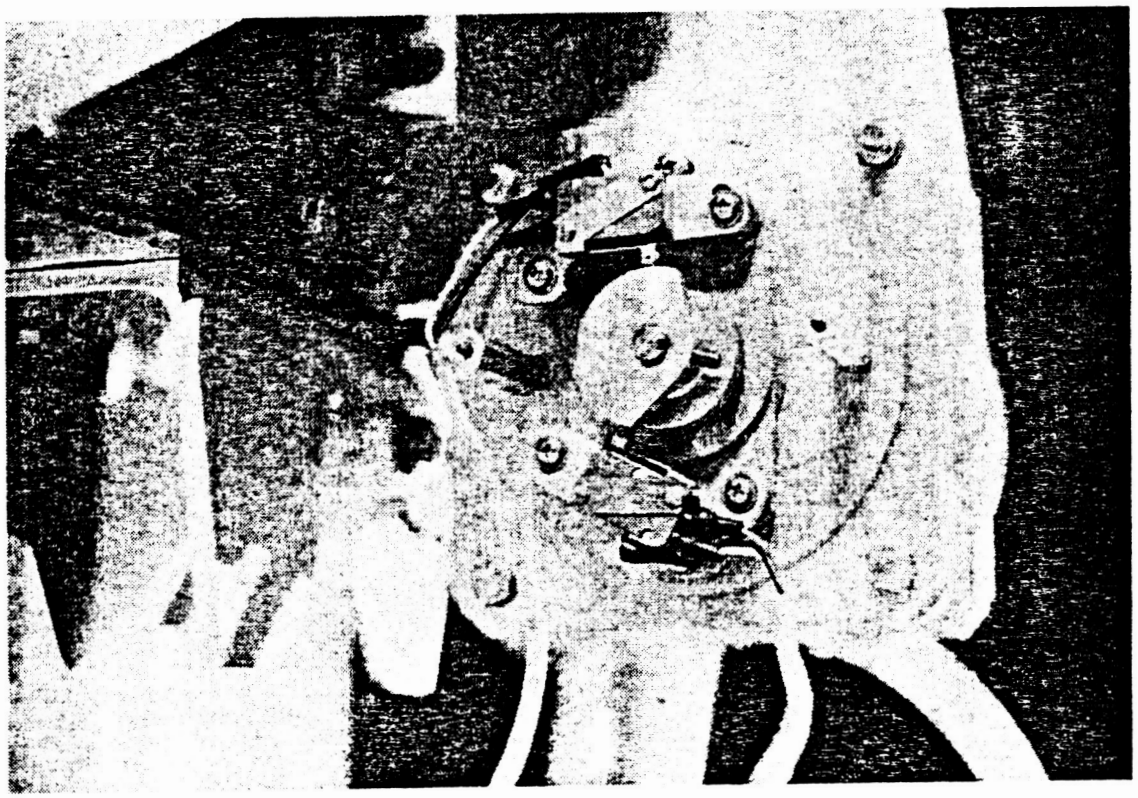

FIGURE 3.7 LATCH IN OPEN POSITION

The test was performed by lowering the upper half of the mechanism (bellows half) using the cable support system down onto the stationary active half. The power up sequence of the control console is contained in the Appendix. The latches were thrown and then retracted several times with no problem. Based on this evidence, the latches were considered to be performing properly and were not adjusted.

However, it was later found that latches did indeed need adjustments because several of them began to oscillate, or chatter, during a validation test of the alignment mode. Figures 3.6 and 3.7 show how the cams should be adjusted at the latch closed position and latch open position, respectively. It was also noted that the latches, which are bolted to the side of the ring have a tendency to be pulled upward a small amount during the high-gain modes of operation. The fact that the latch assembly translates up tends to increase any gap that may exist between the rings, thus introducing some slop between the two latched rings.

3.1.2 Pre-Capture Mode Response Test

The purpose of the pre-capture mode test was to verify that the ring did in fact extend and retract on command from the control computer. The load cells and position pots, which produce the feedback signals for each actuator, had previously been calibrated and were therefore not calibrated at MSFC. However, the zero point was verified.

Initially, the load cell output was zeroed at the full retraction position with the actuators connected to the ring. Upon commanding the ring to an arbitrary extension (less than 18.5") it was seen that the ring moved very roughly. The load cells were re-zeroed at full-extension, and movement of the ring was much smoother. At this point the main power supply failed. It is not certain at this time what caused the failure, but there is the possibility that the power supply could not operate for an extended period of time at the required output voltage of 40V. NASA supplied a spare power supply which operated without any problems for the remainder of the test. When power is cut to the actuators, they can be easily back-driven. If the ring is extended when power is cut, the ring falls with considerable impact to the retracted position. In order to lessen the impact, two 2 x 4 wood boards were placed under the ring in such a way as to avoid interference with the normal operation of the mechanism.

It was the opinion of the MDAC controls engineer that the load cells be zeroed while unconnected to the ring and held in a vertical direction (essentially the load cell would see the actuator weight in that condition). After adjusting the force biases for each actuator, the pre-capture mode was considered to be functioning properly.

3.1.3 Capture Mode Response Test

The purpose of the capture mode test was to approximately verify the 10 lb/in nominal axial spring rate of the active mechanism. Each actuator had a nominal 0.5 lb/in gain (in addition to the 10 lb/in overall axial gain).

It was found if the mechanism was operated with the nominal capture gains, it tended to drift after several seconds. After several iterations it was decided to proceed with a per actuator gain of 7.5 lb/in and an axial gain of 20 lb/in. However, when first attempting to capture dynamically it was recognized that the capture mode gains were too high. Compromising between ring drift and capture capability eventually resulted in using an axial gain of 20 lb/in and a per actuator gain 3.25 lb/in.

3.1.4 Mate and Latch Test

The goal of the mate and latch test was to test the high gain control modes of the mechanism in a somewhat "controlled environment." The 6-DOF is capable of moving to any location within its envelope under manual control, hold this position for any desired time (theoretically) and then "go dynamic." The phrase "go dynamic" indicates that the 6-DOF is under computer control, wherein the computer issues position commands to the 6-DOF based on rigid body dynamic models of the Space Station and the Orbiter. The mass properties used are shown below (expressed in standard orbiter coordinate frame).

Station

Mass = 20945.0 slugs
I_{xx} = 0.1703E9 sl-ft^2; I_{yy} = 0.6928E8 sl-ft^2; I_{zz} = 0.2192E9 sl-ft^2
$I_{xy} = I_{yz} = I_{xz} = 0$
X_{port} = 1.4 ft; Y_{port} = -3.3 ft; Z_{port} = 61.9 ft; (station c.g. to port)

Orbiter

Mass = 7813.0 slugs
I_{xx} = 0.7255E7 sl-ft^2; I_{yy} = 0.9730E6 sl-ft^2; I_{zz} = 0.7541E7 sl-ft^2
$I_{xy} = I_{yz} = I_{xz} = 0$
X_{port} = 0 ft; Y_{port} = 39.0 ft; Z_{port} = -12.6 ft; (orbiter c.g. to port)

For the initial mate and latch tests, the 6-DOF was commanded to a position directly below the upper half mechanism. The separation distance between the two docking rings was such that the active ring could be commanded up (using pre-capture mode) and mate with the upper ring. The

latches are thrown automatically when the 4 contact switches are depressed, therefore capture was actually made while the control computer was in the pre-capture mode. The 6-DOF was then taken into "dynamic mode" with zero velocity initial conditions. Several seconds after entering the high gain attenuation mode the mechanism went unstable, with oscillations at approximately 2 Hz, and was shut down. Contributing factors to this instability will be discussed in the Results and Assessments section. After investigation, it was found that decreasing the nominal lateral translation attenuation gains by a factor of 10 (both rate and position) and adding the force bias command to the force loop produced a stable system in attenuation mode. The initial values of all the control system gains are contained in Ref. 2.

Although it had been found that reducing the transverse translation attenuation gains by a factor of 10 stabilized the system, it was desirable to keep the gain as high as possible for increased performance. By changing the second order filter used in the compensation scheme to have a damping ratio of .6, and reducing the nominal transverse translational gains by a factor of 1/3 (instead of 1/10th) the system was felt to be reasonably well tuned, considering the compromises between stability and performance.

In a nominal run, the system stays in attenuation mode for 180 seconds and then prompts the user to go into the alignment mode. The gains used in alignment are identical to the gains used in the attenuation mode. Upon entering the alignment mode for the first time, the control computer commanded the actuators to exert a very large force (> 2000 lbs) on the upper half and thereby causing the 6-DOF safety software to terminate the test. It was clear that there was some type of transition problem when going from the attenuation mode to the alignment mode. After an examination of the transition software, it was discovered that the call to the initialization routine was not sequenced properly. Modifying the software successfully removed the initial alignment mode transition problem.

It should be noted that after the transition problem from attenuation mode to alignment mode had been solved, there still existed an anomaly with the alignment mode. It was found that when the ring was commanded to retract, for example, the initial response of the actuators was to extend a small amount (approximately 1 in). The actuators would then begin to retract as commanded. This behavior was believed to be caused by the fact that the force biases should actually be programmed as a function of actuator length. The MDAC engineers implemented a change to the software which modified the previously constant force biases to be functions of length. This appeared to fix the alignment mode anomaly for the cases when the ring was centered (i.e., all actuator lengths approximately the same). However, for the cases when the ring was off center, the problem of moving the wrong way momentarily still existed. Post test analysis has shown that the problem could be solved with a more sophisticated algorithm for computing the force bias in each actuator which took into account the angular misalignments, and therefore the changing direction of the weight vector. In order to implement the more computationally intensive force bias

algorithm, it was felt that more computing power than is available with the existing control computer would be necessary. Thus it was decided to let this centering behavior be a "lesson learned," and to move forward with the testing.

3.2 Dynamic 6-DOF Tests

The dynamic 6-DOF tests were the culmination of all the previous functionality tests performed at MDAC-HB, UTC, and at MSFC. By making use of the MSFC 6-DOF, it was possible to simulate the dynamics of the interacting Space Station and Orbiter. The dynamic 6-DOF tests would be used to establish the validity of the design - both hardware and software (control algorithms). Table 3.1 contains the initial conditions at an axial separation of 12 in. that were run. Table 3.2 contains the maximum modulus values of force and torque applied to the 6-DOF sensor package (i.e., space station) during capture and attenuation. As can be seen, some 88 cases were attempted, and for each a brief annotation will be given in this section.

For all the cases attempted, the ring was initially extended to 14.25 in (leg length). After several cases it was found that it was necessary to reduce the per actuator stiffness in the capture mode from 7.5 lb/in to 3.25 lb/in to increase capture capability.

A brief log of each run will now be presented, with a more detailed discussion of several runs to be presented afterwards. Additionally, the data set for each run can be found in the data volume of this report.

Case 1 - Nominal capture, in atten. mode some jitter was observed. Slight amount of misalignment was noted on contact.

Case 2 - Nominal capture - alignment to 14.25". Max. leg extension = 16.75 in.

Case 3 - Nominal capture - align. Relay chatter noted from latches. The 6-DOF F/T sensor deadband was set at approx. 5lb in transverse translation.

Case 4 - Nominal capture - align.

Berthing Mechanism Test Initial Conditions

Case	cap.	no cap.	z-rate (ft/sec)	z-separ (inches)	x-rate (ft/sec)	y-rate (ft/sec)	x misali (inches)	y misali (inches)	x-rate (deg/sec)	y rate (deg/sec	z rate (deg/sec	x misali (degrees	y misali (degrees	z misali (degrees)
1	✔		0.05	12.0	0	0	0	0	0	0	0	0	0	0
2	✔		0.10	12.0	0	0	0	0	0	0	0	0	0	0
3	✔		0.15	12.0	0	0	0	0	0	0	0	0	0	0
4	✔		0.20	12.0	0	0	0	0	0	0	0	0	0	0
5	✔		0.05	12.0	0	0	0	2.0	0	0	0	0	0	0
6	✔		0.05	12.0	0	0	0	3.0	0	0	0	0	0	0
7		✔	0.05	12.0	0	0	0	4.0	0	0	0	0	0	0
7A	✔		0.10	12.0	0	0	0	4.0	0	0	0	0	0	0
8		✔	0.05	12.0	0	0	0	4.5	0	0	0	0	0	0
8A	✔		0.10	12.0	0	0	0	4.5	0	0	0	0	0	0
9		✔	0.05	12.0	0	0	0	-4.5	0	0	0	0	0	0
9A	✔		0.10	12.0	0	0	0	-4.5	0	0	0	0	0	0
10		✔	0.05	12.0	0	0	4.5	0	0	0	0	0	0	0
10A	✔		0.10	12.0	0	0	4.5	0	0	0	0	0	0	0
11		✔	0.05	12.0	0	0	-4.5	0	0	0	0	0	0	0
11A	✔		0.10	12.0	0	0	-4.5	0	0	0	0	0	0	0
12	✔		0.20	12.0	0	0	0	4.5	0	0	0	0	0	0
13	✔		0.20	12.0	0	0	0	-4.5	0	0	0	0	0	0
14	✔		0.20	12.0	0	0	4.5	0	0	0	0	0	0	0
15	✔		0.20	12.0	0	0	-4.5	0	0	0	0	0	0	0
16		✔	0.05	12.0	0	0	0	0	0	0	0	2.0	0	0
16A	✔		0.10	12.0	0	0	0	0	0	0	0	2.0	0	0
17A	✔		0.10	12.0	0	0	0	0	0	0	0	3.0	0	0
18A		✔	0.10	12.0	0	0	0	0	0	0	0	4.0	0	0
18B	✔		0.15	12.0	0	0	0	0	0	0	0	4.0	0	0
19B	✔		0.15	12.0	0	0	0	0	0	0	0	4.5	0	0
20		✔	0.05	12.0	0	0	0	0	0	0	0	-4.5	0	0
20A		✔	0.10	12.0	0	0	0	0	0	0	0	-4.5	0	0
20B	✔		0.15	12.0	0	0	0	0	0	0	0	-4.5	0	0
21		✔	0.05	12.0	0	0	0	0	0	0	0	0	4.5	0
21A	✔		0.10	12.0	0	0	0	0	0	0	0	0	4.5	0
22		✔	0.05	12.0	0	0	0	0	0	0	0	0	-4.5	0
22A		✔	0.10	12.0	0	0	0	0	0	0	0	0	-4.5	0
22B	✔		0.15	12.0	0	0	0	0	0	0	0	0	-4.5	0
23	✔		0.20	12.0	0	0	0	0	0	0	0	4.5	0	0

TABLE 3.1

Berthing Mechanism Test Initial Conditions

Case	cap	no cap	z-rate (ft/sec)	z-separ (inches)	x-rate (ft/sec)	y-rate (ft/sec)	x misali (inches)	y misali (inches)	x-rate (deg/sec)	y rate (deg/sec)	z rate (deg/sec)	x misali (degrees)	y misali (degrees)	z misali (degrees)
24	✔		0.20	12.0	0	0	0	0	0	0	0	-4.5	0	0
25	✔		0.20	12.0	0	0	0	0	0	0	0	0	4.5	0
26	✔		0.20	12.0	0	0	0	0	0	0	0	0	-4.5	0
27		✔	0.05	12.0	0	0	0	0	0	0	0	0	0	2.0
27a	✔		0.10	12.0	0	0	0	0	0	0	0	0	0	2.0
28a		✔	0.10	12.0	0	0	0	0	0	0	0	0	0	3.0
28b	✔		0.15	12.0	0	0	0	0	0	0	0	0	0	3.0
29AX	✔		0.15	12.0	0	0	0	0	0	0	0	0	0	-1.22
29b	✔		0.15	12.0	0	0	0	0	0	0	0	0	0	-3.0
30	✔		0.20	12.0	0	0	0	0	0	0	0	0	0	3.0
31	✔		0.20	12.0	0	0	0	0	0	0	0	0	0	-3.0
32		✔	0.05	12.0	0	0	0	3.0	0	0	0	4.5	0	0
32A		✔	0.10	12.0	0	0	0	3.0	0	0	0	4.5	0	0
32B	✔		0.15	12.0	0	0	0	3.0	0	0	0	4.5	0	0
33	✔		0.20	12.0	0	0	0	3.0	0	0	0	4.5	0	0
34		✔	0.05	12.0	0	0	0	4.5	0	0	0	0	0	3.0
34a	✔		0.20	12.0	0	0	0	4.5	0	0	0	0	0	3.0
35	✔		0.20	12.0	0	0	0	4.5	0	0	0	0	0	3.0
36		✔	0.05	12.0	0	0	0	0	0	0	0	4.5	0	3.0
37	✔		0.20	12.0	0	0	0	0	0	0	0	4.5	0	3.0
38		✔	0.05	12.0	0	0	0	3.0	0	0	0	4.5	0	3.0
38A		✔	0.10	12.0	0	0	0	3.0	0	0	0	4.5	0	3.0
38B	✔		0.15	12.0	0	0	0	3.0	0	0	0	4.5	0	3.0
39		✔	0.05	12.0	0	0	0	-4.5	0	0	0	-4.5	0	-3.0
39a	✔		0.10	12.0	0	0	0	-4.5	0	0	0	-4.5	0	-3.0
40	✔		0.20	12.0	0	0	0	3.0	0	0	0	4.5	0	3.0
41	✔		0.20	12.0	0	0	0	-4.5	0	0	0	-4.5	0	-3.0
42		✔	0.05	12.0	0	0	-4.5	0	0	0	0	0	4.5	3.0
42a	✔		0.10	12.0	0	0	-4.5	0	0	0	0	0	4.5	3.0
43		✔	0.05	12.0	0	0	4.5	0	0	0	0	0	-4.5	-3.0
43a	✔		0.10	12.0	0	0	4.5	0	0	0	0	0	-4.5	-3.0
44	✔		0.20	12.0	0	0	-4.5	0	0	0	0	0	4.5	3.0
45	✔		0.20	12.0	0	0	4.5	0	0	0	0	0	-4.5	-3.0
46	✔		0.20	12.0	0	0.06	0	-4.5	0.15	0	0.05	-1.0	0	-0.3
47	✔		0.20	12.O	0	-0.06	0	4.5	-0.15	0	-0.05	1.0	0	0.3

TABLE 3.1 cont.

Berthing Mechanism Test Initial Conditions

Case	cap.	no cap.	z-rate (ft/sec)	z-separ (inches)	x-rate (ft/sec)	y-rate (ft/sec)	x misali (inches)	y misali (inches)	x-rate (deg/sec)	y rate (deg/sec	z rate (deg/sec	x misali (degrees	y misali (degrees	z misali (degrees)
48	✔		0.20	12.0	0.06	0	-4.5	0	0	0.15	0.05	0	-1.0	-0.3
49	✔		0.20	12.0	-0.06	0	4.5	0	0	-0.15	-0.05	0	1.0	0.3
50	✔		0.20	12.0	0	0.06	0	-0.25	0	0	0	0	0	0
50a	✔		0.20	12.0	0	0.06	0	-2.25	0	0	0	0	0	0
51	✔		0.20	12.0	0	-0.06	0	0.25	0	0	0	0	0	0
52	✔		0.20	12.0	0.06	0	-0.25	0	0	0	0	0	0	0
53	✔		0.20	12.0	-0.06	0	0.25	0	0	0	0	0	0	0
54	✔		0.20	12.0	0	0	0	0	0.15	0	0	3.5	0	0
55	✔		0.20	12.0	0	0	0	0	-0.15	0	0	-3.5	0	0
56	✔		0.20	12.0	0	0	0	0	0	0.15	0	0	3.5	0
57	✔		0.20	12.0	0	0	0	0	0	-0.15	0	0	-3.5	0
58	✔		0.20	12.0	0	0	0	0	0	0	0.05	0	0	2.6
59	✔		0.20	12.0	0	0	0	0	0	0	-0.05	0	0	-2.6
60	✔		0.20	12.0	0	0.06	0	-0.25	0.15	0	0	3.5	0	0
61	✔		0.20	12.0	0	0.06	0	-0.25	0	0	0.05	0	0	2.6
62	✔		0.20	12.0	0	0	0	0	0.15	0	0.05	3.5	0	2.6
63	✔		0.20	12.0	0	0.06	0	-0.25	0.15	0	0.05	3.5	0	2.6
64	✔		0.20	12.0	-0.04	0.04	0	0	0.10	0.10	0.005	2.5	2.5	2.6

TABLE 3.1 cont.

MAXIMUM FORCES/TORQUES

Case	max force	max force	max force	max torq.	max torq.	max torq.
	X	Y	Z	X	Y	Z
1	63	46.5	-125	800	475	230
2	39	41	-310	1300	-510	-300
3	80	-100	-320	1900	-490	-375
4	90	75	-450	2500	600	450
5	80	75	160	750	-800	300
6	125	80	240	1800	700	-410
7	-18	-18	-36	-148	75	-120
7A	120	130	225	1400	-1600	-750
8	19	18	-35	-200	-120	-75
8A	250	160	280	1300	800	430
9	8	-22	-76	-240	43	75
9A	80	60	-150	1400	-420	330
10	-42	27	-42	160	75	-140
10A	-120	75	-170	1250	450	390
11	35	-16	-36	80	-110	-240
11A	130	-60	-220	1400	650	-390
12	-160	-190	-390	2500	600	-650
13	80	125	-225	2400	600	380
14	120	160	260	2400	750	450
15	-140	110	-220	2500	490	480
16	24	35	-44	80	-140	80
16A	80	-49	-190	1250	380	-300
17A	80	70	180	1400	370	300
18A	18	380	-80	125	-170	-125
18B	75	180	-130	1600	-490	-410
19B	-75	-60	-120	1700	380	600
20	4.9	-34	-49	-80	-22	-35
20A	18	-49	-52.5	-140	-44	-180
20B	180	120	275	-2200	-700	-700
21	80	38	-55	-180	380	63
21A	250	-240	-300	1500	700	1200
22	-140	49	-50	60	-250	220
22A	35	38	-90	-75	-390	-90
22B	90	-140	180	1750	-800	550
23	70	60	210	2400	-1800	490

TABLE 3.2

MAXIMUM FORCES/TORQUES

Case	max force X	max force Y	max force Z	max torq. X	max torq. Y	max torq. Z
24	160	80	-270	1750	700	-530
25	-160	-130	225	2500	800	-390
26	-120	150	-380	2400	-800	-550
27	-23	-13	-58	-150	80	150
27A	-70	55	-110	1250	-400	750
28A	25	-31	-100	225	-150	190
28B	0	0	0	0	0	0
29AX	80	60	-180	1800	-380	-750
29B	80	-65	-180	1900	-550	-1750
30	-80	130	-225	2300	530	1300
31	90	70	-190	2300	800	-1700
32	13	26	-35	92	-29	42
32A	-20	37.5	-90	80	-170	-75
32B	110	-90	-185	1600	500	-375
33	-115	-75	-370	2200	600	-410
34	20	-32	-62	-75	-165	150
34A	90	-170	-185	1350	700	1200
35	110	-120	175	2200	900	1250
36	22	39.5	-58	115	200	180
37	-100	140	-195	2100	-550	1300
38	27	27.5	-36	125	90	75
38A	37.5	39	-120	-220	-220	230
38B	-70	85	-180	1800	375	1500
39	24	25	-38	130	140	-170
39A	70	120	175	1950	495	-1800
40	-110	115	-190	1900	600	1750
41	100	145	-320	2400	-1100	800
42	110	45	-120	-190	550	350
42A	-140	-100	-140	1100	800	1400
43	-16	11	-35	-130	90	-75
43A	-240	-150	-425	1600	-850	-550
44	140	-140	-200	1900	900	1400
45	250	110	350	2400	-800	-650
46	-90	140	-320	3300	-700	900
47	160	-80	-175	500	900	650

TABLE 3.2 cont.

MAXIMUM FORCES/TORQUES

Case	max force X	max force Y	max force Z	max torq. X	max torq. Y	max torq. Z
48	130	90	-190	2400	900	1500
49	-205	-40	-380	2700	-1350	-1500
50	-90	170	-280	2100	-700	380
50A	140	155	-255	2400	525	410
51	75	-115	-190	2500	430	-460
52	90	65	-160	2400	650	750
53	-140	125	-440	2400	-600	-640
54	160	90	-400	3800	-850	-700
55	120	95	-280	-800	450	350
56	170	-100	-240	2500	800	750
57	140	90	-200	2350	-800	-600
58	-75	75	-205	2400	-1200	700
59	70	80	-190	2150	-600	-700
60	70	125	-400	3750	500	440
61	-70	150	-225	2100	500	900
62	-100	120	-300	3700	-800	1200
63	140	-125	-250	3750	650	1250
64	125	-140	-220	3300	-750	950

TABLE 3.2 cont.

Case 5 - Reduce per actuator gain to 3.25 lb/in gain change is permanent.
Nominal capture - align.
F/T deadband set at $F_X = F_Y$ = +/- 6.1 lbs
Fz = +/- 9.1 lbs
$T_X = T_Y$ = +/- 11.4 ft-lbs
T_Z = +/- 6.1 ft-lbs

Case 6 - Nominal capture - atten.

Case 7 - No capture.

Case 7A - Ic's same as Case 7, except closing at .1 ft/sec
Nominal capture - atten. Came very close to a leg length exceed (18.5") in leg #4 during align.

Case 8 - No capture.

Case 8A - Same i.c., as case 8, but closing vel. = .1 ft/sec.

Case 9 - No capture.

Case 9A - Closing vel. = .1 ft/sec, nominal capture - align.

Case 10 - No capture.

Case 10A - Closing vel. = .1 ft/sec, nominal capture - align.

Case 11 - No capture.

Case 11A - Closing vel. = .1 ft/sec, nominal capture - align.

Case 12 - Nominal capture - align.

Case 13 - Successful capture - align. Capture latch #2 appeared to be slow to act (approx. 1 sec late)

Case 14 - Nominal capture, but 6-DOF had a computer glitch during the atten. mode. High pitched noise detected from mechanism actuator #5. After repaired, nominal capture - align.

Case 15 - Nominal capture - align.

Case 16 - No capture. It was necessary to remain in pre-capture mode during this run until just before contact to avoid having the ring slide out of position.

Case 16A - Closing at .1 ft/sec. Nominal capture - align.

Case 17A - Nominal capture - align.

Case 18A - No capture.

Case 18B - Closing at .15 ft/sec. Nominal capture - align.

Case 19b - Closing at .15 ft/sec. Nominal capture - align.

Case 20 - No capture.

Case 20A - No capture. Very close to contact of the legs.

Case 20B - Nominal capture - align.

Case 21 - No capture. Barrel actually made contact with leg on the +x side.

Case 21A - Successful capture - atten. Align. not attempted.

Case 22 - No capture.

Case 22A - No capture.

Case 22B - Closing at .15, Nominal capture - atten.

Case 23 - Nominal capture - align.

Case 24 - Nominal capture - align.

Case 25 - Nominal capture - align.

Case 26 - Nominal capture - align.

Case 27 - No capture.

Case 27A - Nominal capture - align.

Case 28 - No capture.

Case 28A - Closing at .1 ft/sec, no capture

Case 28B - Closing at .15 ft/sec, nominal capture - align.
6-DOF data lost, run not repeated.

Case 29AX - Angular misalignment of (-1.22° z angle), .15 ft/sec closing. Nominal capture - align.

Case 29B - Nominal capture - align.

Case 30 - Nominal capture - align.

Case 31 - Nominal capture - align.

Case 32 - Had to change the i.c. to 3.0" y offset because there was no clearance (guide would hit ring face) at 4.5". The k1 (pre-capture mode stiffness) was raised to 30 lb/in to better maintain the ring in nominal position when mechanism tilted over. No capture.

Case 32A - No capture.

Case 32B - Nominal capture - align.

Case 33 - Modified y alignment to 3.0 in (not 4.5). Nominal capture - align.

Case 34 - No capture.

Case 34A - Nominal capture - align. Max leg length approx. 18.1 in (#3)

Case 35 - Nominal capture - align.

Case 36 - Increase $k_1 = 50$, No capture.

Case 37 - Nominal capture - align. Got a force exceed coming out of align.

Case 38 - Change y-misalignment from 4.5 in to 3.0 in for clearance. No capture.

Case 38A - No capture.

Case 38B - Closing at .15 ft/sec. Nominal capture - align. Force exceed coming out of align.

Case 39 - No capture.

Case 39A - Closing at .1 ft/sec. Nominal capture - attenuation, but a torque exceedance. (> 2000 ft/lbs) about z-axis in align. Repeated run twice w/ identical results.

Case 40 - Modified y-misalign. to 3. in. Successful capture - atten. Align left off at 11.5" when command was 14.25". Got a freeze going back to pre-capture.

Case 41 - Nominal capture - atten. but got a z-torque exceed in align.

Case 42 - No capture. Bumped actuator on barrel with the rebound.

Case 42A - Nominal capture - atten. Alignment mode only achieved 9.1" when command was 14.25". Force exceed when going back to pre-capture.

Case 43 - No capture.

Case 43A - Successful capture - atten. Got a z-torque exceed in align.

Case 44 - Successful capture in atten. Alignment mode failed to come close to commanded position, so alignment/retraction was abandoned for rest of test.

Case 45 - Nominal capture, but atten. shook the 6-DOF contact switch, thus ending test.

Case 46 - Nominal capture, but exceeded T_X = 3500 ft-lbs during atten.

Case 47 - Nominal capture - atten.

Case 48 - Nominal capture - atten.

Case 49 - Nominal capture - atten.

Case 50 - Nominal capture - atten. Actuator within 1/4" of contact w/barrel.

Case 50A - Same i.c., as case 50, but y-misalign is -2.25. (correlate w/case 46). Nominal capture - atten.

Case 51 - Nominal capture - atten.

Case 52 - Nominal capture - atten.

Case 53 - Nominal capture - atten.

Case 54 - Nominal capture - atten.

Case 55 - Nominal capture - atten.

Case 56 - Nominal capture - atten.

Case 57 - Nominal capture - atten.

Case 58 - Nominal capture - atten.

Case 59 - Nominal capture - atten.

Case 60 - Successful capture. Failed in atten. with auto 6-DOF freeze. Did not appear to be F/T exceed. Possible 6-DOF ceiling switch activated. Repeat of run - same result.

Case 61 - Nominal capture - atten.

Case 62 - Nominal capture - atten.

Case 63 - Nominal capture - atten.

Case 64 - Nominal capture - atten.

As can be seen from the brief run log, the per actuator gain in the capture mode was reduced from 7.5 to 3.25 lb/in. This presented no stability problems and allowed the active ring to cam into place much easier than with 7.5 lb/in. The drawback to softening the stiffness was that as the 6-DOF was tilted at an angle to achieve some i.c., the ring would tend to slide down to an off-nominal equilibrium position. Clearly this effect is an artifact of testing the mechanism in 1-g rather than a weightless environment. The 6-DOF initialization code expects the docking mechanism to stay in its nominal position before capture. Thus when the ring moves out of position, the 6-DOF does not account for this and hence the actual ring position at contact is not the presupposed initial condition. To avoid this problem, the mechanism was kept in the stiffer pre-capture mode until the moment of contact when the control mode was changed to "capture." As the magnitude of the gravity induced ring sideslip became more apparent, the pre-capture gain was successively increased to 30 and 50 lb/in in cases 32 and 36 respectively. The fact that the initial conditions of cases 32, 33, 38, and 40 had to be modified was attributed to the ring sideslip. This problem is discussed in detail later in this section.

A problem with the alignment mode began to become evident in cases 38B through 44. Not only was the previously seen anomalous centering behavior present, but it was found that the actuator position error was several inches. This error was the cause of the force registered by the 6-DOF re-entering the pre-capture mode. The cause of this problem, which seemed to arise over the course of several runs, was not obvious and was felt to require an in-depth trouble-shooting of the system (see below). With this in mind, it was decided to complete the remaining dynamic cases without entering the alignment mode. Before leaving this topic it should be noted that after running case 14, electronics problems surfaced with actuators #1 and #5. After these problems were fixed, the load cells were re-zeroed. The actuators were connected to the ring, and the ring was down at the fully retracted position when the new zero values were set. The consequences of this was that the force bias numbers input to the program were on the order of 100 lbs, or about twice the previous levels. Several check cases comparing cases previously run indicated no difference in the mechanism behavior when using the new force biases.

It was determined after the testing was completed that if the load cells were "zeroed" at a value of 150 mv when under their own weight (as was previously done during early checkout) the alignment mode problems were apparently solved. Post test analysis predicted this due to the way the load cell electrical offsets are presently handled in the software.

Examination of Table 3.1 indicates that the mechanism was able to capture at all the various misalignments in the matrix if the closing velocity was increased sufficiently. If the closing velocity was raised to .15 ft/sec, all cases in the matrix would successfully capture. Of course from a loads standpoint, minimizing the approach velocity is desirable.

Table 3.2 shows the maximum modulus load applied to the force/torque sensor (i.e., Space Station) for each run. The maximums are extracted from the capture and attenuation modes, not the alignment mode. It was felt that since the alignment mode was not functioning properly, it would be misleading to use the load data from this mode. As can be seen from Table 3.3, the envelope of forces and torques predicted were never exceeded during the test.

TABLE 3.3

DIRECTION	MAXIMUM LOAD	MAXIMUM PREDICTED	CASE NO.
X (lbs)	250	500	8A, 21A, 45
Y (lbs)	380	500	18A
Z (lbs)	450	1200	4
Θ_X (ft-lbs)	3800	5000	54
Θ_y (ft-lbs)	1800	5000	23
Θ_Z (ft-lbs)	1800	2000	39A

Figures 3.8 through 3.25 contain the data output from the 6-DOF facility for Case 4. This particular case has no misalignment and a closing velocity of 0.2 ft/sec. For comparison Figures 3.26 through 3.31 have been included. These figures represent the analytically predicted response of the mechanism to the Case 4 initial conditions. It should be noted that capture occurs at t = 0 seconds on the analytically generated plots, whereas capture occurs at approximately t = 5 seconds into the 6-DOF run. Also the 6-DOF data is expressed in a coordinate frame which is rotated 180° about the y-axis from the analytical frame (See Figure 3.8 and 3.26). The z-position curves show that the 6-DOF behavior is similar in magnitude to the predicted, but the analytical response is sharper, with a quicker response time. The orbiter pitch axis angle (Q_X) shows good agreement between test and analytical data as far as shape and period (≅ 100 sec) are concerned, but the amplitude of the analytical data is approximately 25% lower than the test data. The rate data correlates well between test and predicted response. The z-force value also compares well in shape, with the predicted force some 75 lbs less than the measured force. The pitch axis torque compares quite well, both test and predicted values being just over 2000 ft-lbs. Figure 3.32 contains a portion of the strip chart data taken for Case 4. This data corresponds to actuator number 1.

CASE 4

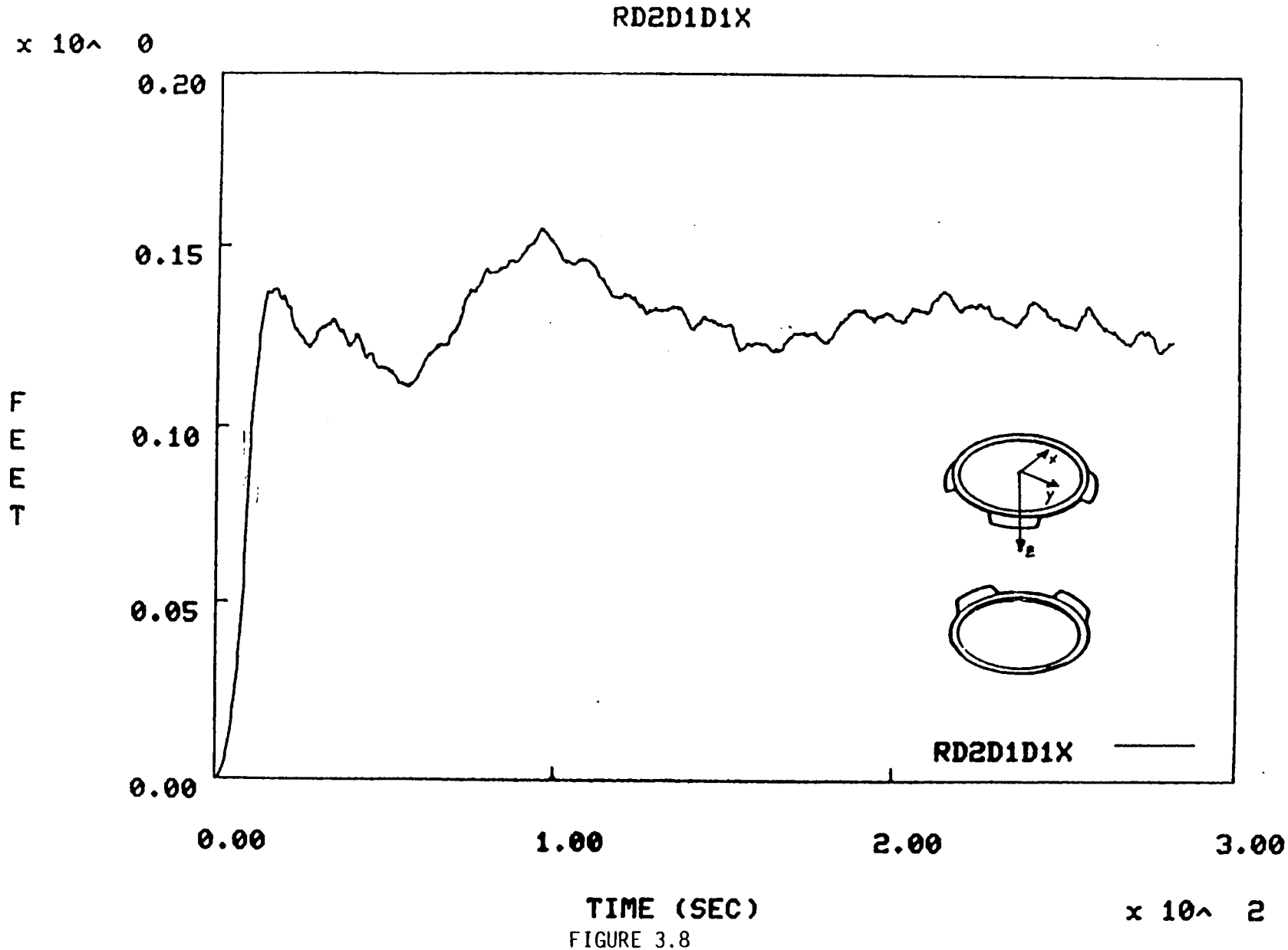

FIGURE 3.8

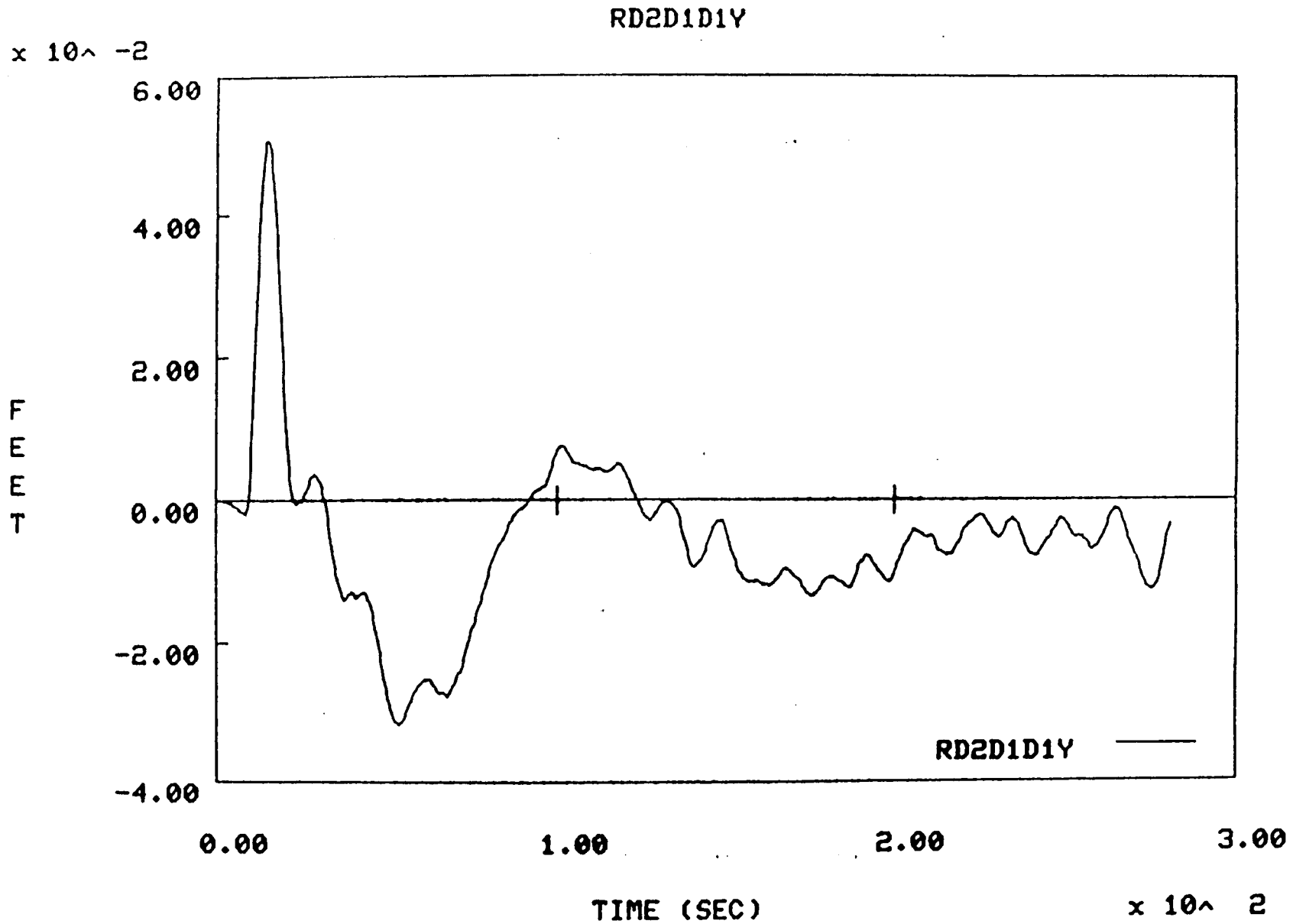
RD2D1D1Y
x 10^ -2
6.00
4.00
2.00
0.00
-2.00
-4.00
FEET
RD2D1D1Y
0.00
1.00
2.00
3.00
TIME (SEC)
x 10^ 2

FIGURE 3.9

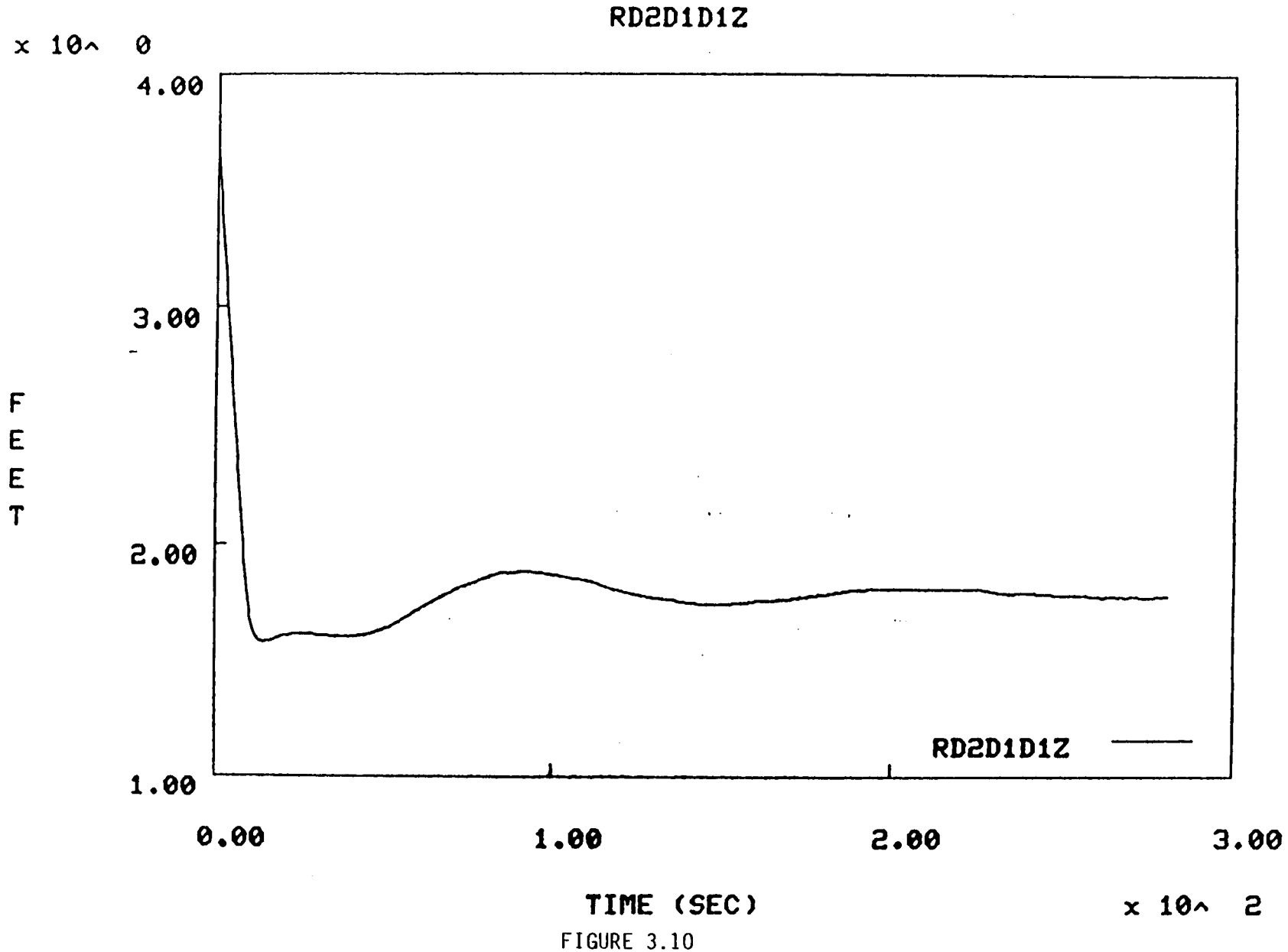
RD2D1D1Z
x 10^ 0
4.00
3.00
2.00
1.00
FEET
0.00
1.00
2.00
3.00
TIME (SEC)
x 10^ 2
RD2D1D1Z

FIGURE 3.10

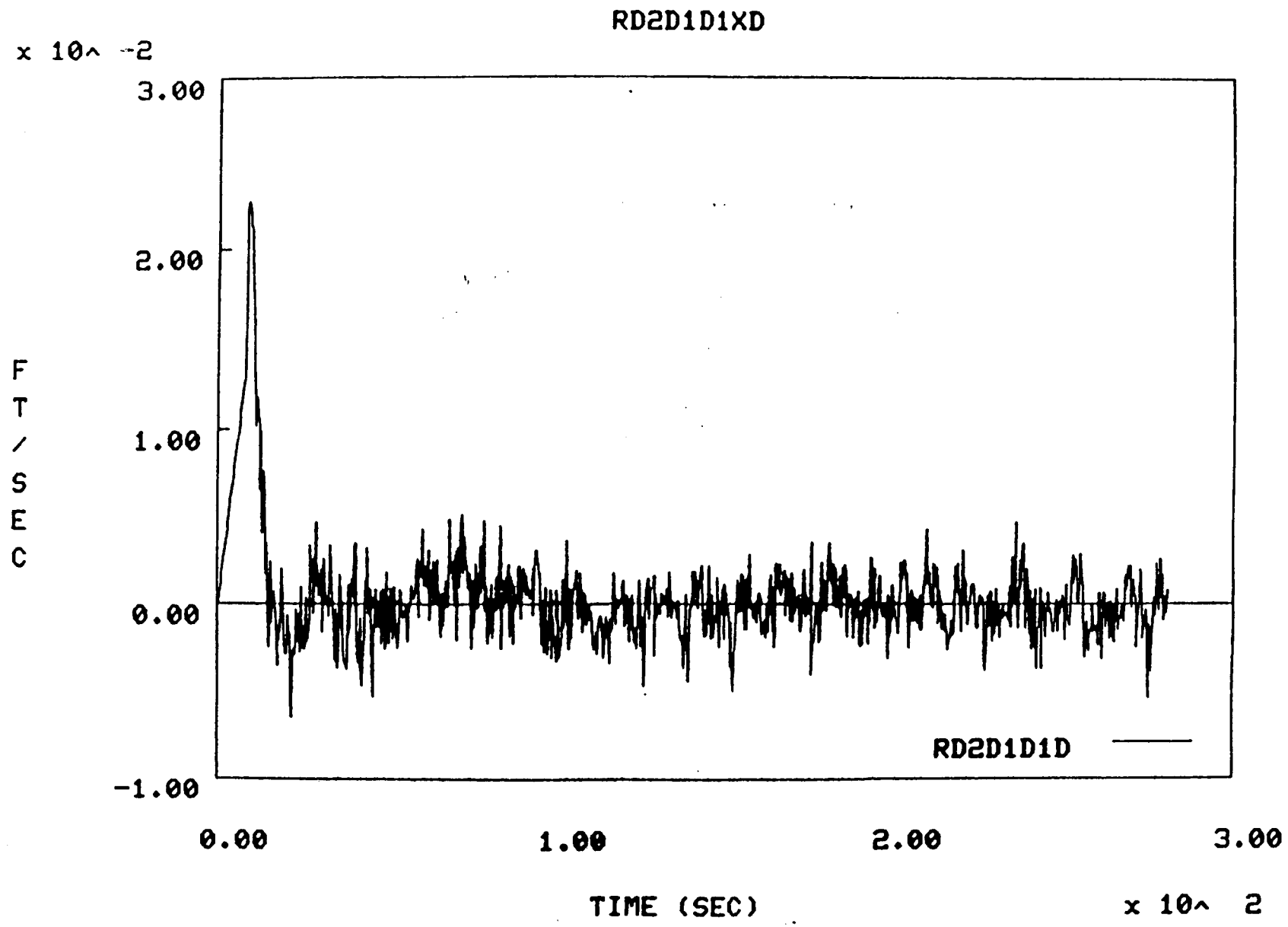
RD2D1D1XD
x 10^ -2
3.00
2.00
1.00
0.00
-1.00
F
T
/
S
E
C
RD2D1D1D
0.00
1.00
2.00
3.00
TIME (SEC)
x 10^ 2

FIGURE 3.11

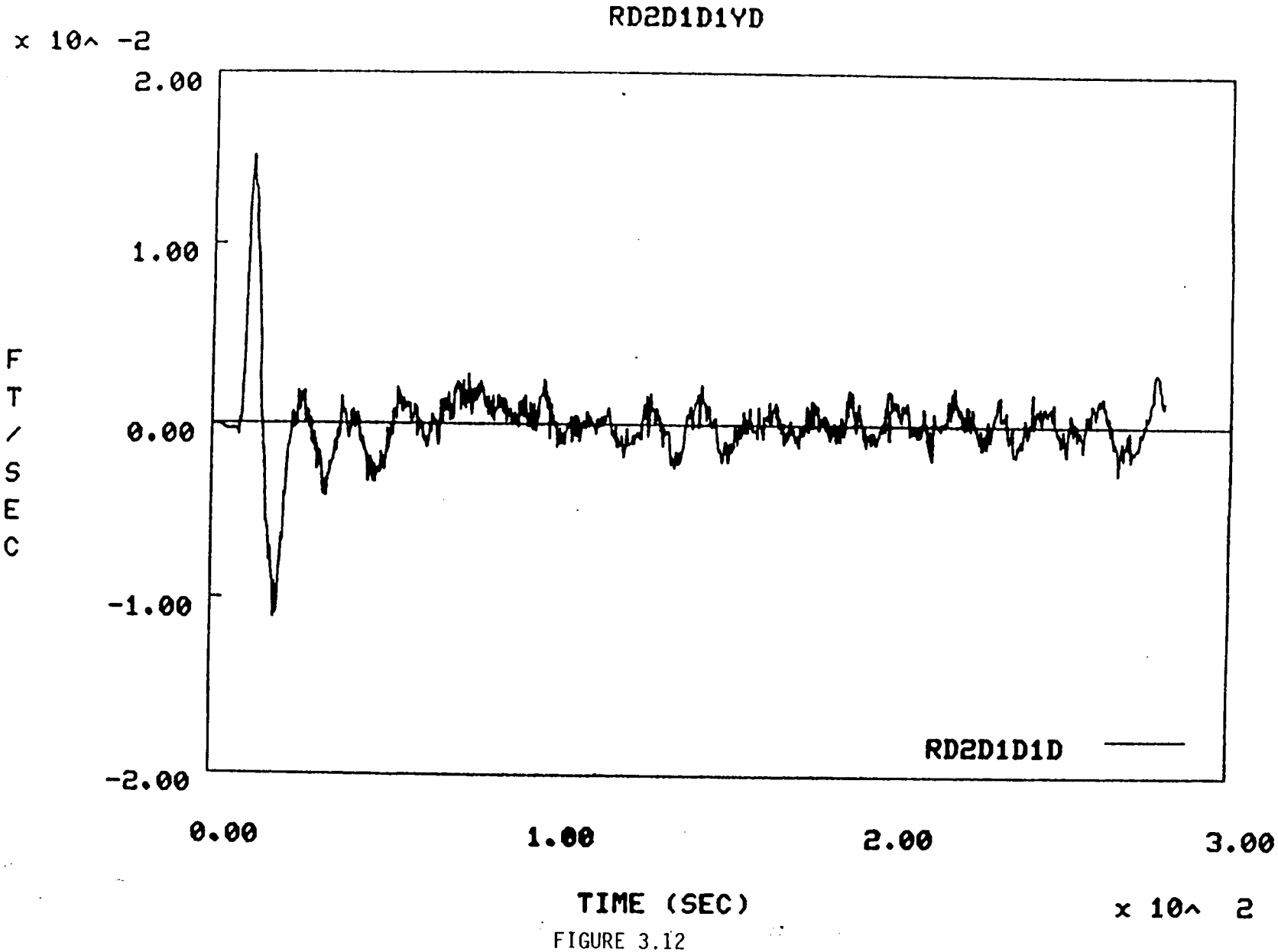
RD2D1D1YD
x 10^ -2
2.00
1.00
0.00
-1.00
-2.00
FT/SEC
RD2D1D1D
0.00
1.00
2.00
3.00
TIME (SEC)
x 10^ 2

FIGURE 3.12

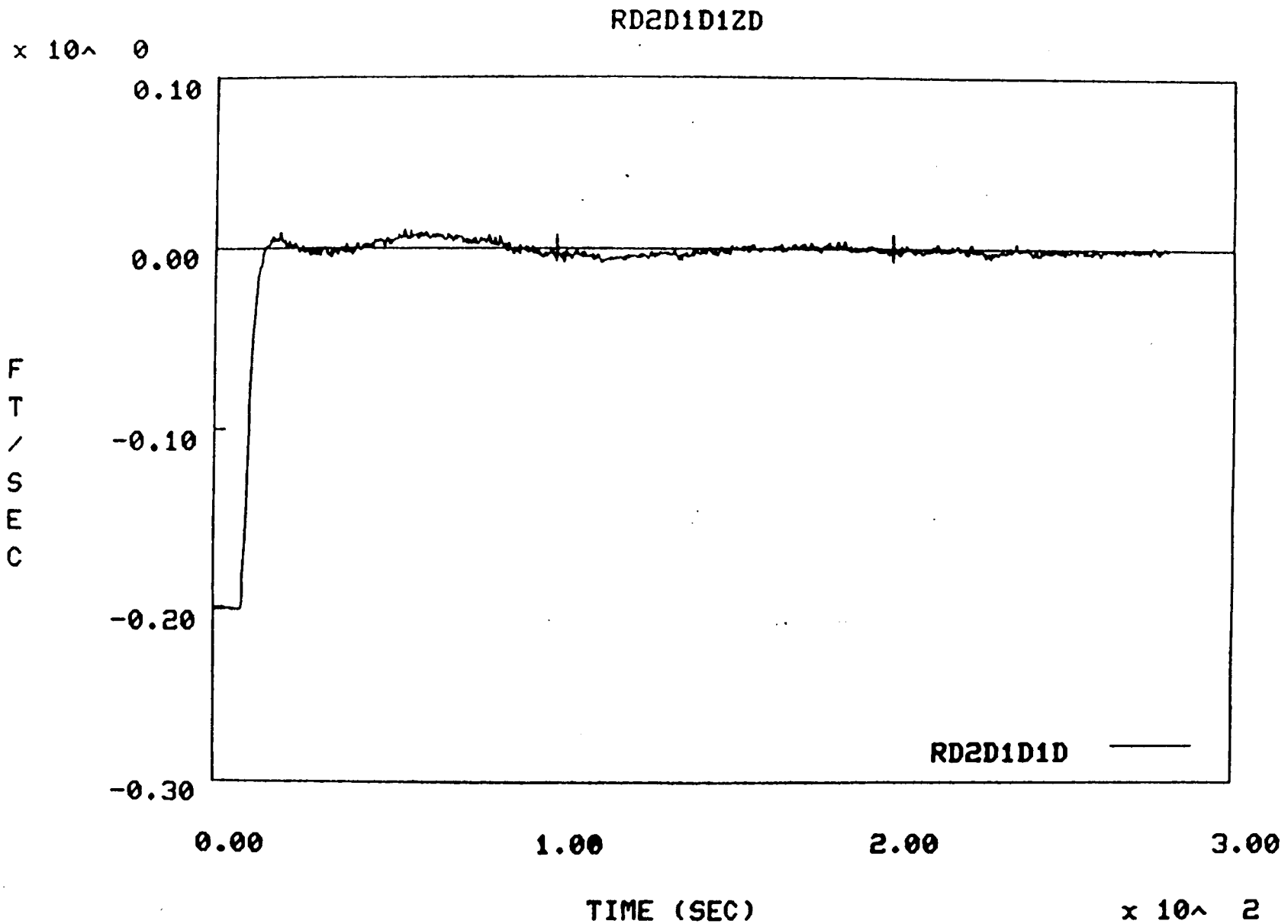
RD2D1D12D
x 10^ 0
0.10
0.00
-0.10
-0.20
-0.30
F
T
/
S
E
C
RD2D1D1D
0.00
1.00
2.00
3.00
TIME (SEC)
x 10^ 2

FIGURE 3.13

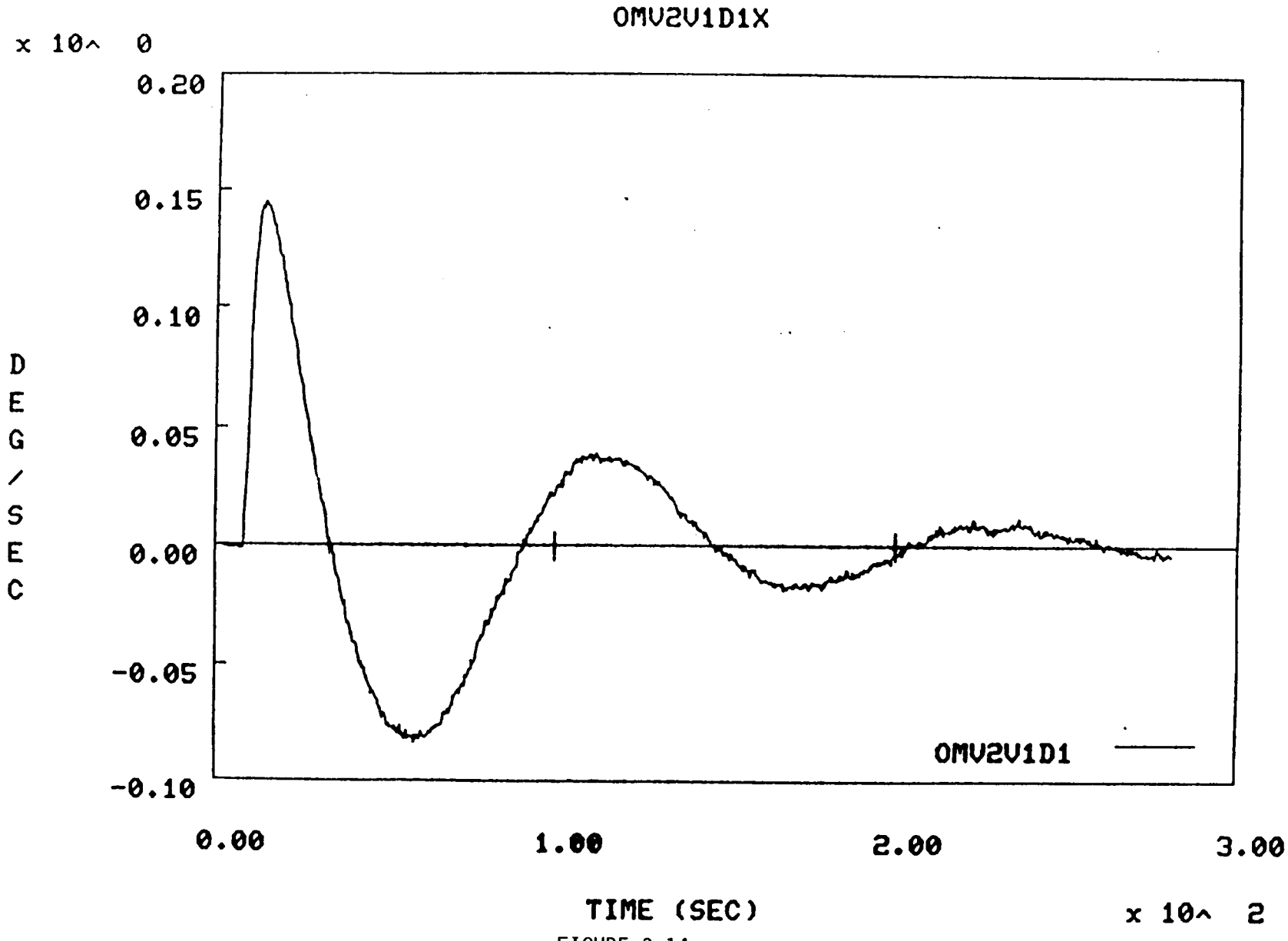
OMV2V1D1X
x 10^ 0
0.20
0.15
0.10
0.05
0.00
-0.05
-0.10
DEG/SEC
OMV2V1D1
0.00
1.00
2.00
3.00
TIME (SEC)
x 10^ 2

FIGURE 3.14

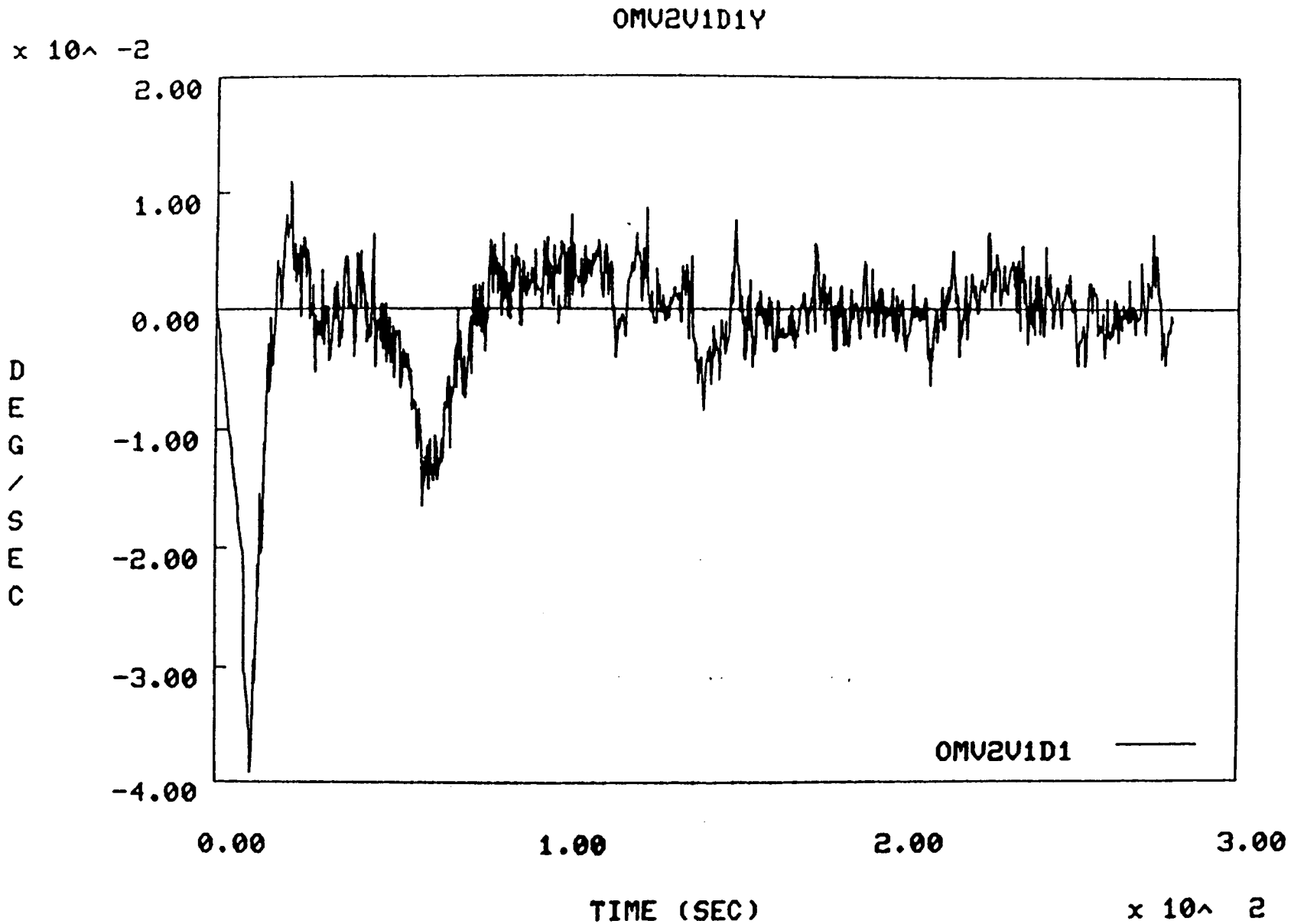
OMV2V1D1Y
x 10^ -2
2.00
1.00
0.00
-1.00
-2.00
-3.00
-4.00
DEG/SEC
OMV2V1D1
0.00
1.00
2.00
3.00
TIME (SEC)
x 10^ 2

FIGURE 3.15

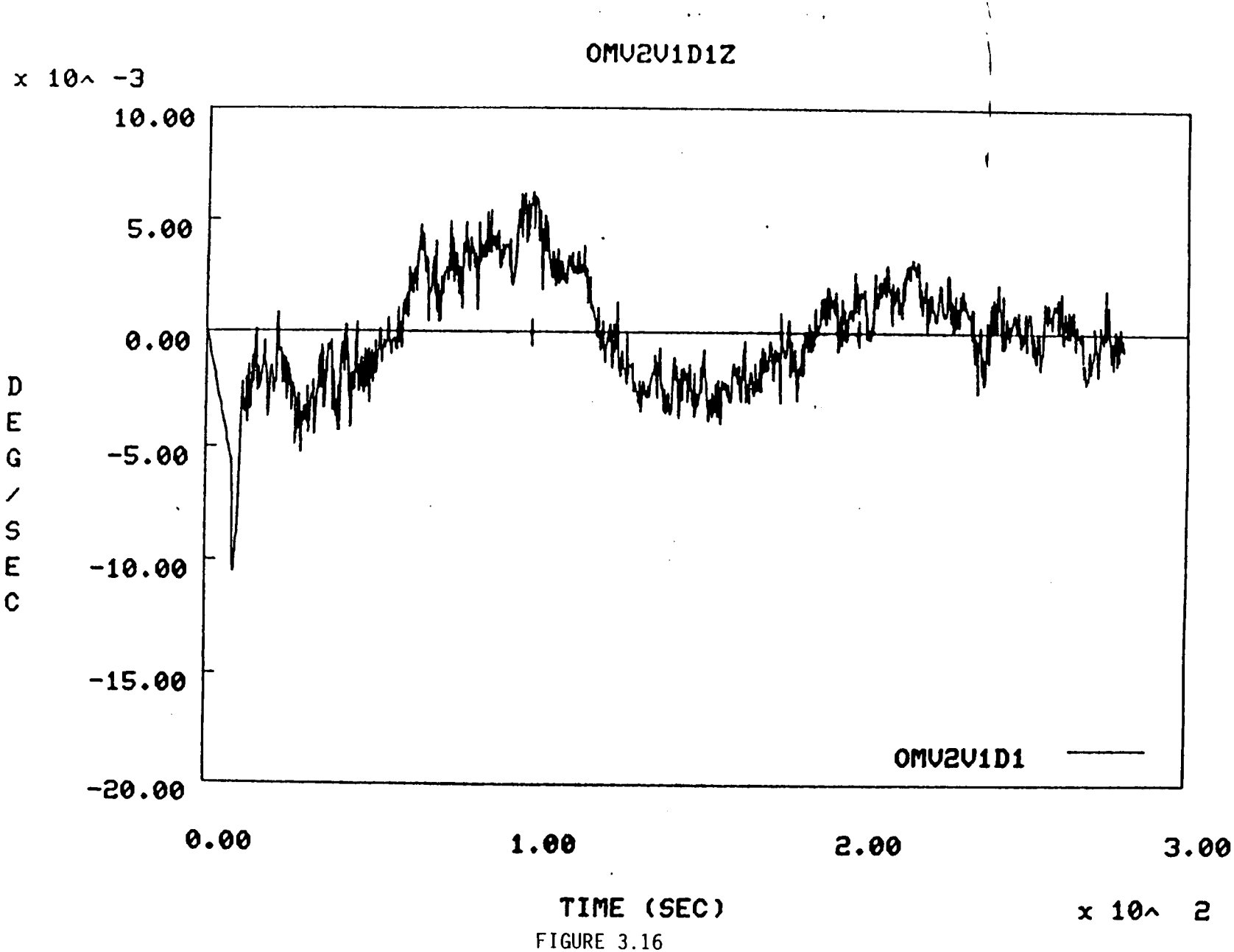
OMV2V1D1Z
x 10^ -3
10.00
5.00
0.00
-5.00
-10.00
-15.00
-20.00
DEG/SEC
OMV2V1D1
0.00
1.00
2.00
3.00
TIME (SEC)
x 10^ 2

FIGURE 3.16

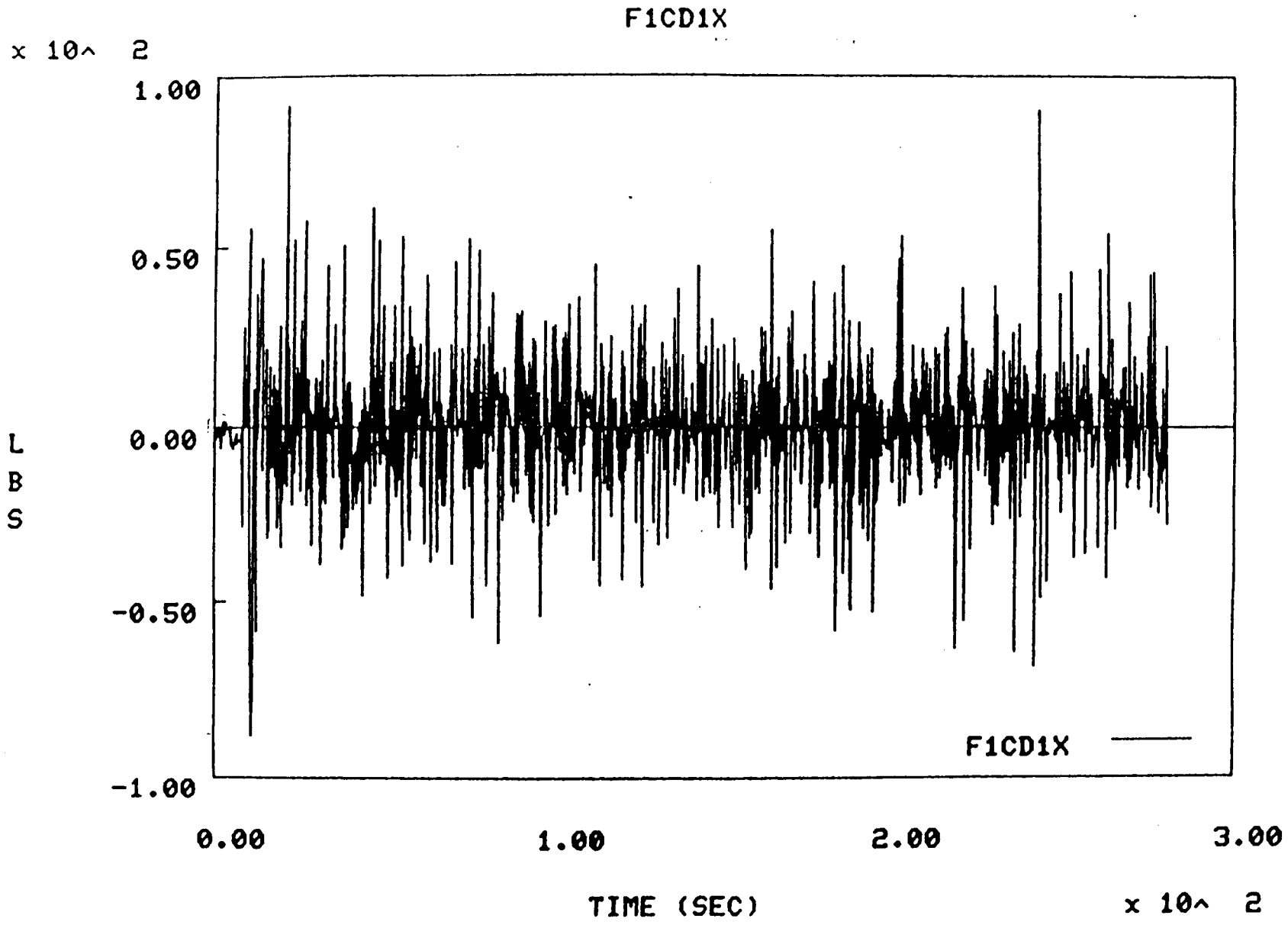
F1CD1X
x 10^ 2
1.00
0.50
0.00
-0.50
-1.00
L
B
S
F1CD1X
0.00
1.00
2.00
3.00
TIME (SEC)
x 10^ 2

FIGURE 3.17

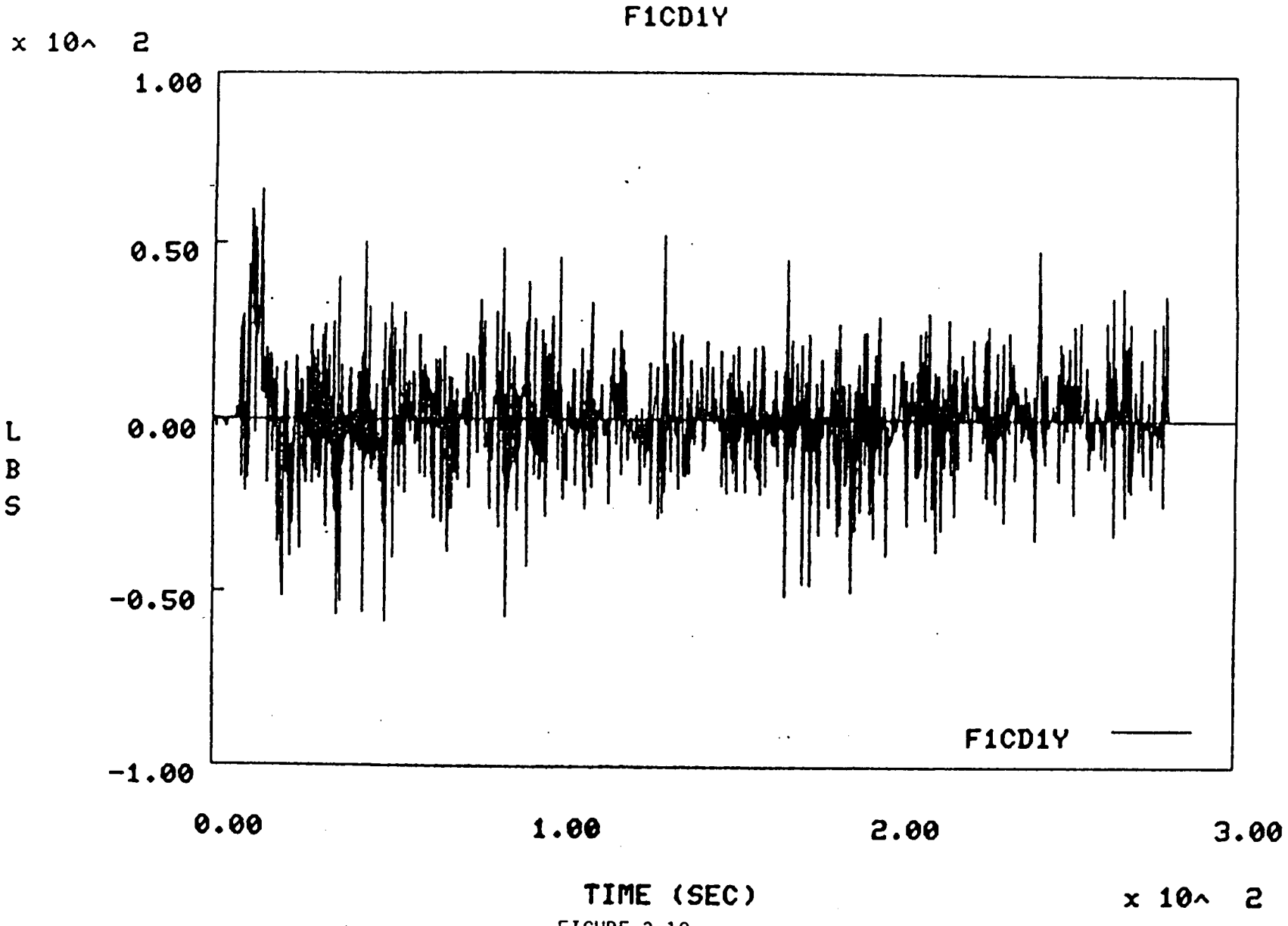
F1CD1Y
x 10^ 2
1.00
0.50
0.00
-0.50
-1.00
L
B
S
F1CD1Y
0.00
1.00
2.00
3.00
TIME (SEC)
x 10^ 2

FIGURE 3.18

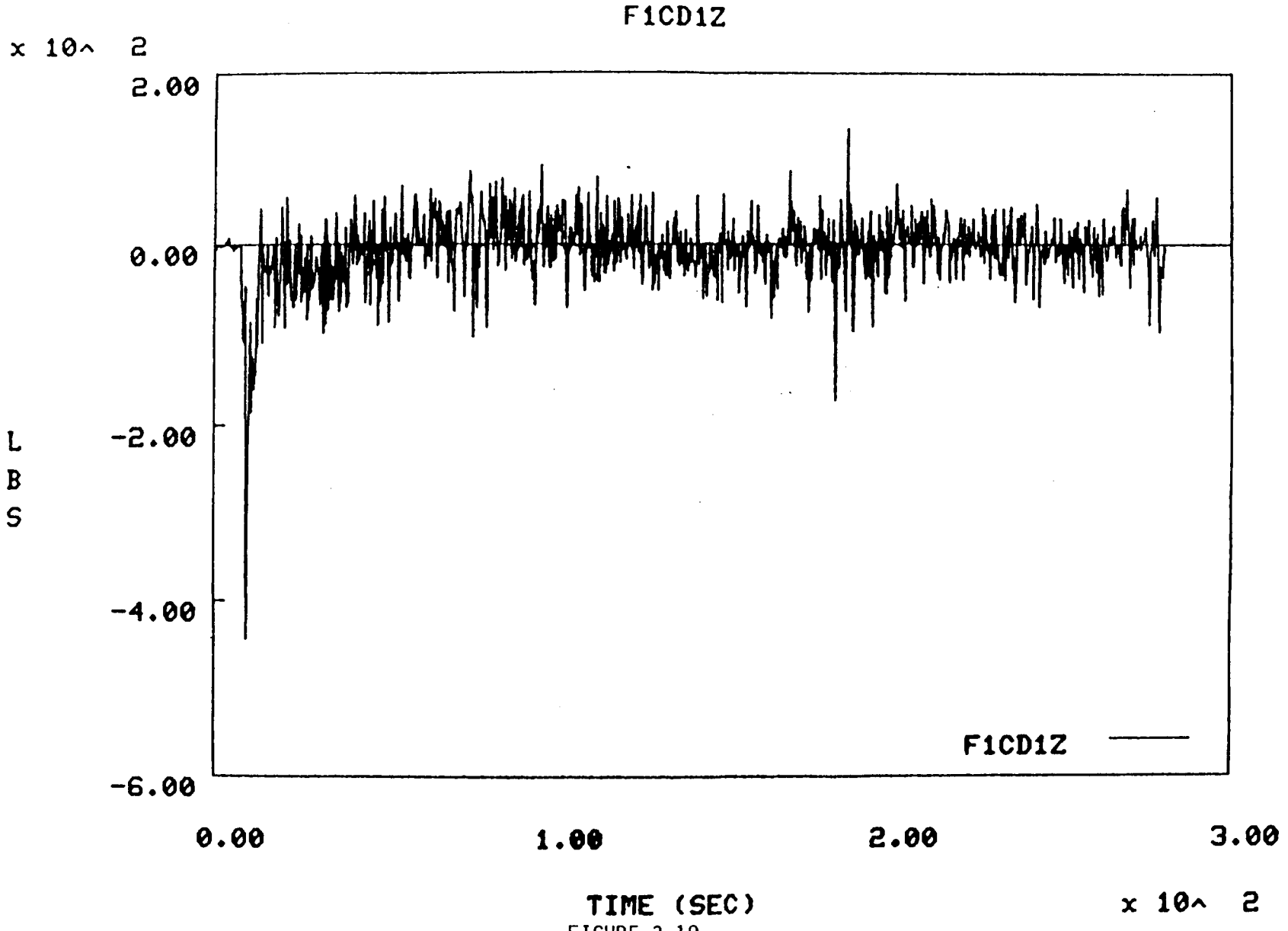
F1CD1Z
x 10^ 2
2.00
0.00
-2.00
-4.00
-6.00
L
B
S
F1CD1Z
0.00
1.00
2.00
3.00
TIME (SEC)
x 10^ 2

FIGURE 3.19

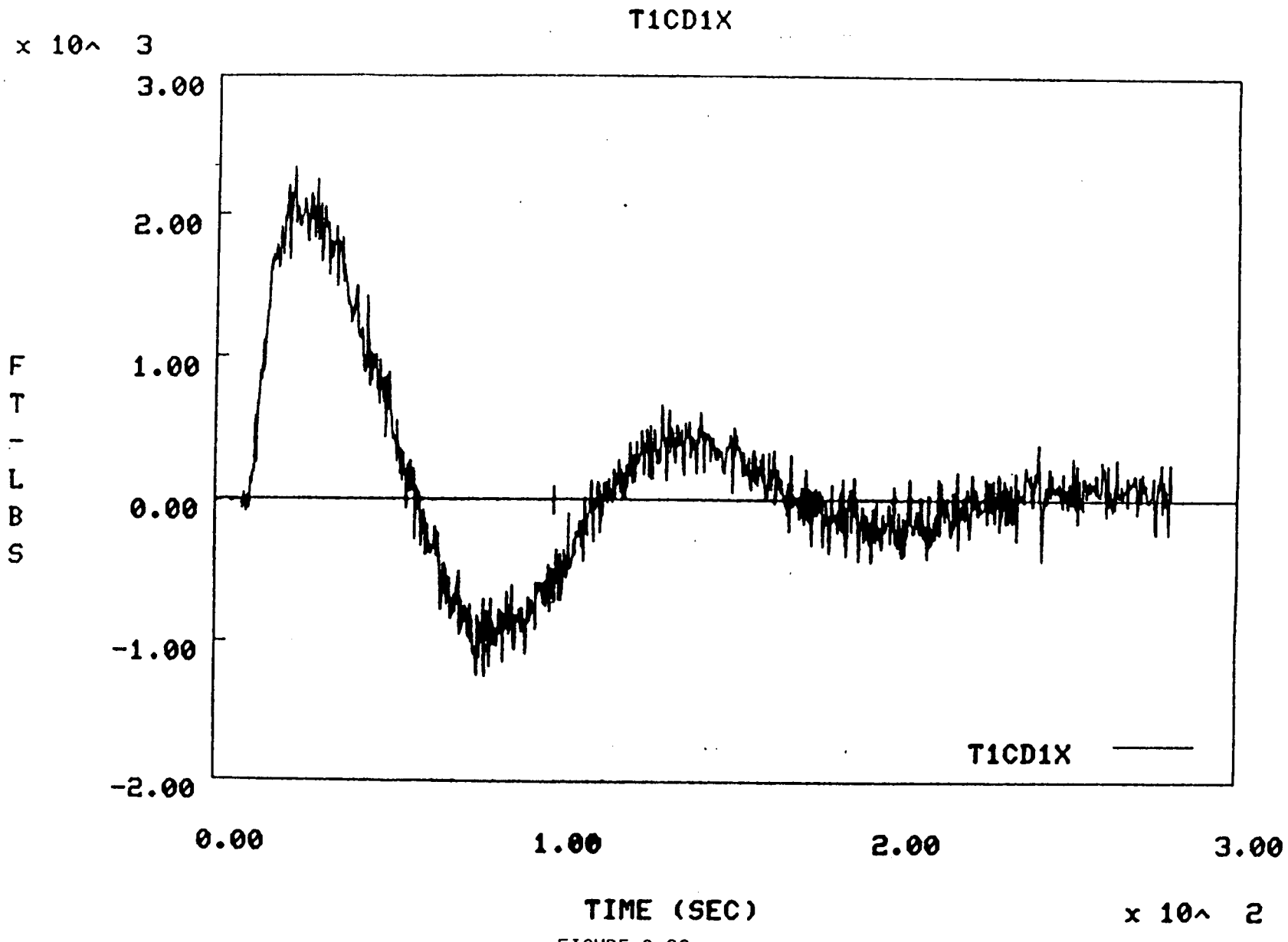
T1CD1X
x 10^ 3
3.00
2.00
1.00
0.00
-1.00
-2.00
F
T
-
L
B
S
T1CD1X
0.00
1.00
2.00
3.00
TIME (SEC)
x 10^ 2

FIGURE 3.20

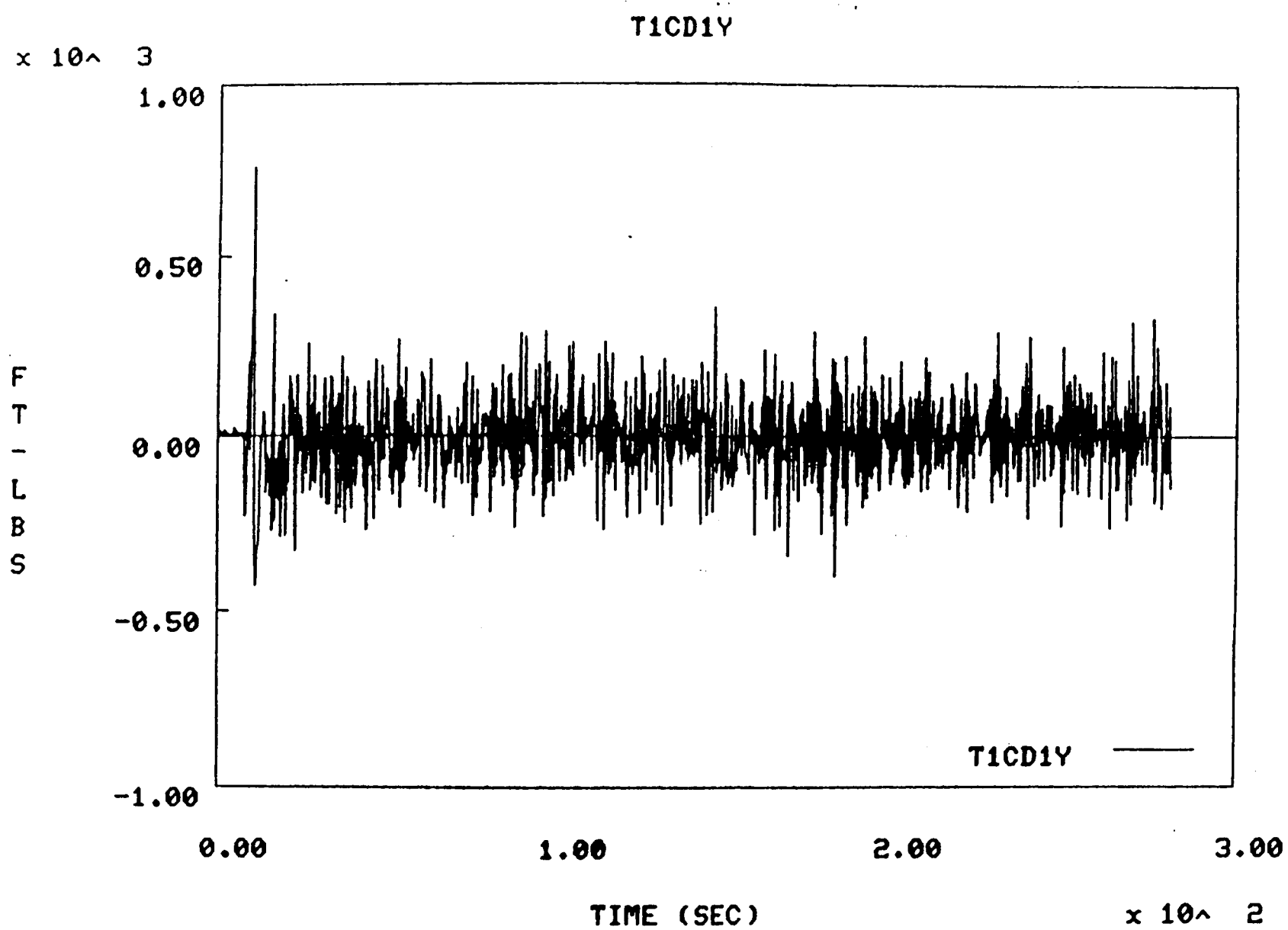
T1CD1Y
x 10^ 3
1.00
0.50
0.00
-0.50
-1.00
F
T
-
L
B
S
T1CD1Y
0.00
1.00
2.00
3.00
TIME (SEC)
x 10^ 2

FIGURE 3.21

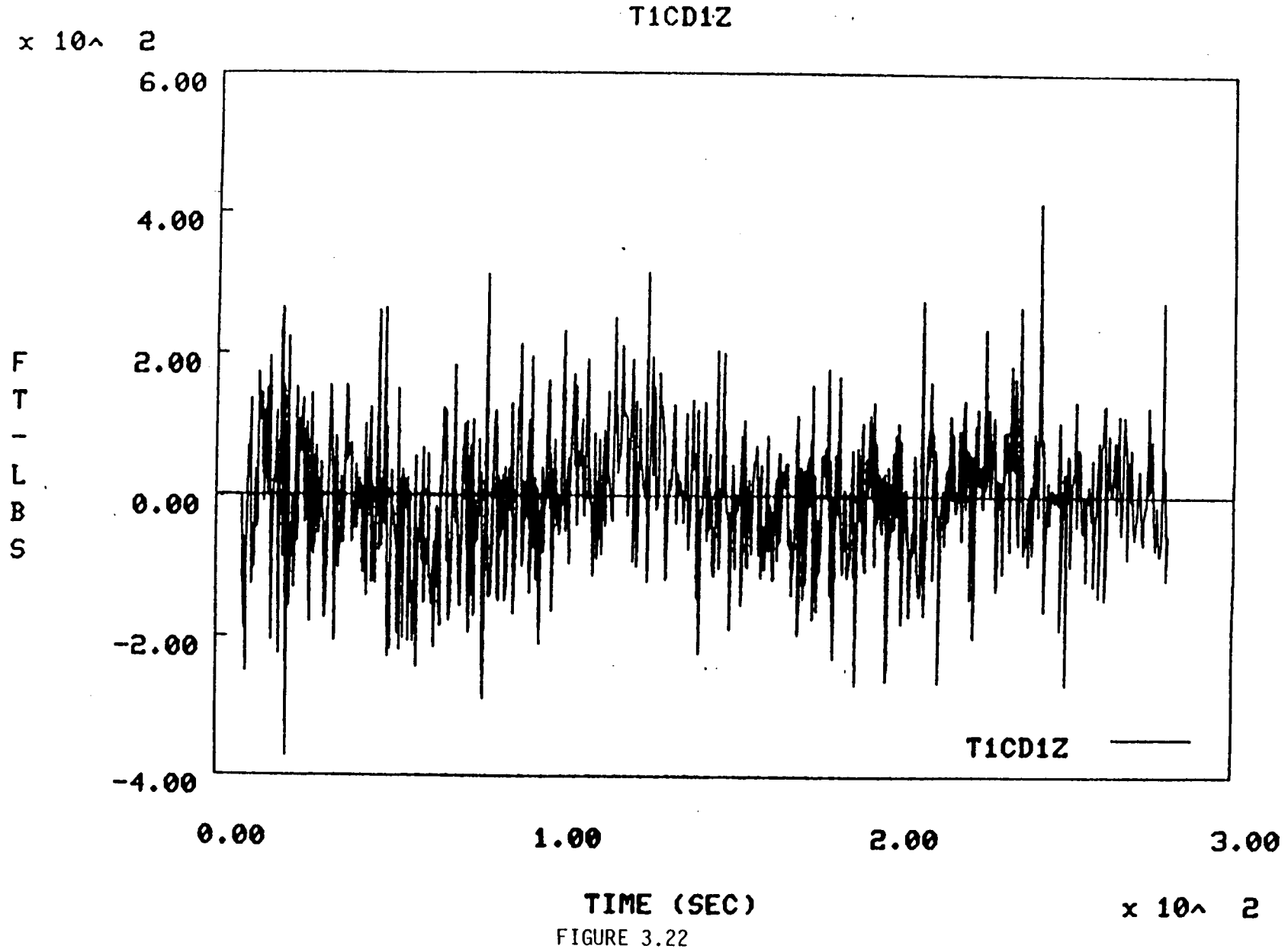
T1CD1Z
x 10^ 2
6.00
4.00
2.00
0.00
-2.00
-4.00
F
T
-
L
B
S
T1CD1Z
0.00
1.00
2.00
3.00
TIME (SEC)
x 10^ 2

FIGURE 3.22

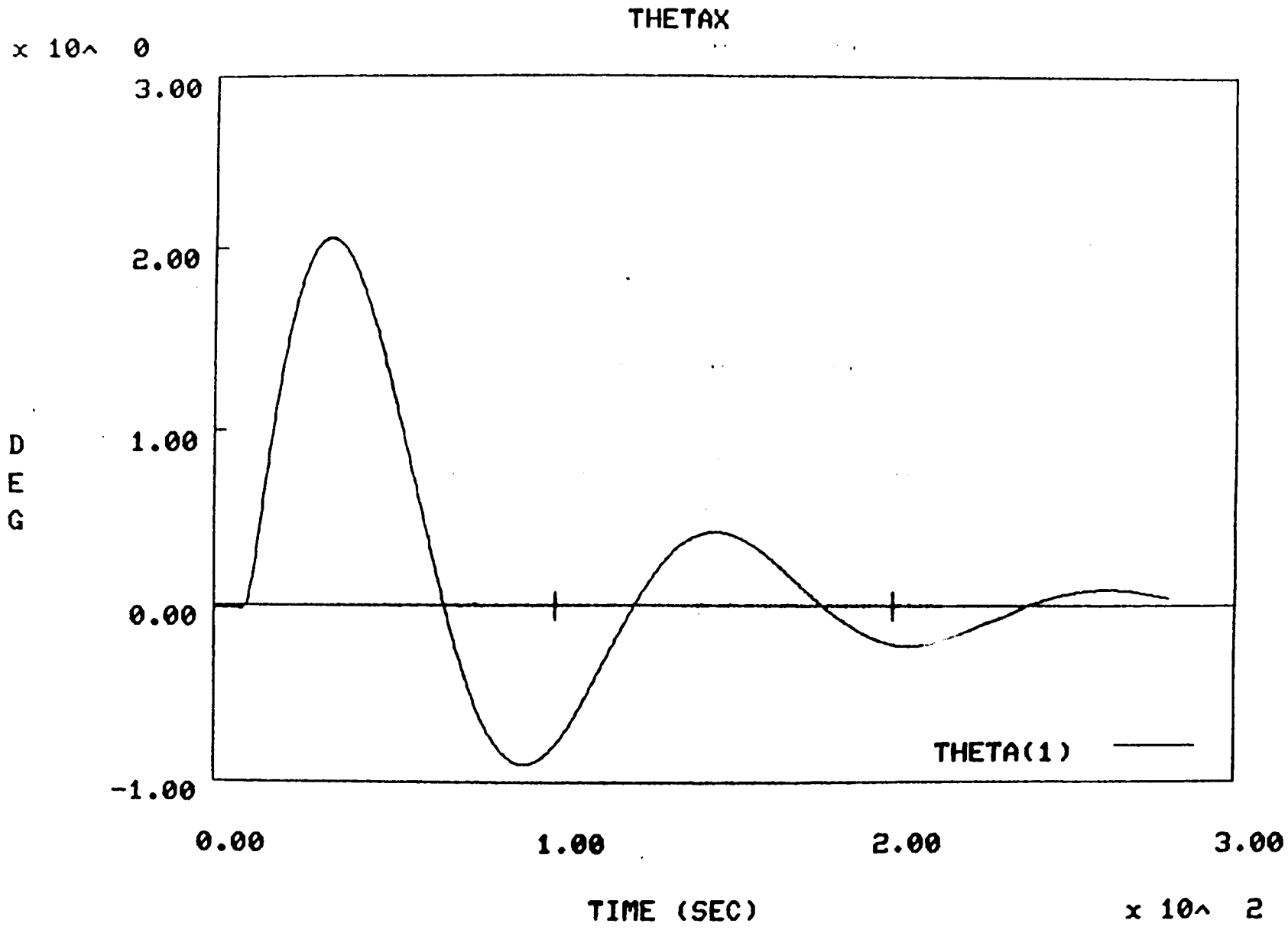
THETAX
x 10^ 0
3.00
2.00
1.00
0.00
-1.00
D
E
G
THETA(1)
0.00
1.00
2.00
3.00
TIME (SEC)
x 10^ 2

FIGURE 3.23

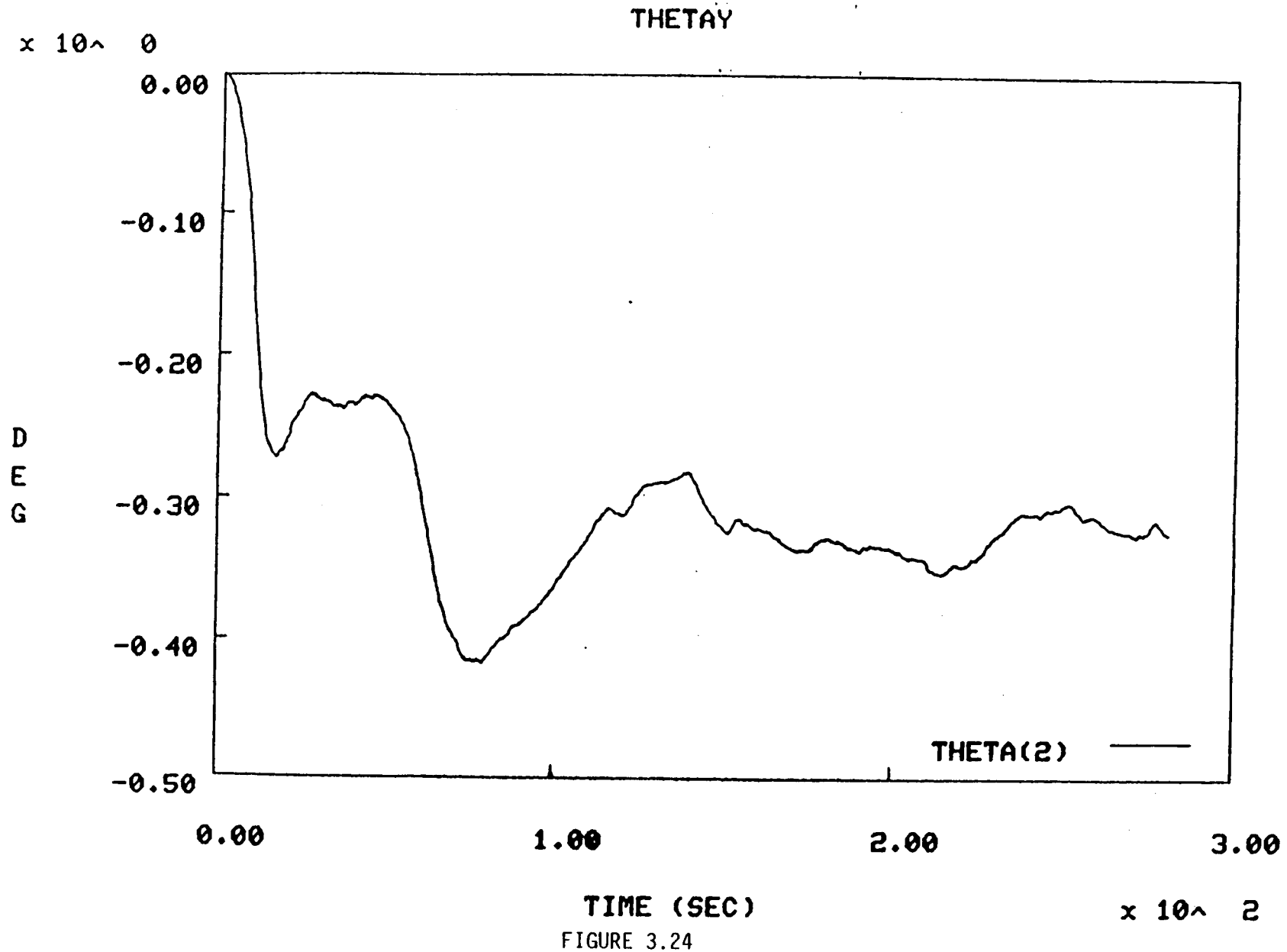
THETAY
x 10^ 0
0.00
-0.10
-0.20
-0.30
-0.40
-0.50
D
E
G
THETA(2)
0.00
1.00
2.00
3.00
TIME (SEC)
x 10^ 2

FIGURE 3.24

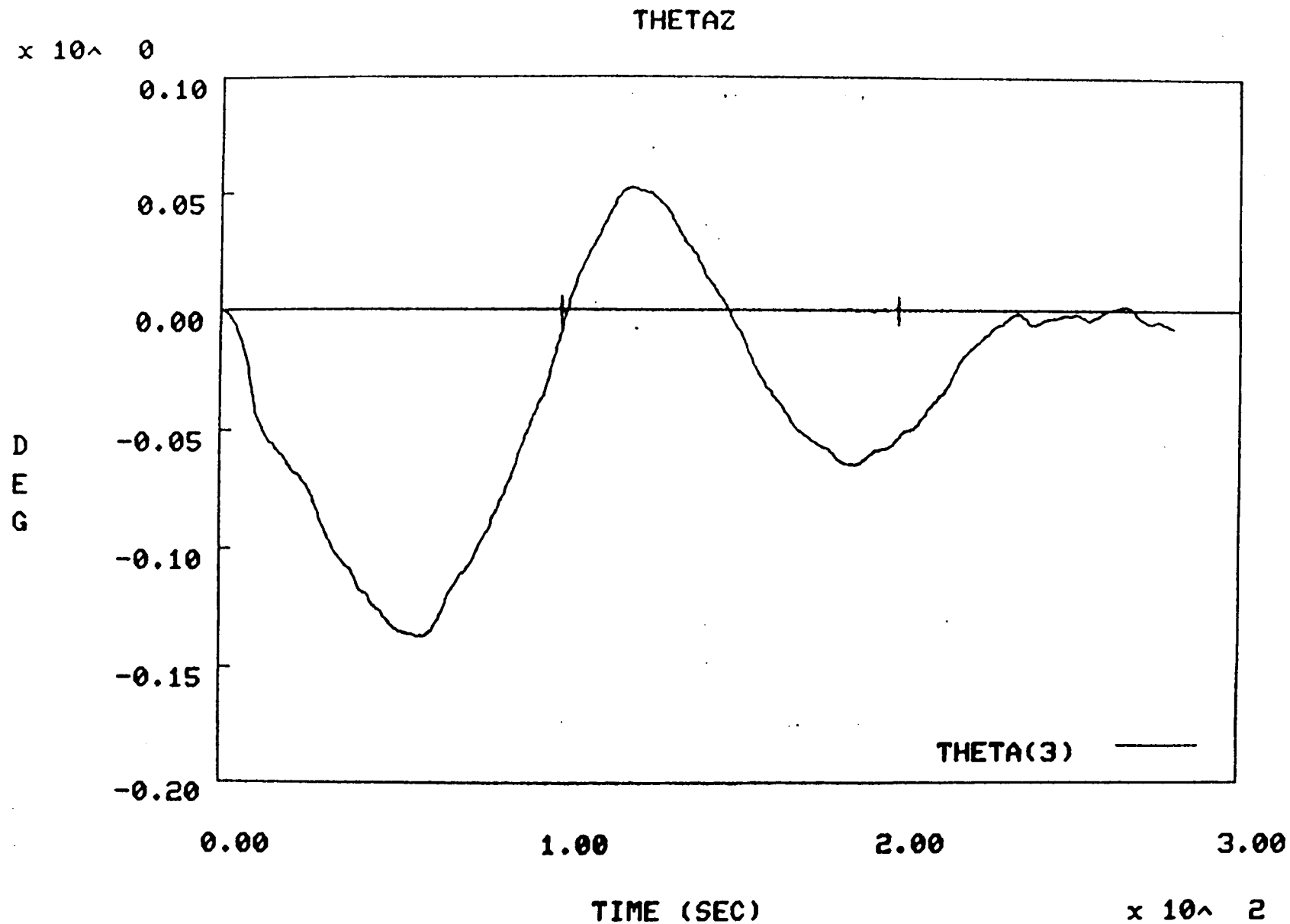
THETAZ
x 10^ 0
0.10
0.05
0.00
-0.05
-0.10
-0.15
-0.20
D
E
G
THETA(3)
0.00
1.00
2.00
3.00
TIME (SEC)
x 10^ 2

FIGURE 3.25

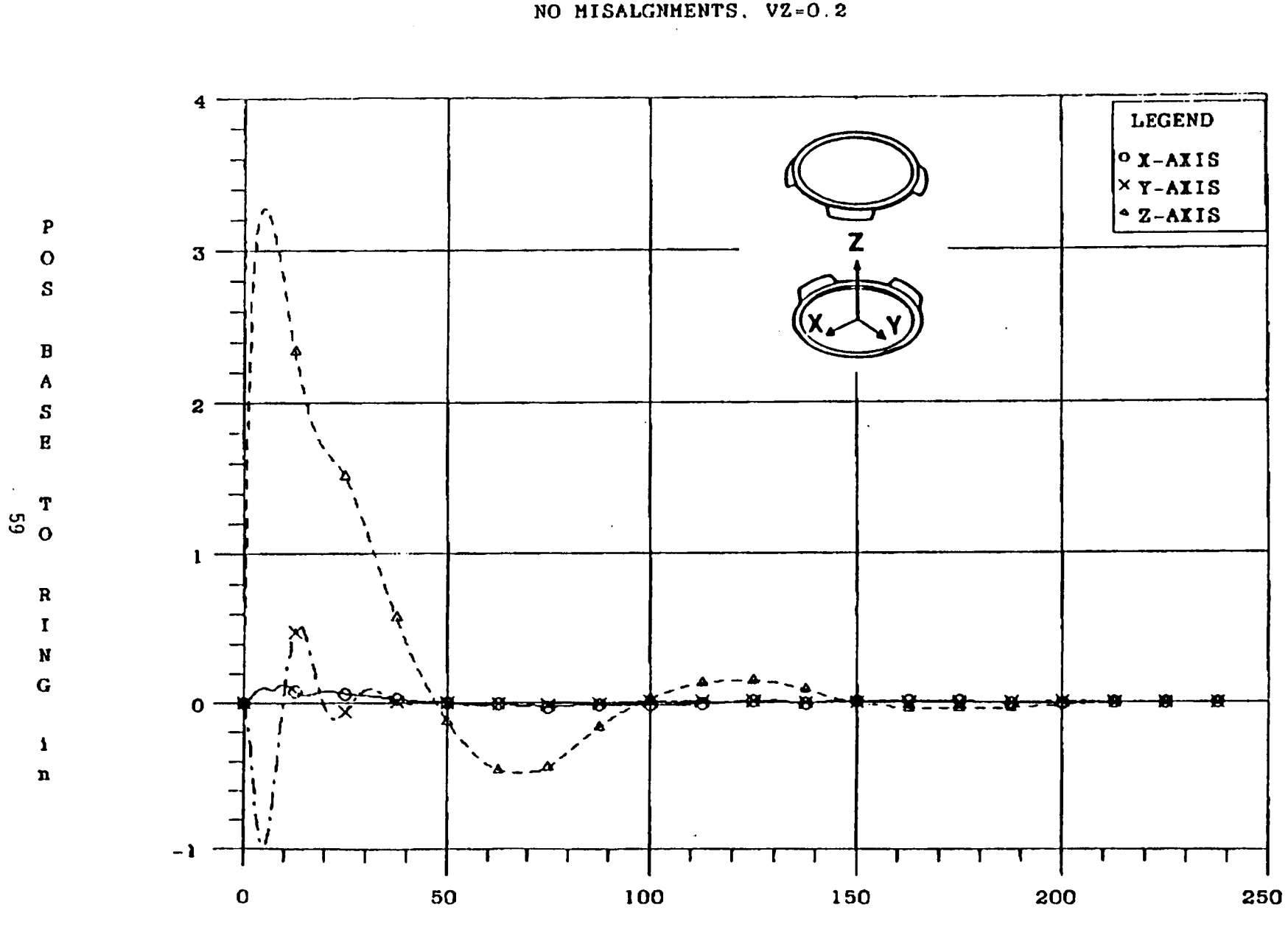
NO MISALGNMENTS. VZ=0.2
LEGEND
X-AXIS
Y-AXIS
Z-AXIS
Z
X
Y
POS BASE TO RING in
4
3
2
1
0
-1
0
50
100
150
200
250
TIME sec

FIGURE 3.26

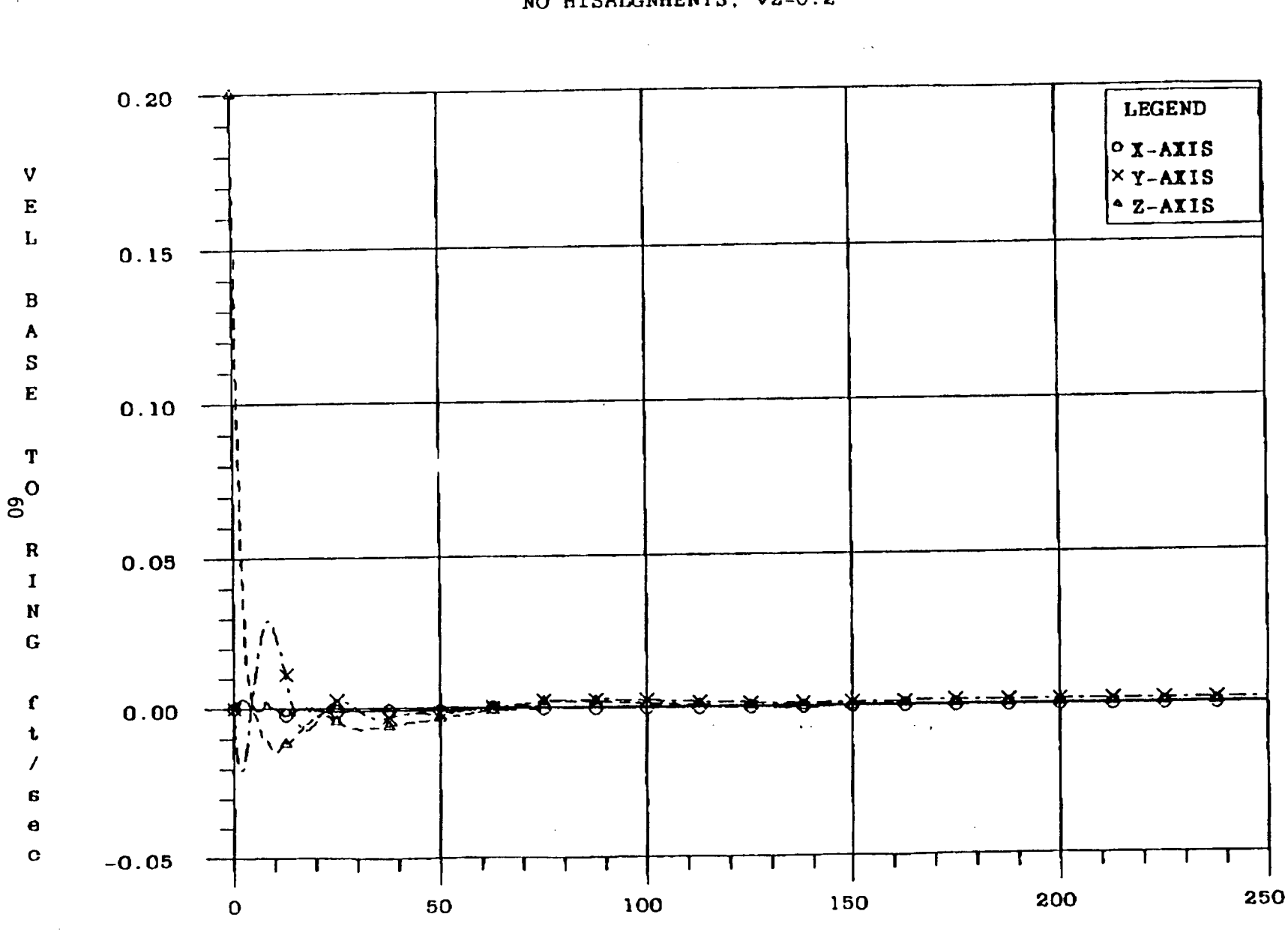
NO MISALGNMENTS, VZ=0.2
LEGEND
X-AXIS
Y-AXIS
Z-AXIS
0.20
0.15
0.10
0.05
0.00
-0.05
0
50
100
150
200
250
VEL BASE TO RING ft/sec
TIME sec
FIGURE 3.27

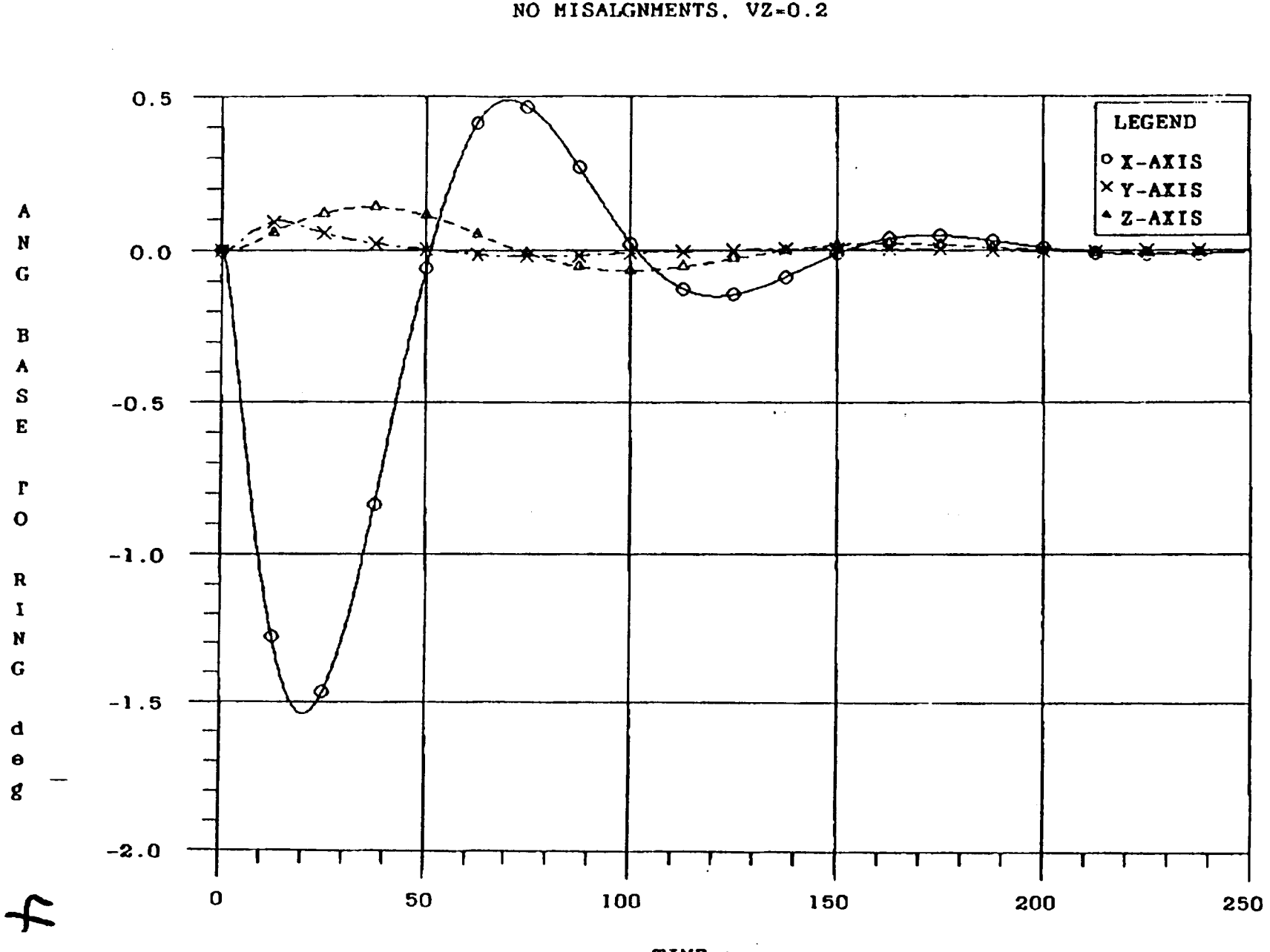
NO MISALGNMENTS, VZ=0.2
LEGEND
X-AXIS
Y-AXIS
Z-AXIS
0.5
0.0
-0.5
-1.0
-1.5
-2.0
0
50
100
150
200
250
ANG BASE FO RING deg
TIME sec

FIGURE 3.28

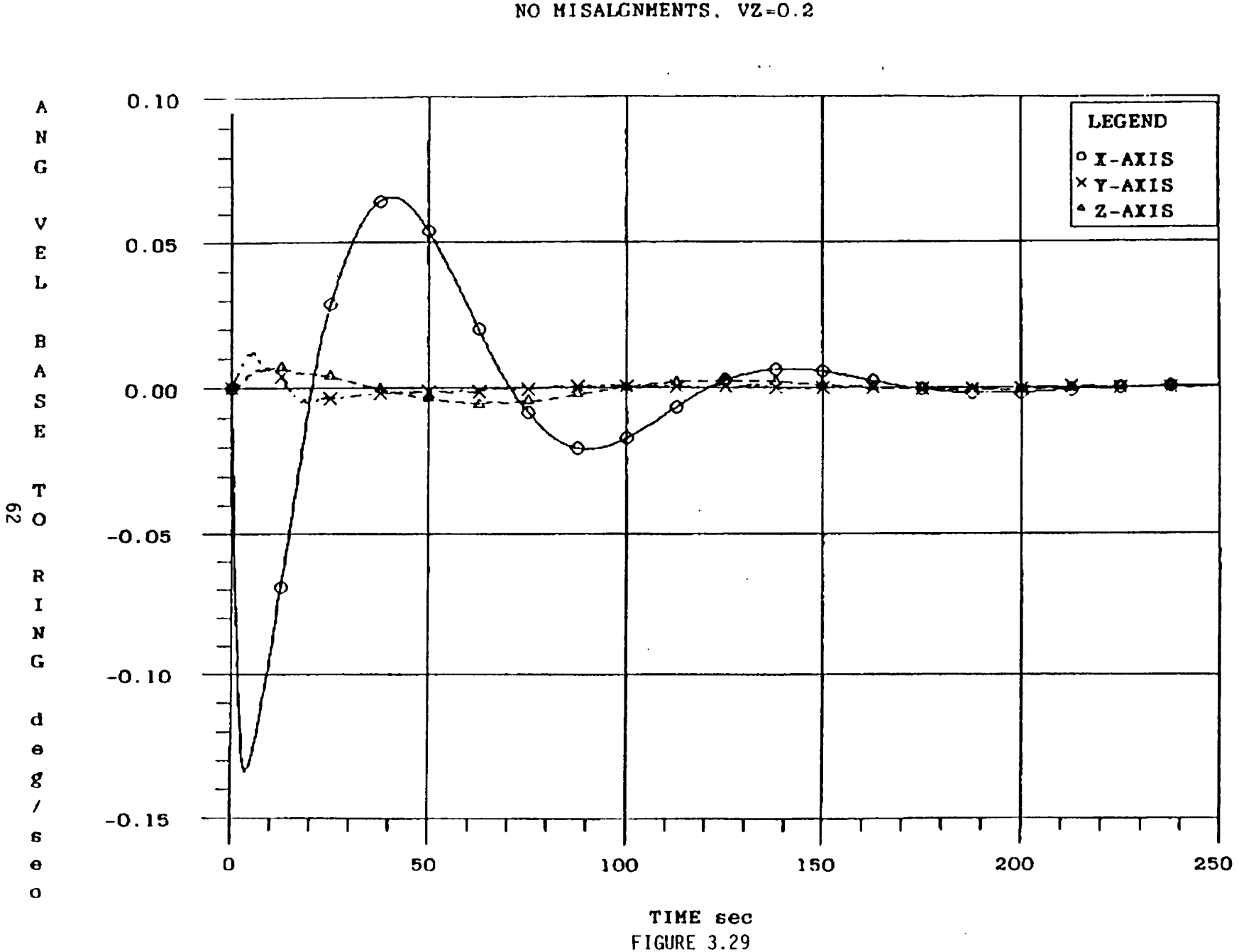
NO MISALGNMENTS. VZ=0.2
ANG VEL BASE TO RING deg/sec
0.10
0.05
0.00
-0.05
-0.10
-0.15
0
50
100
150
200
250
TIME sec
LEGEND
X-AXIS
Y-AXIS
Z-AXIS

FIGURE 3.29

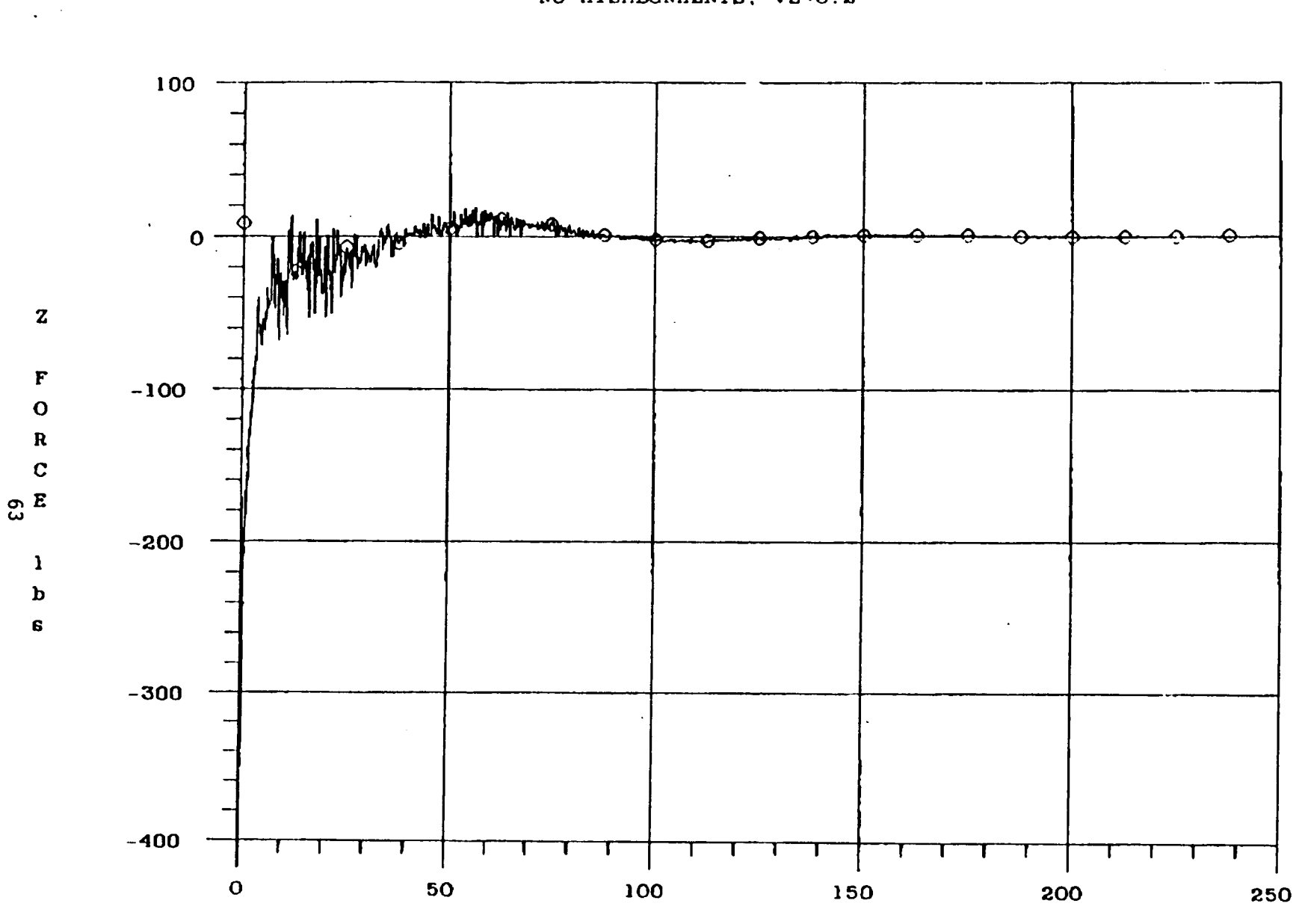
NO MISALGNMENTS, VZ-0.2
100
0
-100
-200
-300
-400
Z FORCE 63 lbs
0
50
100
150
200
250
TIME sec

FIGURE 3.30

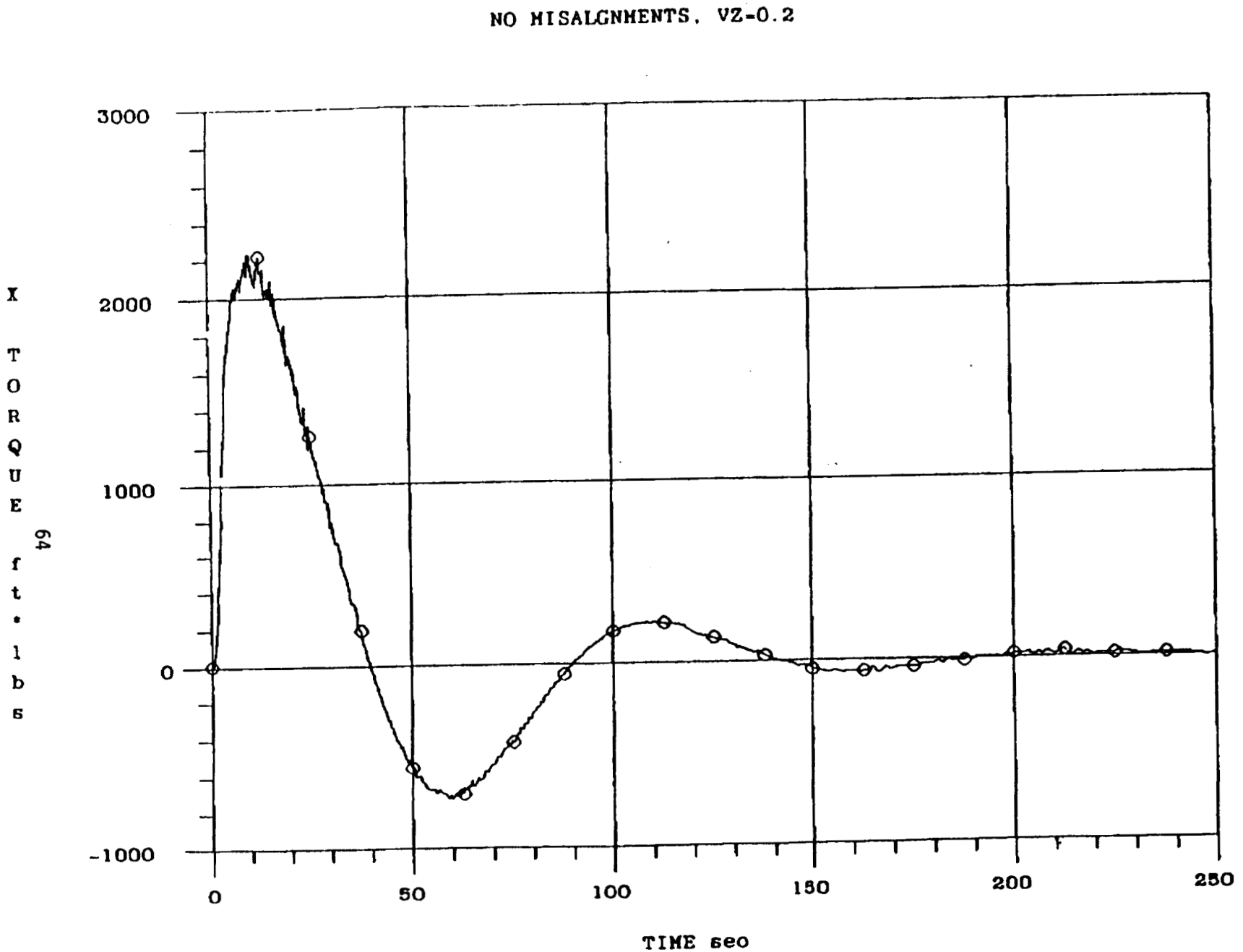
NO MISALGNMENTS. VZ-0.2
3000
2000
1000
0
-1000
X TORQUE ft•lbs
64
0
50
100
150
200
250
TIME sec

FIGURE 3.31

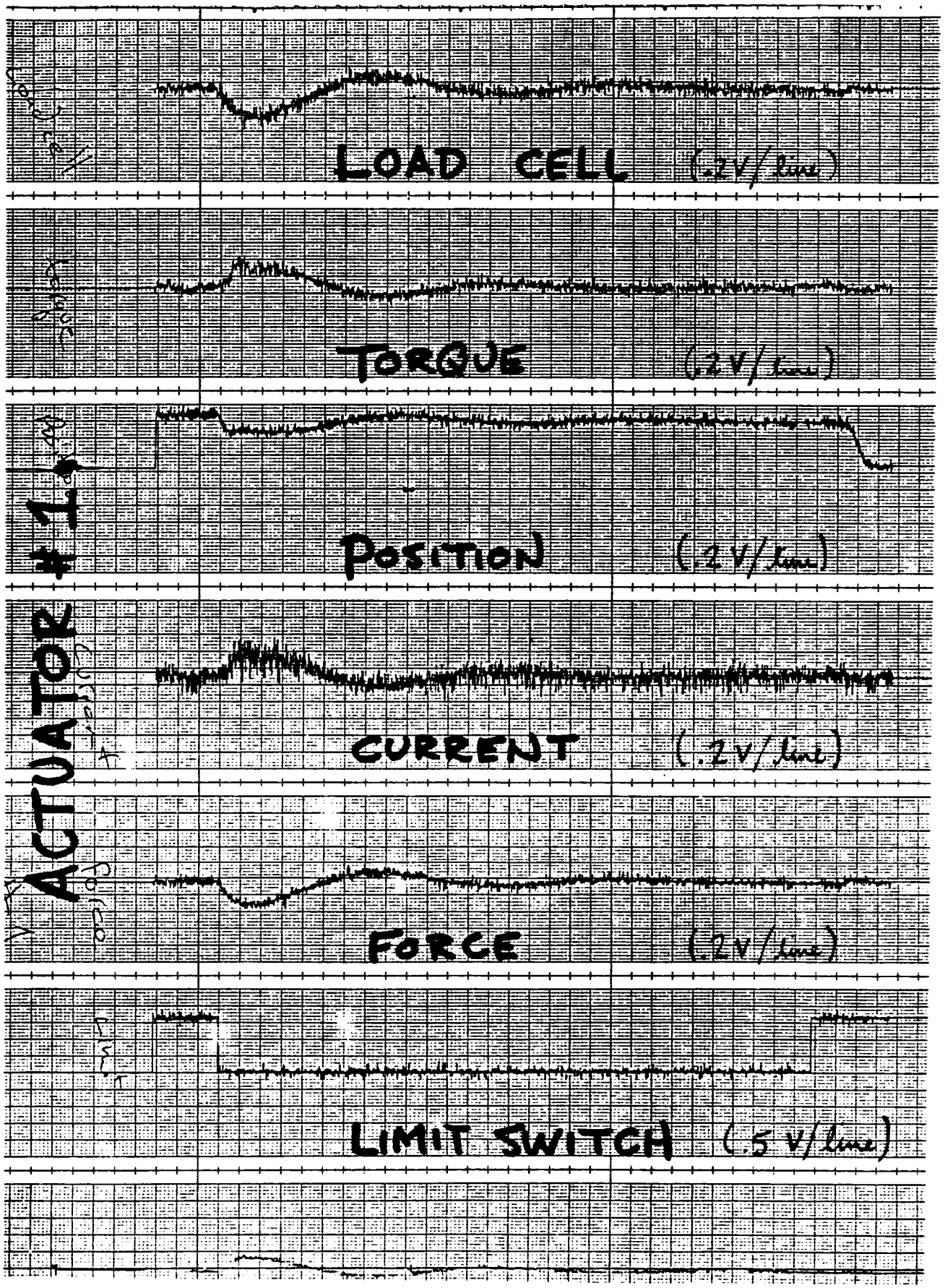

FIGURE 3.32

4. Results and Assessments

This section of the report contains a series of observations and tentative conclusions regarding the behavior of the docking mechanism. Following this, a set of observations of the 6-DOF facility will be presented.

4.1 Observations of Mechanism

The testing of the docking mechanism at UTC revealed several facts about this particular test article. First, it was found that the seal design showed no tendencies to leak under the conditions tested. The bellows flex test indicated that the bellows has a rotational stiffness of approximately 35,000 in-lb/deg. The quick-acting latch test indicated that these latches had the tendency to limit-cycle if the limit-switch cam was not adjusted properly. This problem became apparent again during the MSFC/6-DOF testing. There are several distinct problems which can cause the oscillations. When the two halves of the mechanism are mated, it was found that occasionally the latch roller would bounce off the opposite ring. The latch arm rotates the cam enough such that it engages the micro-switch thereby allowing the motor to drive the latch back into position, thus completing one cycle of oscillation. Due to the cam and limit switch arrangement of the latch, there exists a small deadband during which the latch motor is not active. It was found that minimizing this deadband (by cam adjustment) solved this type of latch behavior. (See Figure 3.6). Also it was found that adjustment of the height of the roller on the end of the latch was important to avoid chattering during the high gain modes. The chattering was caused by the latch (which is under load) opening up enough so that the cam engaged the micro-switch thus allowing the motor to drive the latch arm back into place. After the latch arm was in place, the motor switched off, thereby allowing the latch to open again. This cycling occurs at a high enough frequency to make a chattering noise.

Over the course of the dynamic testing, only one true instability was found to exist. This instability was found when entering the high-gain mode with the original set of gains (See Ref. 2). The oscillation of the system occurred at approximately 2 Hz. The 6-DOF support structure is suspected to have natural mode in the 2-3 Hz range. Certainly if the structure does indeed have a mode at 2-3 Hz this would be detrimental to the performance of the docking mechanism controller since it was designed under the assumption that no flexible modes were present. Upon reduction of the transverse translation gains in the high-gain modes, stability was achieved.

Immediately obvious to an observer watching the active ring being commanded up and down (in pre-capture mode) is that the ring does move as smoothly as one might expect. It appears that some of the actuators may be working against each other as the ring is moving. This type of motion is most probably due to the relatively large amount of friction inherent in the ball-screw

actuator. The force loop bandwidth is 1 Hz which implies that it takes about a second for the force loop to react to a given force command. This can cause the jerk seen in the mechanism when it is moving slowly.

Due to the way the actuators were designed, the weight of the cable is partially supported by the actuator. As can be seen in Figure 4.1 the load carrying bracket which secures the cable is mounted above the load cell - thus the load cell will detect this weight. The quick-acting latches were wired in such a way that the weight of their cables will be detected also (see Figure 4.2). In fact, due to the helical nature of the cable bundles, the load transmitted to the load cell is most likely a function of ring height.

While in the pre-capture and capture modes, the ring position was found to be significantly influenced by its own weight. Since the lateral stiffness of the active ring is quite low in the low gain modes, tilting the 6-DOF at some angle would cause the ring to slide over as if sliding down an incline to a new equilibrium point. It should be emphasized that this is strictly an artifact of testing the mechanism in a one-g environment.

One-g compensation was provided for in the initial design by having a force bias term for each actuator necessary to hold up the ring weight. The original intention was to position the ring in pre-capture mode (which has relatively high gains) and store the forces required to hold the ring at the desired capture position. At the beginning of capture these values would now become the new force biases. It was found however, that a one time sample of the forces at the beginning of capture lead to a random calculation of these values (due to noise in the analog to digital converters bringing the position signal into the computer and noise in the potentiometer electronics. Several methods of fixing this problem were considered (including averaging the force values over some time period). It was decided to store fixed values of force biases for all control modes with compensation of these values as a function of axial (z-axis) position. This worked well until large angular misalignments were introduced later in the test matrix. It became obvious that a better one-g compensation would be required to avoid having the ring "fall" to the side. This would require knowledge (and feedback to the mechanism software) of the 6-DOF orientation and position. This was not feasible given the additional interface requirements and the lack of computer resource to perform the necessary compensation. This was considered a lesson learned and can be compensated for in any future testing when additional resources are available.

Figure 4.3 shows how close the actuators are to contacting the back edge of the guide in the retracted position. Figure 4.4 shows the gouging on the back edge of one guide that has occurred. This seems to indicate that more clearance is necessary.

Given the size of the misalignment envelope within which capture must be guaranteed, it appears that the guides are just big enough to accommodate the misalignment with very little safety

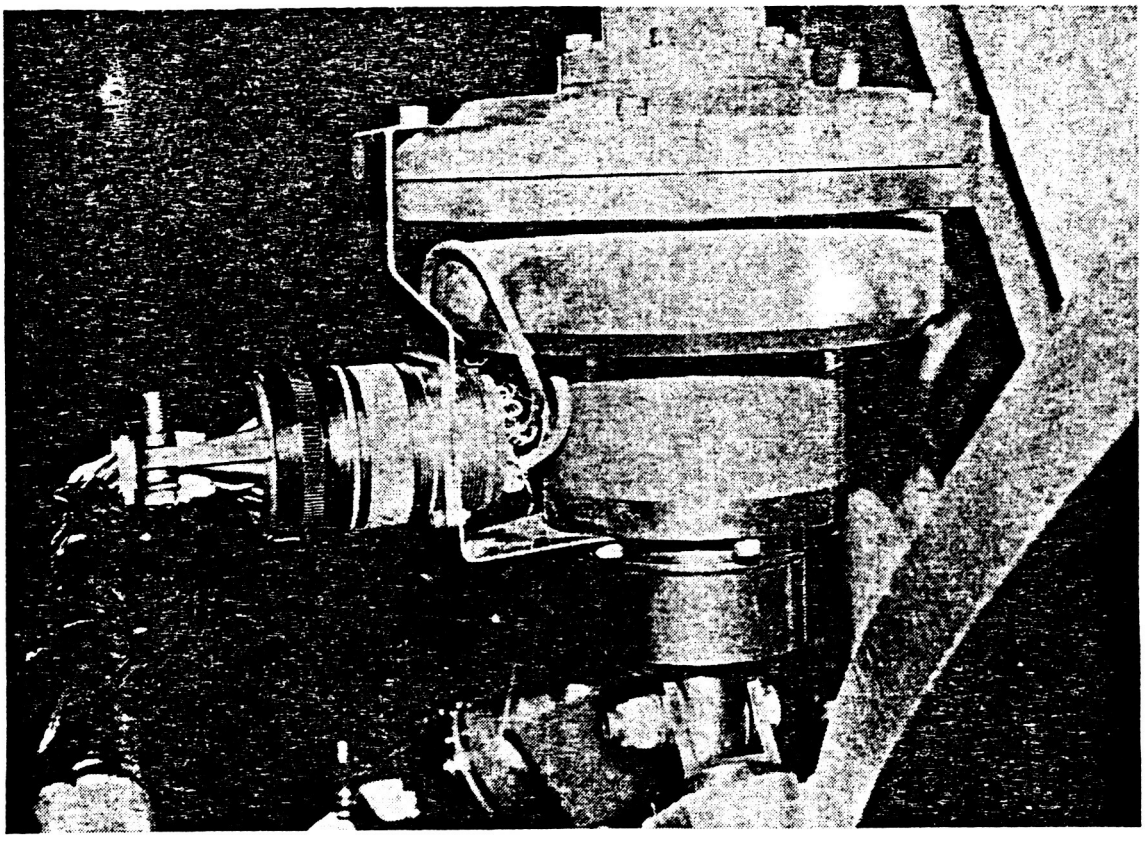

FIGURE 4.1

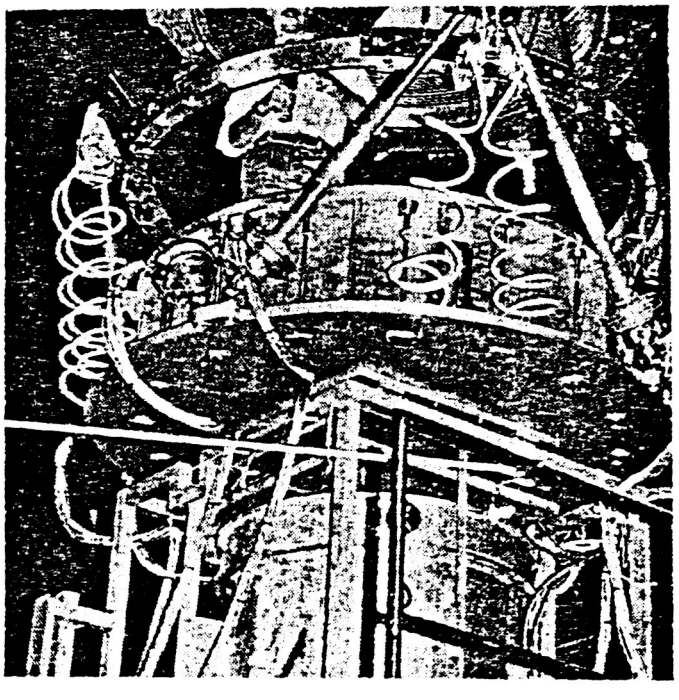

FIGURE 4.2

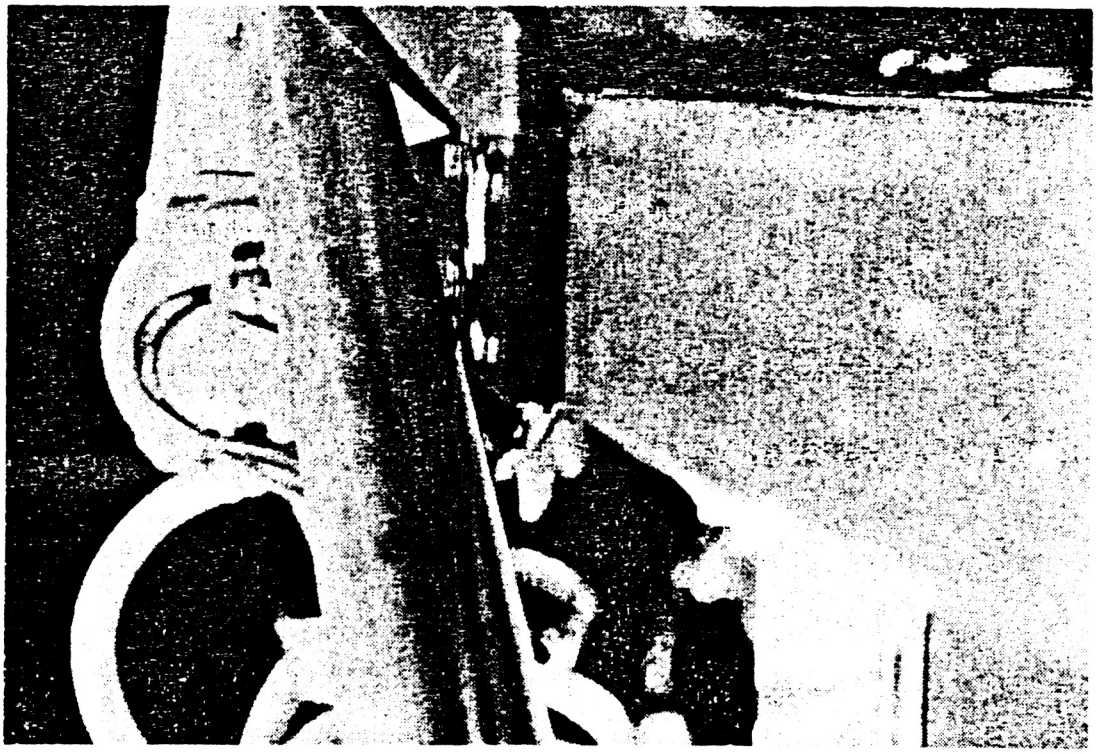

FIGURE 4.3

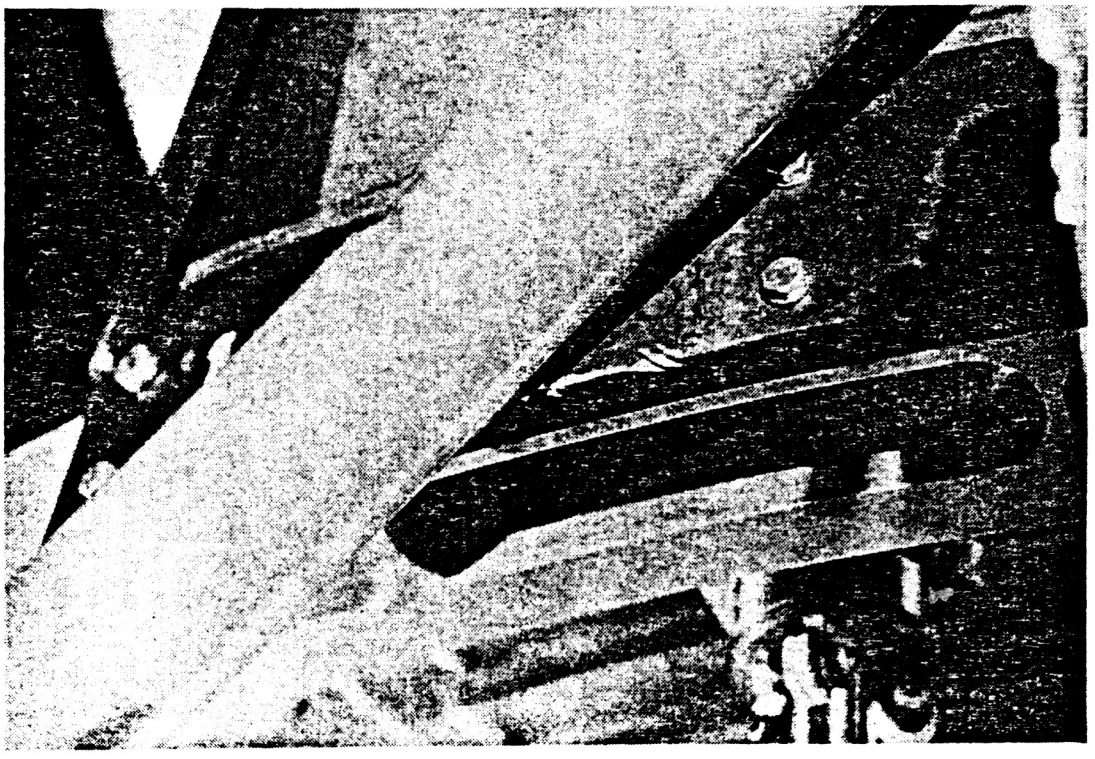

FIGURE 4.4

margin. Several cases were run where the guides contacted on the outside edge of the ring (as opposed to the ring face) by the smallest of margins.

4.2 Observations of 6-DOF Simulation Facility

The docking mechanism test performed at MSFC were by no means designed to validate the 6-DOF motion simulator. Several weeks before the mechanism was installed at the 6-DOF, NASA engineers performed a calibration of the facility. Satisfied with results of these tests, the mechanism was installed and testing begun. The results of the docking tests are predicated on the assumption that the 6-DOF was behaving dynamically as the Space Station - Orbiter pair. This assumption appears to be valid, however, several observations of the 6-DOF behavior merit discussion.

Probably the first item noted about the 6-DOF/docking mechanism set up was the flexibility of the upper mechanism rocking on the ceiling support structure. It appears that a mode exists at approximately 2 Hz when the upper mechanism half is suspended. It should be noted that a similar mode was analytically predicted some six months before testing and all organizations (NASA, MDAC, UTC, CDy) were alerted to its possible presence. NASA engineers found after the testing was completed that some increase in stiffness could be gained by pre-loading the safety tensile link (a mechanical fuse). Due to the fact that the support structure must neck down to force/torque sensor, designing a stiffer support system would be a significant task.

It was also noted that the pneumatic safety system under the active mechanism half seemed to have some motion associated with it. This motion was probably due to the vertical piston rocking back and forth within the tolerances of its fittings.

As a means of preventing drift of the 6-DOF, a deadband of approximately 50 lbs is introduced into the force/torque sensor data path. It was found that this value was too large to ensure the proper behavior of the docking mechanism. As a compromise between simulation fidelity and drift the deadband values were reduced to $F_X = F_Y = +/- 6.1$ lbs, $F_Z = +/- 9.1$ lbs, $T_X = T_Y = +/- 11.4$ ft-lbs, and $T_Z = +/- 6.1$ ft-lbs. Certainly the ideal case would be one in which no deadband is necessary.

As a matter of fortunate circumstance, the 6-DOF neutral position is well within the stroke of the docking mechanism actuators should the rings be latched together. As a means of pushing the 6-DOF performance as high as possible, the VAX/750 (the 6-DOF control computer) is run at the same priority as VMS (the VAX operating system). This results in sporadic computer system crashes, during which the simulator returns to the neutral point. Several such computer crashes occurred during the mechanism testing, however, none resulted in a problem for the docking mechanism.

5. Recommendations

The following is a list of items which were noted during the course of testing, where design improvements should be considered for future systems.

1. More computing power. The current AT-compatible running at 10 mhz is simply pushed to its limit. Debugging existing software is even difficult in the current set-up. See Appendix for more detail.

2. Connector types. Solder pin connectors are favored over the crimp pin type used. Also, standardizing to fewer types may have advantages.

3. Quick-acting latch cams. A larger range of adjustment would be desirable for the cam.

4. Capture Signal. The current software switches the controller into high-gain mode after the contact switches are depressed. No consideration is given to whether or not the latches have actually been thrown. Thus a latch failure may indirectly induce an instability (because high-gain modes are unstable if not latched). This was demonstrated during testing when the latch power supply failed.

5. Cables. Shield entire cable on each external cable bundle; also add a protective jacket for each bundle.

6. Computer control. The computer should control the sequencing of power up and down (not just issue instructions).

7. Long reach (berthing) latches. The latches should have some sort of torque control. Currently when driven at maximum speed the stalling torque is large enough to damage the latch.
8. Emergency stop. E-stop switch would be desirable which freezes the ring without dropping it. (Needed for 1-g testing).

9. Operation manual. Manual describing actual operation, trouble-shooting, and parts list.

10. Improved one-g compensation bias in software.

11. Store computed 6 DOF orientation and rate information (as well as computed forces and torques) calculated in the mechanism computer. This would help for comparison of actual vs. predicted result evaluation.

Recommendations for further tests to be performed on the mechanism, are as follows.

1. Calibrate load cells. Perform actual calibration (not just establishing zero) and determine noise characteristics as well as frequency response.

2. Calibrate position pots. Same as above.

3. Perform frequency response tests of mechanism. In order to characterize the unmodeled dynamics, the FRF tests should be performed for all control modes.

4. Modify the capture software to limit the position gain feedback. This will provide enough feedback to hold the ring still prior to contact but will limit the effect of the spring at large offsets during contact/capture.

5. Rerun some of the test matrix after better one-g compensation is designed into the software.

6. Perform position and accuracy tests on both the 6-DOF and docking mechanism. This is required to perform detailed post test analysis and provide inputs to update the simulation models.

5.2 Conclusions

The intent of this report has been to document the testing of the MDAC designed docking and berthing mechanism. The prototype mechanism testing was performed with a goal of establishing the validity of docking with an active electromechanical system. This proof-of-concept goal was achieved.

As might be expected with a prototype system, a number of items (both hardware and software) required trouble-shooting. While the majority of problems were solved, some proved more elusive. Perhaps the most apparent is the anomalous behavior of the alignment mode. However, given adequate time, the remaining problems can be solved.

The mechanism was shown to be capable of capturing if the initial conditions are within the misalignment envelope bounded by the test matrix. However, for some of the more severe misalignments, a minimum closing velocity of between 0.1 and 0.15 ft/sec was required. This required closing velocity can almost certainly be improved upon by refinement of the 1-g compensation technique. The test results concerning the minimum velocity required needed to capture is not felt to be indictative of the true performance capability of the electromechanical system. Any conclusions drawn concerning the capture capability should come after new testing is done with an improved one-g compensation routine.

6. Final Assessment and Recommendations for Phase C/D

Since May 1985, where the Berthing Mechanism Advanced Development program stated, several concepts for docking/berthing the Orbiter to the Space Station have been explored. This Advanced Development program was based on the concept of using a telescoping "docking module" installed in the forward end of the Orbiter cargo bay. It was also assumed that the Orbiter must dock with any standard Space Station module interface. These assumptions led to the berthing mechanisms designs that encompassed the standard 50 inch square Space Station hatch opening and thus, dictated the size and geometry of the mechanisms.

Currently the docking mechanism concept for the Orbiter/Space Station is under study and the final concept to be mechanized has not been selected. The objective of exploring these alternate concepts is to minimize the weight to be carried to orbit by the Orbiter and to install as much of the docking mechanism and pressurized transfer tunnel as possible on the Space Station.

The Berthing Mechanisms Advanced Development program developed two mechanism halves each for a different purpose. Although the design is androgynous, and the halves mate with each other, two separate sets of requirements were met.

The flexible half was designed to be used within the closed loop module pattern and provide two degrees of freedom of motion. The attenuating half was designed to be mounted on the STS Orbiter "Docking Module" and provide capture, attenuation alignment and retraction of the Orbiter to Space Station.

The design of the flexible berthing mechanism half including the guide system, the capture latches, the structural latches, the flexible two ply aluminum bellows, the cable bellows restraint system, and seals are all directly applicable to the module-to-module interface currently part of Work Package 1 under the direction of NASA MSFC.

Although the attenuation half that was developed will not fit directly into the concepts now under consideration, the proof-of-concept has been established for the use of an active, computer controlled, electromechanical capture and attenuation system.

6.1 Current STS/SSPE Attachment System Status

Figure 6-1 illustrates the MDAC proposed phase C/D baseline docking system approach. It used the technology developed under the advanced development program for an active electromechanical system. The hatch size and thus the docking/berthing mechanism was smaller in diameter than the R&D prototype. Long stroke attenuator/actuators were used to extend the capture frame eliminating the need for a telescoping docking module and thus reducing weight.

The current SS/STS docking/berthing assessment program has the purpose to identify and assess the impacts and program risks associated with the different docking concepts. The approach is to qualitatively and quantatively compare the various concepts and using evaluation criteria such as: Orbiter weight and CG location, cost reliability, maintainability, safety and operational flexibility, interface complexity, development risk and docking loads, select the system concept to be used for Space Station. This study plan calls for recommendations to be presented by 15 January 1989.

Figures 6-2 and 6-3 illustrate the docking mast concept currently being considered. Figures 6-4 and 6-5 illustrate a passive attenuation system to be used with the mast concept as proposed by RI. Figure 6-6 illustrates an active probe and drogue system using the computer controlled electromechanical attenuator/actuator concepts developed by this Advanced Development program. Figure 6-7 illustrates a docking module concept utilizing the existing Orbiter airlock. This concept moves the airlock from the crew compartment aft into the cargo bay potentially improving the Orbiter's forward CG problem. This concept would fully utilize the technology developed by this program. Figure 6-8 illustrates a concept utilizing an external airlock, the docking mast and an active load attenation design concept.

6.2 Conclusions

The selection of the STS Orbiter to Space Station docking system concept and final design will be the product of trade studies currently underway. The technology developed under this R&D contract will be a major contributor to the data base to be used in conducting these trades. In addition to the docking technology derived, the following designs, illustrated in Figure 6-9, have been demonstrated and apply to the Phase C/D Space Station design:

A. Quick acting capture latch

B. Long reach capture latch

C. Guide design

D. Multi ply large diameter, aluminum bellows pressure vessel

E. Cable pulley bellows pressure restraint system

F. Structural latches

G. Module to module interface sealing system

H. Umbilical cross-over concept

I. Hatch design concepts

J. Structural design concepts and fabrication technique of large space mechanisms

K. Computer controlled, electromechanical, capture, attenuation, alginment and retraction system

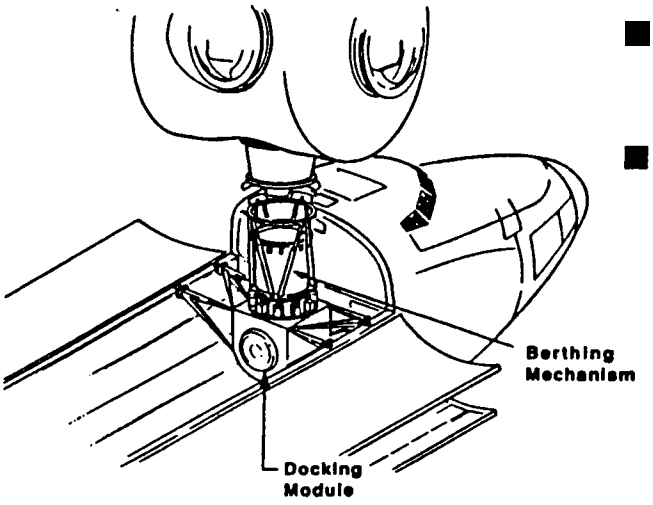

Key Issues

- **Separate docking module increases Orbiter up/down weight**
- **Compatibility with large lateral misalignment (±8.0 in)**

DOCKING MODULE CONCEPT

STS/SSPE ATTACHMENT SYSTEM Internal Airlock

FIGURE 6-1

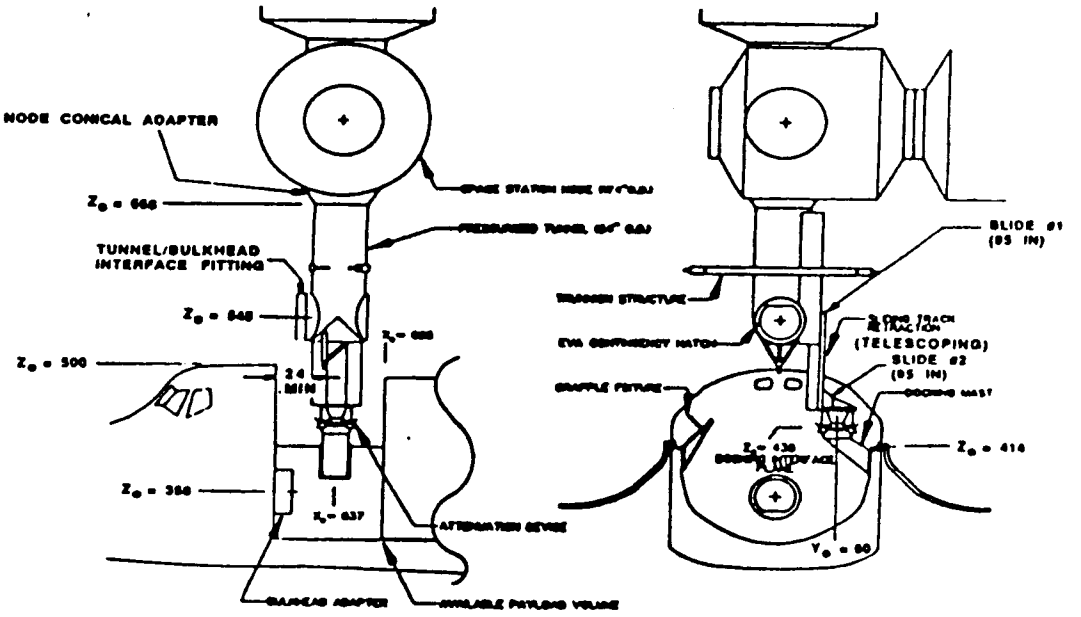

ORBITER/STATION DOCKING MAST ATTACH SYSTEM

INITIAL CONTACT CONFIGURATION

FIGURE 6-2

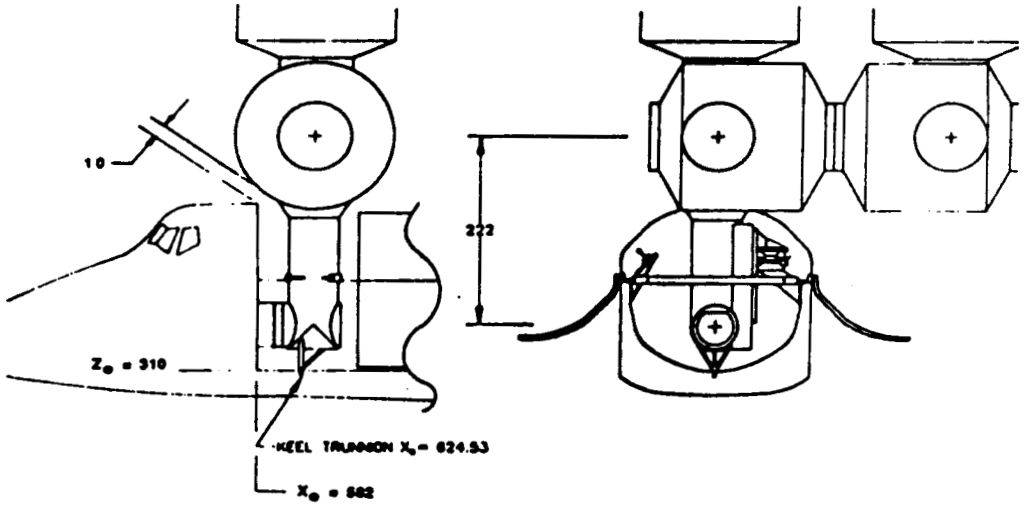

ORBITER/STATION DOCKING MAST ATTACH SYSTEM
FULLY DOCKED CONFIGURATION

FIGURE 6-3

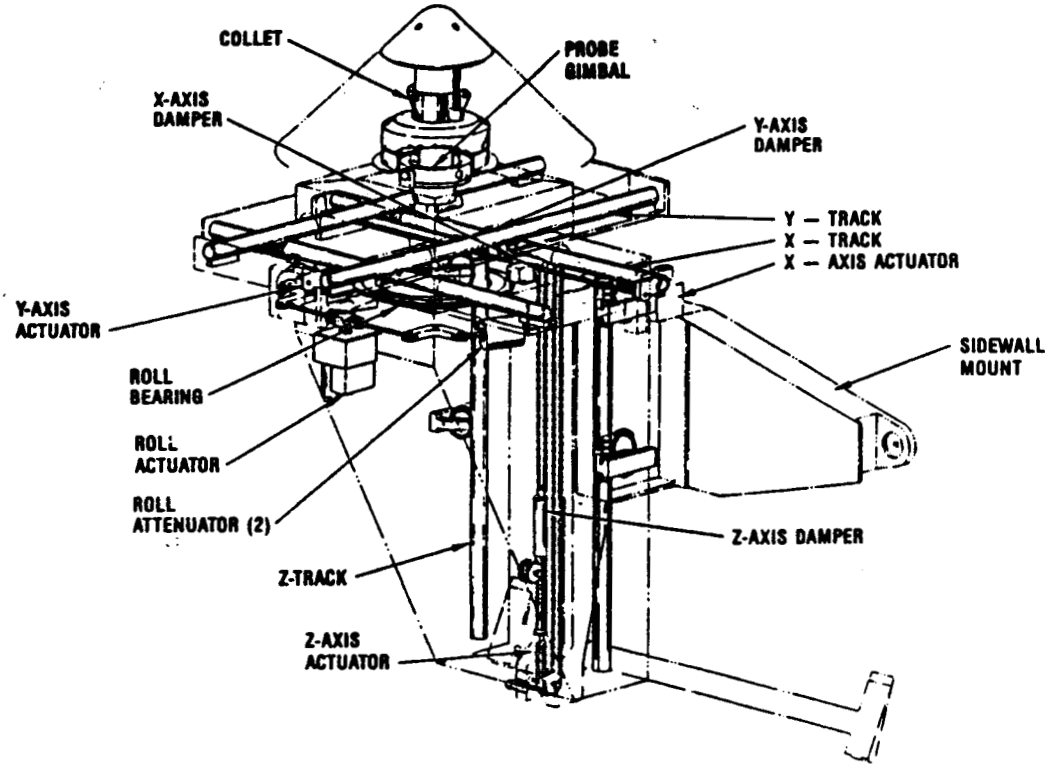

Design Concept Accepts Misalignment Requirements and Has Passive Attenuation

FIGURE 6-4

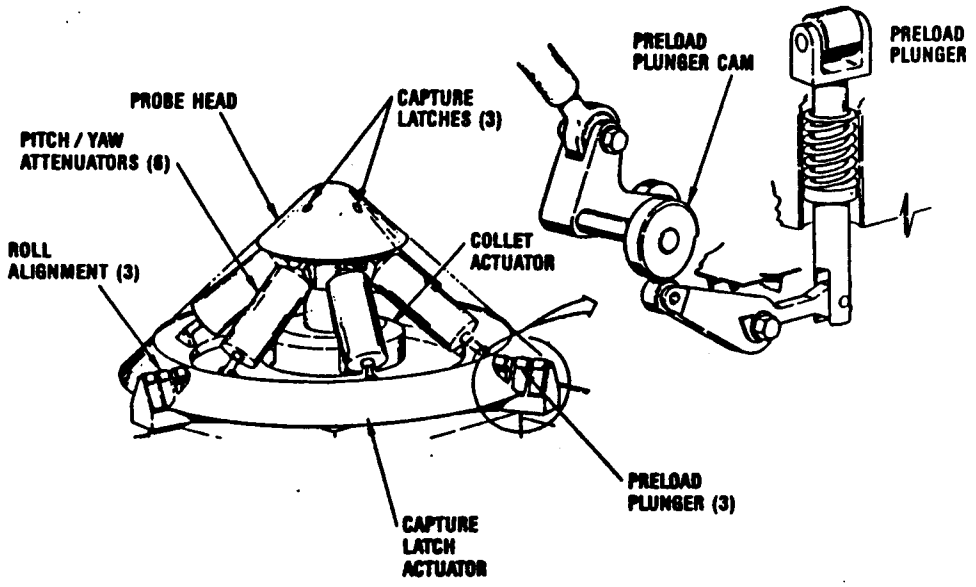

Probe Design Has Passive Attenuation

FIGURE 6-5

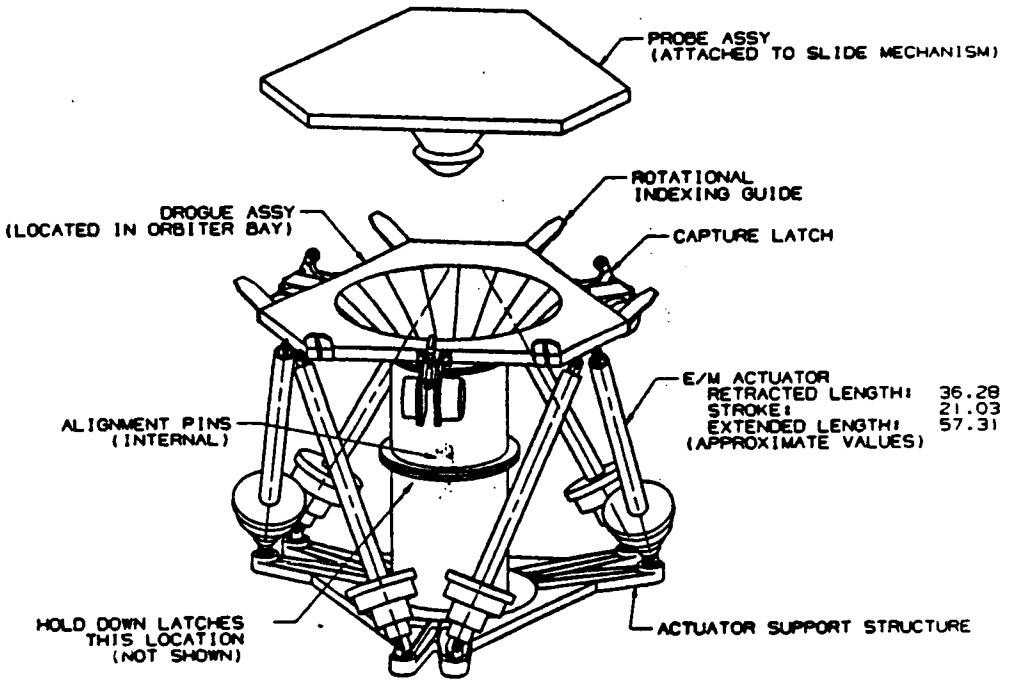

ACTIVE LOAD ATTENUATION DESIGN CONCEPT (6 ACTUATORS)

FIGURE 6-6

ORIGINAL PAGE IS
OF POOR QUALITY

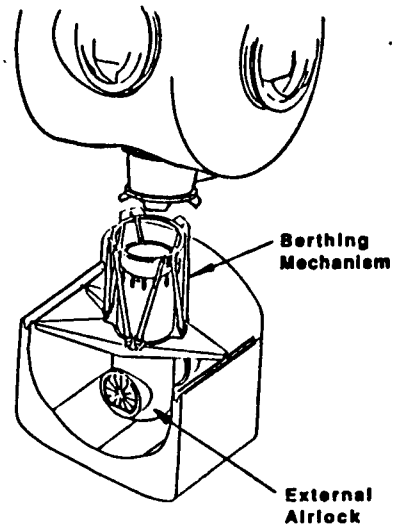

Key Issues

- Retention of berthing mechanism and airlock in cargo bay (weight concern)
- Compatibility with large lateral misalignment (±8.0 in)
- External airlock (replaces cabin airlock)

DOCKING MODULE CONCEPT
External Airlock

FIGURE 6-7

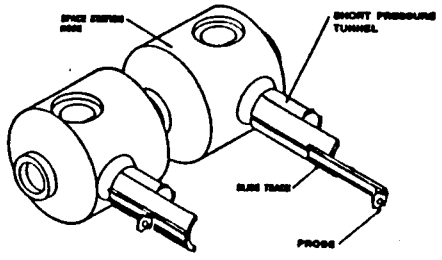

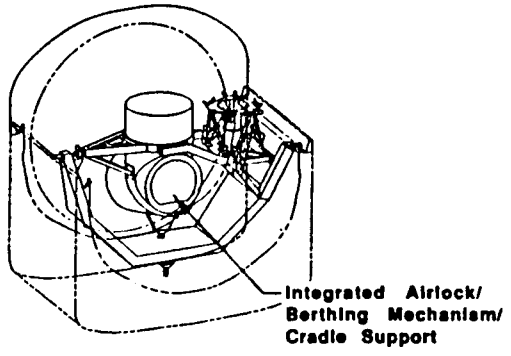

Key Issues

- Additional on-orbit maintainability (pressure tunnel and slide mechanism remain with Station)
- MSC Orbiter berthing (MSC reach capability exceeded with extended slide mechanism
- Compatibility with large lateral misalignments (±10.5 in)
- Attaching to vehicles besides Station (requires target vehicle to carry tunnel and slide mechanism)
- Long cantilevered slide attached to short tunnel section

DOCKING MAST CONCEPT
External Airlock

FIGURE 6-8

ORIGINAL PAGE IS
OF POOR QUALITY

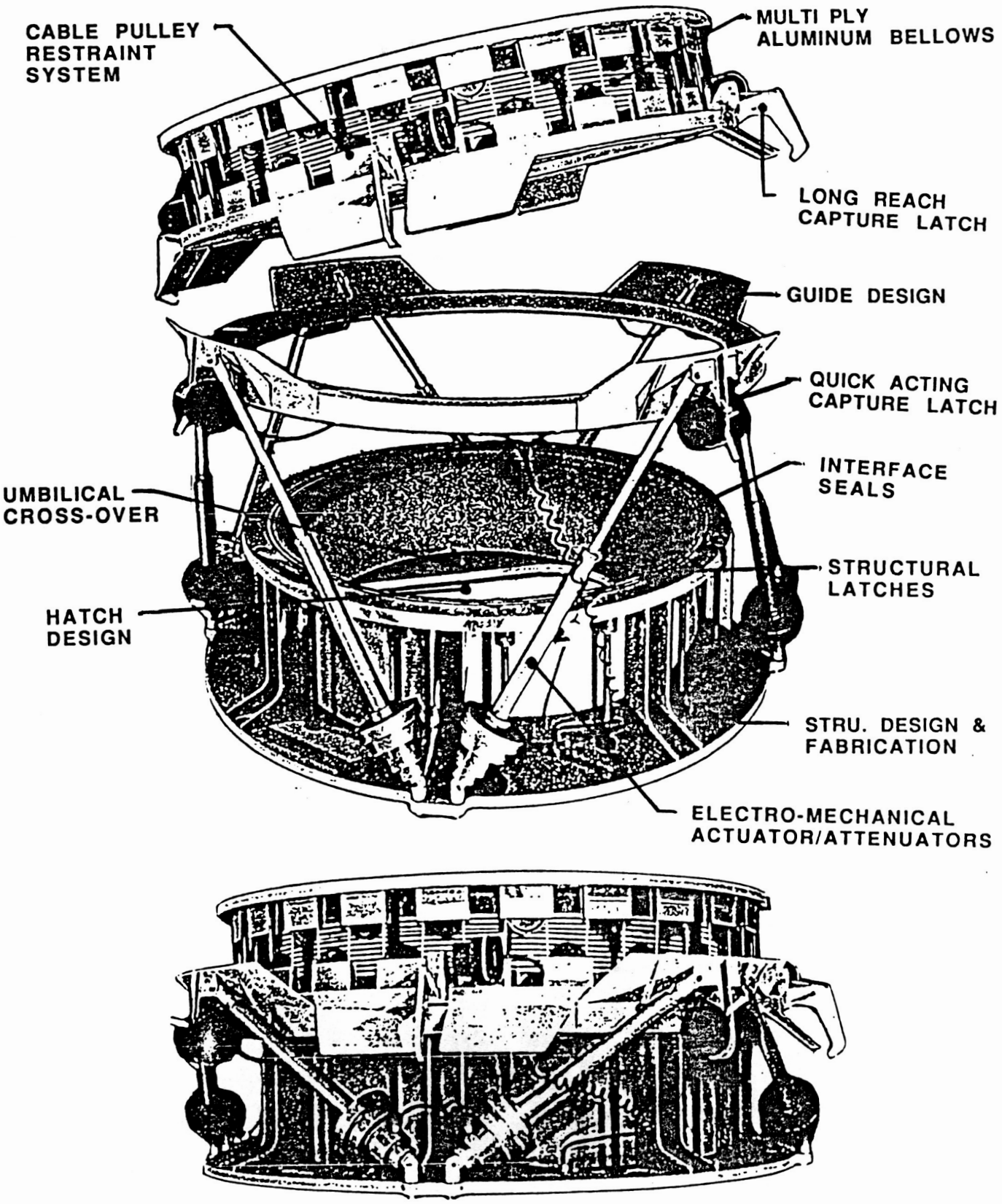

FIGURE 6-9. BERTHING MECHANISM DEVELOPMENT DEMONSTRATION ITEMS

7. References

1. Space Station Berthing Mechanisms Study Program Test Plan (IDRL - 11), Control Dynamics Company, November 1987.

2. McDonnell Douglas Memorandum A3-960-DBB-SS-M-8700552, "Berthing Mechanism Program Control System Design Requirements," T. Alt and D. Buchanan, April, 1987.

8. Appendix

SPACE STATION BERTHING MECHANISM TEST RACK

POWER-UP SEQUENCE

I. INITIAL SWITCH POSITIONS

The state of the direction and **RUN/STOP** switches on the Boston Gear controllers (FLEXTURE CAPTURE LATCH CONTROLS) does not matter (but it is helpful if they are all set for the same direction). The pot setting doesn't matter either (but it is helpful if they are all set to the same position). The momentary **MOVE MOTOR** switch must be in the normal, center off (middle) position. If the long reach capture latches (Boston Gear controllers) are not going to be used, the **RUN/STOP** switches on each controller should be moved to the STOP position.

The card cage switch (**ACTUATOR CONTROLLER INPUTS**) should be in the grounded position for power-up.

The attenuating capture latches **CAPTURE/RETRACT** switch should be in the CENTER OFF position. NOTE: THERE IS NO AUTOMATIC SAFETY POSITION FOR THIS SWITCH. IF THE SWITCH IS LEFT IN AN ENABLED POSITION (CAPTURE OR RETRACT) WHEN POWER IS APPLIED, THE MOTORS MIGHT START RUNNING.

The actuator motor **UP TO INHIBIT ACTUATOR OUTPUTS** switch should be in the UP POSITION. The actuator **UP TO ZERO LOAD FORCE FEEDBACK** switch should be in the UP POSITION (to zero the feedback loop).

The power switch to the large power supply (below the blower) should be OFF. The corse and fine voltage adjust and current adjust controls should all be full counter clockwise (zero setting).

The **MASTER POWER** switch should be in the OFF or DOWN position.

II. INPUT POWER

Input power is a 3 phase, 4 wire type of system with a safety ground (total of 5 wires). The input voltage is 110-120 volts (RMS) from any leg or phase to neutral and 208 volts between any two legs or phases.

The test rack is fused for a 60 amp line. External fusing should consist of the same size (60 amp) breaker. The large power supply is fused for 30 amps (also a breaker). The 28 volt power supply is fused for 20 amps, the 24 volt power supply is fused (F1) for 6.25 amps, and the +/-15 volt power supply is fused for 2 amps (F2).

III. POWER TURN-ON SEQUENCE

The computer should be turned on and fully operational before power is applied to the test rack.

The **MASTER POWER** switch can now be moved to the UP (on) position. This will activate all of the internal fans and power supplies except for the actuator controller power supply. At this point, any

of the capture latch systems (either long reach or quick acting) can be used.

To apply power to the actuator controllers, the power switch to the large power supply (below the main blower) must be turned ON (moved to the UP position). This supplies power to the actuator controller output stages but no voltages should be detected at the controllers outputs at this time.

Adjust the current control up until it is at 3/4 of full scale.

Adjust the corse voltage up until the meter reads 40 volts (plus or minus one volt).

To enable the actuator controller outputs, the actuator motor **UP TO INHIBIT ACTUATOR OUTPUTS** switch must be moved to the DOWN position. When this is done, power will be available at the actuator controller outputs.

The card cage switch (**ACTUATOR CONTROLLER INPUTS**) should now be moved to the CONNECTED (UP) position to unground the actuator inputs. Any offsets or voltages present on the analog board outputs will now appear on the actuator controller outputs.

The last switch to be thrown is the **UP TO ZERO LOAD FORCE FEEDBACK** switch. This switch should be moved to the DOWN position to activate the force feedback loop and make the analog control system complete.

The Berthing Mechanism Test Rack should now be fully operational.

BMCPS Lessons Learned / Recommendations

I. Development History

The BMCPS (Berthing Mechanism Control Program Software) was developed on a JS286 (IBM AT clone) under DOS 3.2 using Borland's TurboPascal Version 3.02A for editing, compiling and linking. Assembly language routines (Intel 30286 assembly) were assembled using Microsoft Macro Assembler Version 4.0. Qua Tech's Labstar Version 2.0 canned routines were used for control of the DAC and ADC cards.

The computer system was specified by the GN&C group and purchased as a package from CyberResearch. It consisted of the JS286 (including monitor, keyboard, high-density floppy drive and hard disk) and the Qua Tech digital analog boards (1 DAC, 4 ADC's, 2 screw terminal panels, 2 PXB's and connecting cables). The Pascal and assembler packages were purchased separately.

Documentation used were the manuals for the software packages, Norton's Programmer's Guide to the IBM PC and various Intel reference manuals on the microprocessor and support chips. The Norton Guide proved to be very useful with easily understandable text and helpful examples.

II. Lessons Learned

The BMCPS was originally intended to be written entirely in Pascal. However, due to a 50 Hz cycle time requirement, several high computational sections had to be rewritten in assembly in order to meet time constraints. TurboPascal Version 3.02A has a complex process for linking external routines and only allows parameter passing on the stack, thus forcing subroutine calls to have a large number of arguments (in one case, 42). TurboPascal Version 4 allows for global variable access in external routines with a simplified linking procedure and should be used for future releases. However, the current Labstar version will not work with version 4, but Qua Tech is working on this problem. Alternatively, Ada compilers are now available for the 30286/30386 computers. Ninety percent of the code could be directly converted to Ada (Ada is based on Pascal) with recoding needed only for system-specific items, i.e. interrupt vector loading.

The Qua Tech boards proved to very difficult to implement. The manuals were poorly written and, in some cases, contradictory. A hardware interrupt was needed to initiate the 50 Hz cycle and the Qua Tech manuals indicated that the ADC board had this capability. In practice, the board would not work and subsequent fixes recommended by Qua Tech support personnel did not remedy the situation. We ended up building our own board to generate the necessary signal.

The only debugger available was a crude one provided with the system. It would not allow debugging inside the interrupt service routine (ISR), where most of the problems arose. The most significant problem encountered was a floating point overflow which would cause a lockup. After two weeks of work and many false leads, the problem was diagnosed to be a failure to save/restore the state of the math coprocessor upon entry-to/exit-from an external subroutine. This was corrected with the addition of two instructions in each subroutine. A debugger capable of working in an ISR would have found the problem almost immediately. TurboPascal Version 4 does have a sophisticated debugger, although it is unknown whether it will work in an ISR.

III. Recommendations for future upgrades and related projects

1. Use a faster machine. The JS286 is a 10 MHz machine, there are now 25 MHz machines available on the market, i.e. the IBM PS2/model 70.

2. Include a data recording capability. Time constraints precluded the storage of intermediate calculation results, which made debugging and system tuning difficult.

3. Buy support contracts when purchasing equipment. Attempts to receive help from CyberResearch and Qua Tech were met with bureaucratic resistance.

4. Inclusion of the software group early in the design phase. The software group was brought in after computer selection and preliminary software design were completed. Several problems could have been avoided by input from the SW group during this phase (i.e. computer selection, complier selection, etc.)

5. Purchase of a printer and a low density floppy drive. Hard copy listings of the software were unwieldly to obtain due to the lack of a printer and a low density drive (computers with low density cannot read high density discs).

6. Use TurboPascal Version 4 or higher. Newer versions have a debugger and ease the use of external subroutines.

7. Purchase a machine with a user accessable Programmable Interval Timer (PIT) with interrupt generation capability. A PIT would have alleviated the problems arising fromthe lack of hardware interrupt needed for cyclic ISR initiation.

8. Different ADC and DAC cards. The Qua Tech boards failed on numerous occasions during test and integration, resulting in down-time while repairing or replacing the boards. They also failed to perform as specified and support response was too slow.